2019

Discovery and Development of KDM4B Inhibitors to Target Periodontal Disease Progression

Joy Elizabeth Kirkpatrick
Medical University of South Carolina

Discovery and Development of KDM4B Inhibitors to
Target Periodontal Disease Progression

Joy Elizabeth Kirkpatrick

A dissertation submitted to the faculty of the Medical University of South Carolina in partial fulfillment of the requirements for the degree of Doctor of Philosophy in the College of Graduate Studies.

Department of Drug Discovery and Biomedical Sciences

2019

Approved by:

Chairman, Advisory Committee _____
Patrick M. Woster

_____
Craig Beeson

_____
Chad Novince

_____
Yuri Peterson

_____
Ozlem Yilmaz

Dedication

I dedicate this dissertation to Felix Gerasco, who has provided me with unconditional love throughout the completion of this work.

Table of Contents

List of Figures

List of Tables

Key to Symbols and Abbreviations

Aa	Aggregatibacter actinomycetemcomitans
BMDM	Bone marrow derived macrophages
CEJ	Cemento-enamel junction
CFU	Colony forming units
dOCP	defined osteoclast progenitors
ELISA	Enzyme linked immunosorbent assay
FBS	Fetal bovine serum
GAPDH	Glyceraldehyde 3-phosphate dehydrogenase
H3	Histone 3
H3K4	Histone 3 lysine 4
H3K9	Histone 3 lysine 9
IL	Interleukin
KD	Knockdown
KDM1A	Lysine demethylase 1A
KDM4B	Lysine demethylase 4B
KO	knockout
LPS	Lipopolysaccharide
LSD1	Lysine specific demethylase 1
MAPK	Mitogen activated protein kinase
M-CSF	Macrophage colony stimulating factor

MEMα	Minimum essential medium alpha
MMP	Matrix metalloproteinase
mRNA	Messenger ribonucleic acid
NF-κB	Nuclear factor kappa b ligand
OB	Osteoblast
OC	Osteoclast
OPG	Osteoprotegrin
PBS	Phosphate buffered saline
PCR	Polymerase chain reaction
PDL	Periodontal ligament
RANK-L	Receptor activator of nuclear factor kappa b ligand
RNA	Ribonucleic acid
TBST	Tris buffered saline with Triton X-100
Th	T helper
TLR	Toll like receptor
TNF-α	Tumor necrosis factor alpha
TRAP	Tartrate resistant acid phosphatase
uCT	Micro computed tomography
WT	Wild type

Abstract

JOY ELIZABETH KIRKPATRICK. Validation and Development of KDM4B Inhibitors to Target Periodontal Disease Progression. (Under the direction of PATRICK WOSTER).

Periodontal disease (PD) affects nearly half of the adult United States population and is characterized by bacterial-driven inflammatory bone loss. Traditional and emerging treatments for periodontitis management do not typically target the host immune response, which is the major source of tissue damage. The demethylation activity of lysine-specific demethylase 1 (KDM1A) at histone 3 lysine 4 leads to a decrease in pro-inflammatory cytokine transcription. By contrast, lysine specific demethylase 4B (KDM4B) is a histone demethylase that specifically demethylates histone 3 trimethyllysine 9 (H3K9me3). Interestingly, previous data has shown that cross talk between these two enzymes leads to a balanced system wherein lysine 9 methylation serves as a prerequisite to lysine 4 demethylation by KDM1A. The studies outlined in this dissertation will exploit this crosstalk for the design of new potential therapies for PD. *The central hypothesis of this dissertation is that promotion of KDM1A activity by introduction of a specific KDM4B inhibitor will alleviate PD by controlling the overactive immune system in diseased areas, enabling the host to better manage the disease*. This hypothesis was tested through completion of the following Specific Aims: Specific Aim 1: To mechanistically define the role of KDM4B in periodontal inflammation; Specific Aim 2: To design a novel inhibitor of KDM4B for adjunctive treatment of PD inflammation, and Specific Aim 3: To evaluate novel and known KDM4B inhibitors for in vivo activity as anti-inflammatory agents. KDM4B inhibition prevented the *A.a*-induced immune response *in vitro* and *in vivo*. KDM4B inhibition also reduced osteoclast formation in vitro and bone loss in vivo. KDM4B activity is heightened in periodontal disease in clinical tissues as well as in murine calvarial tissue sections treated with *A.a*. KDM4B inhibition mediated immunosuppression relies on the concurrent overactivation of KDM1A. Computational chemical screens identified several hit scaffolds, one of which was optimized using phenotypic screen guided binary QSAR. From an extensive in silico derivative library, 25 novel derivatives were synthesized, 8 of which caused significant immunosuppression.

Chapter 1: Background and Significance

1.1. Periodontal Disease

1.1.a. Clinical Significance and Epidemiology

Periodontitis is a chronic oral inflammatory condition that destroys the supporting tissues of teeth, resulting in irreversible damage including bone loss and tooth loss. Currently, this disease affects 42% of dentate adults in the United States. There is higher prevalence of the disease associated with adults 65 years or older, Mexican-Americans, non-Hispanic blacks and smokers.[1] Severe periodontal disease is estimated by the world health organization to be the 11th most prevalent disease globally.[2] Although traditional therapies performed by clinicians are effective for a large proportion of patients, these measures come at a cost, with 20% of out-of-pocket health expenditure coming from dental treatment.[3] This is largely due to a derisory ability to control the disease which is a direct result of our inadequate understanding of the underlying disease pathophysiology.

1.1.b. Clinical Diagnosis

While a consensus for diagnosis of specific periodontal diseases has been difficult to achieve due to the complexity of the disease,[4] the American Academy of Periodontology suggests that a diagnosis can be reached by a combination of clinical measurements. These measurements seek to identify the extent of inflammatory involvement by measuring probing depth, clinical attachment loss (CAL) and bleeding on probing (BOP) combined with the extent of alveolar bone loss which can be measured radiographically.[5] Probing depth is measured by inserting a periodontal probe into the gingival sulcus in

health or periodontal pocket in disease while applying light pressure. Probing depth measures the linear distance from the base of the sulcus or pocket to the gingival margin, where a measurement of < 4 mm is considered healthy. Clinical attachment loss measures the linear distance from the depth of the sulcus or pocket to the cementoenamel junction (CEJ), which may be more accurate as it eliminates variability in clinical crown size, accounting for differences in gingival recession and excess between patients. While extensive literature supports clinical attachment loss as the most important measurement in diagnosis of periodontal disease, this is commonly not measured clinically, and while inferior, probing depth is taken in its place.[6-7] Nevertheless, increases in these measures demonstrate that there has already been apical migration of the connective tissue attachment of the periodontal ligament, which connects the cementum of the tooth to bone. When the force of tension from the periodontal ligament onto the bone is lost, the bone remodels and there is a net loss of bone in the area,[8] which can be seen radiographically. In a complementary process, inflammatory mediators associated with periodontal lesions activate bone resorbing osteoclasts. This combination of events can lead to drastic levels of bone loss, which can involve the furcation, result in severe fremitus, or result in the ultimate extreme: tooth loss.

In addition to taking linear measurements to assess alveolar bone loss, soft tissues are assessed for bleeding. In an intact gingival sulcus of a healthy patient, junctional epithelium serves to protect the underlying connective tissue from exposure to the oral environment. Unlike other types of epithelium, junctional epithelium contains relatively few desmosomes and occasionally has gap junctions.[9] Inter-cellular spacing is also much higher even when compared to the adjacent sulcular or gingival epithelium. Lastly, while

the junctional epithelium has something that resembles a basement membrane, it is structurally unique, lacking several major components such as collagen IV and VII. Therefore, the normal physical barrier contained within most types of epithelium is not existent in the junctional epithelium.[10] Because of this, immune cells such as polymorphonuclear leukocytes (neutrophils), macrophages, lymphocytes and dendritic cells can continuously sample the environment and respond to an overwhelming insult. When the inflammatory cells are chronically activated, such as is seen in the presence of specific so-called “perio-pathogens” or in the presence of a large mass of plaque or calculus, the periodontal ligament collagen fibers detach from the root cementum of the tooth, resulting in transformation of the junctional epithelium to long junctional epithelium. At this point, the healthy gingival sulcus has fully transformed into a periodontal pocket, where overgrowth and leakiness of blood vessels is a common occurrence.[11] In the case that there is any bleeding at all, this is considered unhealthy and is recorded in the patient’s chart. Lastly, plaque index is a measure of the patient’s current plaque load, which has been established with little debate as the initial causative agent of periodontal disease. Overall, clinical measurements to diagnose periodontal disease aim to evaluate three main factors: oral hygiene, inflammation and bone loss.

According to the 1999 consensus report on periodontal classifications,[12] periodontal disease is classified based on whether it is chronic or aggressive, and again by whether it is generalized or localized.[13] Aggressive periodontitis presents in patients who are otherwise healthy, but exhibit rapid bone and attachment loss. This is thought to be attributed to an underlying genetic predisposition, as it is seen in families.[14] Although not universally present, patients generally have elevated levels of *A.a* in their biofilms, and

have a disproportionate immune response to the amount of plaque present with hyper-responsive macrophages.[15] In chronic periodontitis, the amount of bone and attachment loss directly correlates with the plaque load and subgingival calculus is commonly present. This form of disease can be associated with other systemic diseases and has a slow rate of progression, According to this classification system, both forms of disease can either be localized, where ≤ 30% of total sites are diseased, or generalized, where >30% of sites are diseased. While this classification system proved useful to clinicians and researchers for several years, it did not address the complexity and confounding variables within periodontal diseases, nor did it have a valid justification for differentiating between chronic and aggressive periodontal disease.

In 2018, a new international classification system for periodontal disease was developed following the 2017 World Workshop on the Classification of Periodontal and Peri-Implant Diseases and Conditions.[16] This current classification system groups chronic and aggressive periodontitis under one category of disease (periodontitis) and has only two additional disease classifications that can be considered periodontal disease: periodontitis as a direct manifestation of systemic disease, and necrotizing periodontitis. Within periodontitis, disease is further defined by stages I through IV, and grades A, B, and C. Stages increase based on severity, complexity and extent and distribution of disease, and grades increase based on both direct and indirect evidence of progression as well as risk factors. Necrotizing periodontal disease is periodontal disease where there is necrosis of the papilla, bleeding and pain and is classified into two categories based on the affected patient population: chronically, severely compromised patients and temporarily or moderately compromised patients. Periodontitis as a direct manifestation

of systemic disease is diagnosed by identification of a rare host immune modulating systemic disease. In the absence of a rare systemic disease or necrotizing lesion, where there is an interdental CAL at ≥ 2 non-adjacent teeth or CAL of ≥ 3mm at ≥2 teeth, the disease is considered periodontitis and should be staged and graded according to its characteristics. In addition to these three main forms of periodontal disease, additional separate diagnoses exist for periodontal abscesses as well as endo-periodontal lesions. In a periodontal abscess, there is localized accumulation of pus within the periodontal pocket. In endo-periodontal lesions, there is a pathologic communication between periodontal and pulpal tissues where either one causes the other or they occur simultaneously.[16] While the clinical diagnosis of aggressive periodontitis has been eliminated, the characteristic presentation can be alternatively described as Stage III.C with a molar incisor pattern.[16] Periodontal disease classification has undergone many changes over the years and will continue to evolve as more information is discovered.

1.1.c. Pathogenesis: Introduction

The specific pathway that leads to initiation and progression of periodontal disease has been debated for decades. In the 1970s, several groups had committed to the "co-destructive factor" hypothesis,[17] suggesting that traumatic occlusion or other mild injuries adjacent to plaque and calculus was enough to initiate destruction of periodontal tissues.[18-19] By 1980, the critical importance of the exaggerated immune response in the etiology of periodontal destruction had been established. The co-destructive factor hypothesis was disproved; removing the source of trauma in the presence of inflammation had no effect on bone regeneration or connective tissue attachment, while resolution of inflammation in the presence of trauma produced this effect.[20-23] These data suggested there was rather

a “continuous disease” hypothesis, where the disease would progress continuously until intervention or tooth loss. Unfortunately, inflammation is a very complex process, and the periodontium is a very complex site, and newer studies were suggesting that periodontal disease was a dynamic, multi-factorial process that wasn’t continuous or predictable.[24-25] In 1984, Socransky et. al suggested a systemic factor for the progression of periodontal disease for the first time, pointing to a correlation of periodontally destructive events with specific life events such as pregnancy. This breakthrough study also fed into the conversation regarding different forms of periodontal disease, and the importance in distinguishing between them for accuracy of further research.[26]

What has remained constant over the years is the importance of plaque and calculus for the initiation of periodontal disease. The development of calculus generally progresses through three distinct phases: pellicle formation, plaque development and calcification. The pellicle is a thin biofilm layer of mainly protein that forms on teeth naturally throughout the day. Plaque on the other hand, is a microenvironment that contains living microorganisms such as bacteria, viruses and fungi as well as an extracellular matrix of salivary proteins and food particles.[27] This microenvironment has the potential to undergo specific changes which confer benefits to the survival of more pathogenic bacteria.[28] For periodontal disease, potential for true detriment depends primarily on the third stage, calcification. Calcium salts from saliva and dietary sources can incorporate into the intricate plaque lattice and form a mineralized and tightly adhered mass to the tooth structure. This allows for adherence of new biofilm upon its surface, leading to a host tissue response in the form of immune activation as well as detachment from the tooth to move away from the growing mass.[27] Additionally, calculus can bar off

viable microbial environments from things that might otherwise keep them at bay.[29] Calculus is tightly adhered to the tooth structure, requiring professional removal by clinicians using either scalers or ultrasonic cleaners. Because of this well-defined progression of events centered on biofilms, it is of critical importance to educate patients on at home and in office oral hygiene measures. The use of soft-bristled toothbrushes, floss and regular dental visits may have the potential to prevent most cases of periodontal disease.

1.1.d. Pathogenesis: Inflammation

Unfortunately for some patients, the discussion of prevention is too little too late, and calculus has been present long enough to elicit an immune response. The human body has two main pathways by which it fights off damaging insults: innate and adaptive immunity. Innate immunity innate immune cells such as macrophages and neutrophils detect evolutionarily conserved molecular patterns shared by all pathogens and mount a non-specific immune response.[30] On the other hand, adaptive immune cells such as T and B lymphocytes have receptors specific to a single pathogen and mount a memory-based immune response.[30] Periodontal disease develops through activation of both innate and adaptive immunity. The focus of this dissertation is on the innate immune response, and more specifically on macrophages, which have the capability to phagocytose pathogens process their antigens and signal to other immune cells through antigen presentation as well as secretion of cytokines and chemokines.[30] When calculus is present on the surface of the tooth, macrophages that continually sample their environment commonly find danger associated molecular patterns (DAMPs) that are secreted by damaged or dying vascular and epithelial cells.[31-32] On the other hand, the pathogenic gram-negative

bacteria housed by the calculus mass have lipopolysaccharide (LPS) on their cell surface which is made pathogenic by the carbohydrate or O-antigen portion of its structure. LPS can act as a pathogen associated molecular pattern (PAMP) and directly activate macrophages through binding to a specific pattern recognition receptor (PRR) on their cell surface. These receptors are called Toll-like receptors (TLR) and of the 11 classes found in humans, TLR-4 is specifically activated by periopathogenic LPS.

Activation of these TLRs results in signaling through the cell in a well-studied inflammatory cascade. This signaling ultimately results in activation of nuclear factor kappa beta (NF-κB), a transcription factor responsible for creation of inflammatory cytokines such as IL-1β, IL-6 and TNF-α. First, TLR-4 activation is initiated through homodimerization following complex assembly with LPS, CD14 as a co-receptor, MD-2 as an adapter, and LPS-binding protein as a cofactor.[33] Following successful binding of LPS, TLR-4 signals to either myeloid differentiation factor 88 (MyD88) or toll/interferon receptor domain containing adapter-inducing interferon B (TRIF) and these are named the MyD88 dependent and independent pathways, respectively.[34] In the MyD88 dependent pathway, another split in the pathway occurs where either IκB kinase (IKK) activates NF-κb or mitogen-activated protein kinases (MAPKs) activate activating protein 1 (AP-1). Both NF-κb and AP-1 are transcription factors that produce IL-6, IL-1b and TNF-a. In the MyD88 independent pathway, IFN-β is produced through activation of Interferon Regulatory Factor-3 (IRF-3) via TRAF-family-member-associated NF-κB activator

(TANK)-binding kinase 1 and IKKs.[35] Several of these cytokines can reliably be found in the gingival crevicular fluid of periodontally diseased hosts,[36] and the use of these cytokines as a biomarker has been under investigation for several decades.[37] These pro-

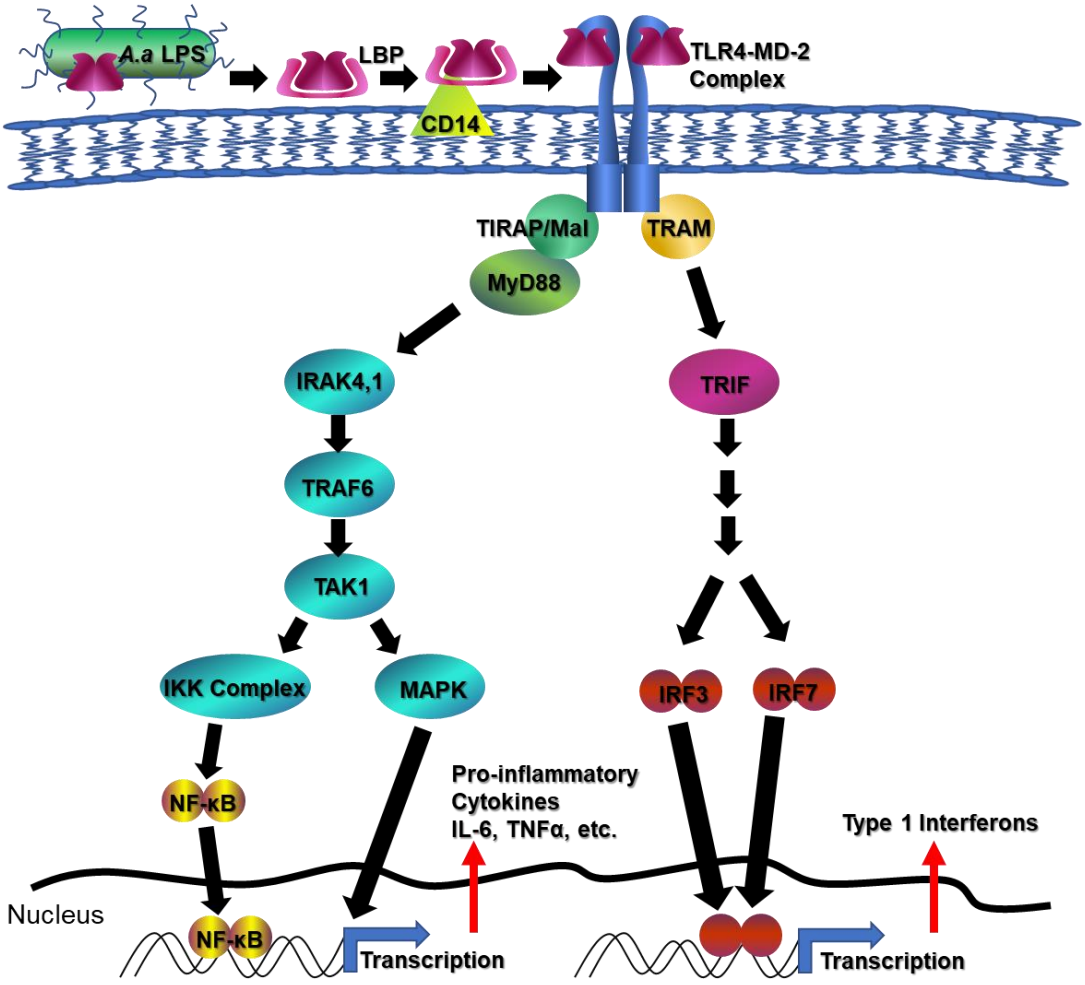

Figure 1.1. Inflammatory cascade initiated by bacterial lipopolysaccharide resulting in production of pro-inflammatory cytokines.

inflammatory cytokines initiate signaling cascades to attempt to re-establish periodontal homeostasis.[38] Unfortunately, calculus is a fortified mass that is largely impenetrable by these forces while the host tissues, on the other hand, are highly susceptible to damage. In a perfect world, the immune response would be able to clear the calculus and spare

the host of any damage. In reality, the opposite happens: host tissues suffer while the calculus and bacteria it houses thrive even more. (**Figure 1.1**)

Interestingly, macrophages play a dual role in periodontal disease depending on how polarized they are towards inflammation or resolution. Classically activated or M1 macrophages can secrete pro-inflammatory cytokines to recruit additional immune cells to the site. These macrophages are activated by exposure to lipopolysaccharide or IFN-γ. On the other hand, pro-resolving macrophages or M2 macrophages have more anti-inflammatory capabilities.[39] M2 macrophages can be further broken down into M2a, M2b, or M2c depending on their specific activating factors.[40] In periodontal disease, there is an imbalance in the M1/M2 ratio, where M1 macrophages predominate for the purpose of clearing microbes. This imbalance leads to tissue destruction characteristic of periodontal disease.[41] Many studies have been conducted to understand the dynamics that govern polarization of macrophages towards one subset or another, as tight control of these processes could prove useful therapeutically. For example, KDM4D knockdown in fibroblasts results in IL-12 gene repression.[42] IL-12 is associated with M1/Th1 immunity, as opposed to IL-10 which would drive the immune system towards M2/Th2 immunity.[43] Additionally, JMJD3 has been shown to be induced by LPS stimulation in macrophages.[44] This epigenetic enzyme demethylates H3K27me3 to H3K27me and its activity is critical for macrophage polarization into the M2 or anti-inflammatory state.[45] The KDM4B/KDM1A axis is likely involved in this process heavily, as previous literature has shown that inhibition of the KDM4 family induces apoptosis in M1 macrophages and conversely introduction of a KDM1A inhibitor promotes expression of M1 markers and decreases M2 markers.[46-47]

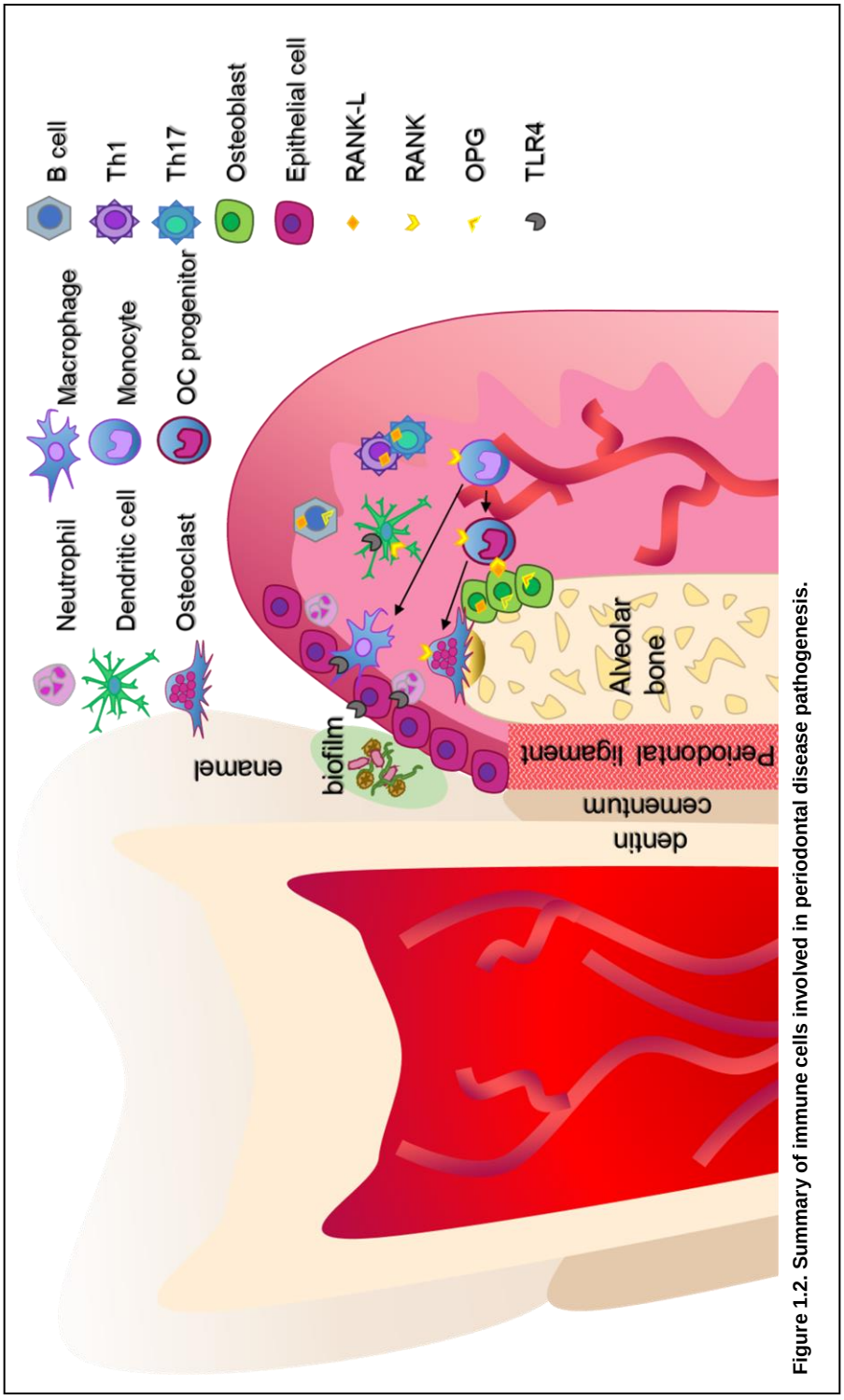

Figure 1.2. Summary of immune cells involved in periodontal disease pathogenesis.

In addition to macrophages, there are several other important immune cells that play a key role in progression of periodontal disease. (**Figure 1.2**) Although it is impossible to detail every cell involved in addition to all of their diverse functions, a brief overview will be provided. Gingival epithelial cells are a primary barrier to bacterial invasion as they line the connective tissue where periodontal inflammatory destruction is initiated and therefore

provide a mechanical barrier. Neutrophils, also known as polymorphonuclear cells or PMNs, are a hallmark of acute inflammation.[48] They are recruited by IL-8, which is secreted by junctional epithelial cells following injury.[49] Neutrophils secrete granules that are generally protective but when aberrantly released can cause tissue and extracellular matrix damage. Additionally, neutrophils are short lived and the accumulation of dead cells in the periodontal tissues leads to additional tissue damage.[50] Dendritic cells (DCs) are professional antigen presenting cells that survey their environment and have the most potent T cell activating function of all cells in the body.[51] Thus, DCs are a major connecting point between innate and adaptive immunity and have been shown to affect periodontal disease pathogenesis positively and negatively.[52] In fact, dendritic cells can differentiate into bone-resorbing osteoclasts, causing bone loss directly.[53] Additionally, adaptive immunity plays a role in periodontal disease pathogenesis. CD4+ T cells, also known as T helper cells, play a central role in immunity and have several subsets. For example, Th1 and Th17 cells are pro-inflammatory and are directed toward intracellular pathogens and bacteria, respectively.[54] Both of these cell types are positively correlated with chronic periodontitis in humans,[55] and inhibition of differentiation of either cell type confers protection from destruction.[56-57] Th17 cells are upregulated in response to microbial dysbiosis[56] as well as mechanical damage,[55] both of which have been thought to contribute to pathogenesis of PD. B cells, which produce antibodies, are another adaptive immune cell type involved in PD pathogenesis. While B cells produce antibodies to bacterial antigens, they are also able to promote destruction of host tissues through production of anti-self antibodies.[58] In fact, B cell deficient mice do not develop bone loss following bacterial infection, suggesting a pathologic role of these cells likely through stimulation of osteoclasts and other immune cells.[59] While many other immune cells play

a role such as natural killer cells,[60] endothelial cells,[61] fibroblasts,[62] myeloid derived suppressor cells[63] and more, it is increasingly clear that pathogenesis of periodontal disease is a complex process that is difficult to accurately model by using a single cell type and this will continue to challenge the field for some time.

1.1.e. Pathogenesis: Bacteria

In 1998 Socransky et. al. proposed that there are five main complexes of bacterial species that colonize periodontally diseased sites.[64] This study implicated the "red complex" of bacteria as being highly correlated to deep pocket depths and bleeding on probing.[64] These pathogens include: *Porphyromonas gingivalis, Treponema denticola, and Tannerella forsythia*.[64] More recently, Hajishengallis et. al. proposed the "keystone pathogen hypothesis" which suggests that single, lowly abundant microorganisms lead to a dysbiotic periodontal microenvironment.[65] This study suggested that *Porphyromonas gingivalis* was a keystone pathogen that if targeted individually, could result in resolution of inflammatory periodontal damage by stabilizing the dysbiotic microbial community.[65] More recently it was discovered that this model was oversimplified, and periodontal disease was dependent on a complex process leading to dysbiosis and altered overall subgingival flora rather than the mere presence of one or more specific periopathogens.[66] This model, termed the polymicrobial synergy and dysbiosis (PSD) model, considers that the polymicrobial biofilm is interdependent and pathogenic as a system rather than singly dependent on a keystone or red complex pathogen.[66] Further studies have identified individual species related to specific disease subsets, such as *Aggregatibacter actinomycetemcomitans (A.a)*, which has been uniquely associated with aggressive and highly destructive forms of PD.[67] While we have not yet been able to successfully use

the presence of specific pathogens as a screening device for progressive versus non-progressive lesions or for classification of periodontal diseases,[15] we have used this information to enhance our understanding of the biologic mechanisms at play and augment our *in vitro* and *in vivo* experimental models by using the bacteria that are most commonly associated with the disease to better replicate the disease process.

1.1.f. Pathogenesis: Bone Loss

A critical hallmark of periodontal damage is alveolar bone loss. Bone resorption is mediated by osteoclasts (OCs), while bone formation is mediated by osteoblasts (OBs). Under normal homeostatic balance, OBs and OCs constantly signal to each other to maintain a constant level of bone turnover. More specifically, osteoblasts produce receptor activator of nuclear factor kappa b ligand (RANK-L), which is a critical activator of osteoclasts. On the other hand, osteoblasts also secrete osteoprotegerin (OPG), which can inhibit the RANK-L signal by irreversibly binding to its receptor.[68] In periodontal disease, there is imbalance in this process, and a net catabolic effect occurs by an increased osteoclast to osteoblast activity ratio.[69] In fact, osteoclast formation can be induced by pro-inflammatory cytokines secreted by both innate and adaptive immune cells, such as TNF-α and lL-1.[70] These same cytokines have been shown to deactivate osteoblasts, directly linking inflammation to the osteoblast-osteoclast activity ratio.[69] Additionally, macrophage colony stimulating factor (M-CSF) is a pro-inflammatory cytokine critical for the activation of both macrophages and osteoclasts,[71-72] that is secreted primarily by osteoblasts in response to pro-inflammatory signals.[73] This results in an iterative cascade of macrophage and osteoclast activation which eventually results

in inflammatory-driven bone loss. Thus, in hyper-inflammatory conditions, osteoclast actions are heightened more than osteoblast actions, resulting in a net loss of bone. (**Figure 2**)

1.1.h. Treatment Modalities

Current and traditional therapy to treat periodontal disease includes scaling and root planing (SRP).[74] Scaling involves mechanical debridement of plaque biofilms and calculus from clinical crowns using scalers, and root planing requires access to the root surfaces using surgical and non-surgical measures for the same purpose.[75] This treatment has undergone continual refinement to involve an extensive array of instruments including ultrasonic scalers, which use ultrasonic energy to assist in removal of biofilms,[76] although the foundational technique and principles have not changed since its conception. The basic concept is that by disrupting plaque biofilms, the host immune system will discontinue its attack on this altered environment and the tissue inflammation and subsequent cellular damage will stop. Unfortunately, complete removal of the entirety of the plaque by clinicians is highly unlikely,[77] and nevertheless there are some patients who recur after therapy[76]. In fact, in aggressive periodontitis (currently referred to as stage III.C periodontitis), clinical attachment loss occurs in patients with a very limited plaque load.[78] Due to the limited ability of SRP to completely heal the entire periodontally diseased population, several adjunctive therapeutics have been developed over the years.

Initially, extensive research was conducted testing the use of systemic antimicrobial therapy for treatment of periodontal disease. Over the years, several antibiotics have been tested for treatment of PD, such as penicillin, augmentin,

clindamycin, amoxicillin, metronidazole, tetracycline, doxycycline, minocycline, azithromycin and more.[79-83] Considering that antibiotic overuse has led to a widespread issue with antimicrobial resistance,[84-85] the marginal benefits have limited the use of systemic antibiotic use to severe cases of disease.[86] Local antimicrobials have been shown to be less effective than systemic antimicrobials but nevertheless are still used clinically.[87] For example, PerioChip® and Atridox® are both bioresorbable discs either loaded with chlorhexidine gluconate or doxycycline hyclate, respectively.[88] Arestin® is minocycline hydrochloride loaded in extended release nanoparticles.[89], Periogard® is a chlorhexidine mouth rinse formulation.[90] Unfortunately, clinically relevant improvements are not generally produced by using these drugs, and they still carry unwanted side effects.[91] Because of these factors, local antimicrobials are not currently considered standard of care treatment, although they are commonly implemented as a last resort for desperate and severe cases.[92]

Because the host immune response is the source of tissue destruction in periodontal disease, extensive research has been conducted toward targeting the host immune response. Several groups have demonstrated that non-steroidal anti-inflammatory drugs (NSAIDs) are efficacious in reducing periodontal destruction. For example, indomethacin and flurbiprofen have been shown effective in reducing periodontal destruction when given systemically in animals.[93] Interestingly, even topical application of an NSAID can reduce the destructive effects of periodontal disease.[94] Unfortunately, some of these effects were marginally significant, and when taken into clinical trials, were unable to produce statistically significant increases in clinical attachment or bone regeneration.[95] While NSAIDS are an obvious choice considering significantly more prostaglandins have been found in the gingival crevicular fluid of more

aggressive and destructive periodontal diseases,[96] many cell types are at play and play a contributing role in the pathogenesis of the disease that are not directly involved in the COX pathway. Additionally, NSAIDs have consistent side effects and chronic use is generally contraindicated to prevent damage.[97] Nevertheless, further exploration of treating periodontal disease with NSAIDs is ongoing and could produce exciting data in the future. Most recently, an innovative cyclic treatment schedule has been used, reducing bone loss and inflammation in a randomized controlled clinical trial.[98]

In addition to NSAIDs as host modulation therapy, many studies have suggested that inhibition of matrix metalloproteinases (MMPs) represent a promising therapeutic strategy for treating periodontal disease. MMPs are enzymes mainly secreted by fibroblasts that are responsible for maintenance of tissues through breakdown of extracellular matrix components.[99] There are 23 different MMPs, all of which are endogenously inhibited by tissue inhibitors of MMPs (TIMPs).[100] MMP-2, -8, -9 and -13 are commonly studied with respect to periodontal disease because they are increased in either the gingival crevicular fluid or gingival tissues of periodontally diseased individuals.[99] In periodontal disease, the MMP/TIMP ratio is increased resulting in a net breakdown of tissues.[101] Although doxycycline was originally designed as a semi-synthetic tetracycline, at sub-antimicrobial doses this compound has been shown to inhibit matrix metalloproteinases -8 and -13, and therefore has been marketed for treatment of periodontal disease as a host modulation therapy under the trade name Periostat®.[102] Minocycline is another tetracycline analogue[103] that has been evaluated as an MMP inhibitor in several diseases such as multiple sclerosis, vascular neurological disorders as well as periodontal disease.[104] Small molecule MMP inhibitors have also been developed, such as batimastat, marimastat, prinomastat and rebimastat.[105] Lastly,

monoclonal antibodies to MMPs have been developed and are currently being evaluated for treatment of tumor metastases.[106-107] These antibodies will likely be evaluated for host modulation therapy for periodontal disease in the near future.

Bisphosphonates (BPs) present an additional potential therapeutic class that could help mediate periodontal health in the over-inflamed host. BPs are pyrophosphate analogues that adsorb selectively to hydroxyapatite surfaces in bone and prevent breakdown of bone tissue through multiple independent mechanisms.[108] In short, BPs inhibit osteoclast function and recruitment, leading to a reduction in alveolar bone loss.[109] Thus, these compounds have been implicated in diseases where bone loss is a clinical issue such as osteoporosis,[110] osteogenesis imperfecta[111] and periodontal disease.[112] Bisphosphonates have even been shown to exhibit anti-tumor activity through decreasing production of VEGF, inhibiting cellular proliferation and causing cell cycle arrest.[113] Unfortunately, osteonecrosis of the jaw (ONJ) is a common adverse outcome associated with bisphosphonate use. First described in 2003,[114] bisphosphonate related osteonecrosis of the jaw (BRONJ) is an area of uncovered bone persisting for at least 8 weeks in the maxillary and mandibular bones. The pathophysiology of the disease is poorly understood but several theories have been proposed[115] including avascular necrosis, drug toxicity, reduced bone turnover due to compromised osteoclast-osteoblast interactions as well as inflammation such as is seen in periodontal disease.[116] More recently, ONJ has been linked to the usage of anti-resorptive medications other than just bisphosphonates and thus has been renamed medication related osteonecrosis of the jaw (MRONJ).[117] Second to BPs, ONJ is commonly seen in patients taking denosumab, a monoclonal antibody targeting RANK-L.[118] While several additional medications have also been shown to correlate with ONJ incidence,[119] periodontal disease has been

correlated with disease development.[120-122] Considering these facts, the potential use of an anti-resorptive medications to treat periodontal bone loss has been employed with extreme caution.

Based on the data presented above, there is an urgent need for development of novel treatment strategies for periodontal disease. The ideal agent would be a small molecule that could be applied topically, would interrupt the pathways that activate the inflammatory response, and prevent bone loss. This dissertation will describe our attempts to develop such an agent through structure-based design and structural optimization of potential lead compounds.

1.2. Epigenetics

1.2.a. Introduction

The term epigenetics refers to reversible and heritable changes in the expression of DNA that do not involve changes in the primary DNA sequence. Over the last decade, there has been a dramatic increase in the study of epigenetic control mechanisms that play a role in the development of cancer and other diseases. The first epigenetic targeting therapeutic was technically FDA approved in 1968, but the fact that this drug, 5-azacytidine, acted through an epigenetic mechanism was only discovered in 2004.[123] In that same year, the first reversible histone demethylase enzyme, KDM1A, was discovered.[124] Since then, a plethora of additional epigenetic modifying enzymes have been discovered, and various epigenetic mechanisms have been targeted for treatment of various diseases.

Epigenetics contrasts with genetics, the study of inherited DNA alterations, because epigenetic modification does not alter the DNA but rather alters the differential

expression of specific genes. Epigenetic changes are generally initiated in response to internal and external stimuli, and these processes are mediated through several different mechanisms within a cell. There are two basic mechanisms for the epigenetic control of gene expression: methylation of DNA at CpG islands in promoter regions of DNA and post-translational modification of histone proteins. The focus of this dissertation is on histone methylation/demethylation, specifically the demethylation activity of KDM4B and to a lesser extent KDM1A. This section will explore the general concepts of epigenetics, the mechanism of KDM4Bs enzymatic activity, some of the effects of that activity and finally how and why KDM4B has been targeted for drug development.

1.2.b. Histone Modifications

DNA is organized into tightly wound chromatin so that it can fit into the nucleus of a cell. Chromatin can either be relaxed euchromatin or condensed heterochromatin, depending on how tightly DNA is bound around nucleosomes, and this alters the accessibility of transcriptional machinery for purposes of replicating and expressing these genes. Nucleosomes consist of histones H1, H2A, H2B, H3 and H4, each of which has amino-terminal tails that are accessible for modification. (**Figure 1.3**) Histone methylation and acetylation are widely studied, while phosphorylation, ubiquitination, sumoylation and citrullination of histone tails have been less well characterized. These groups are generally transferred to very specific histone tails by “writers” and to be removed require an entirely separate set of very specific enzymes called “erasers”. For example, histone methyltransferase G9a is a writer capable of specifically transferring methyl groups to histone 3 lysine 9 (H3K9) and is only active in converting the mono-methylated form into the di- or tri-methylated form.[125] On the other hand, to remove these marks requires an

eraser: histone demethylase KDM4B. To add to the complexity, the specificity of these enzymes is not always overlapping, as KDM4B has additional activity on the trimethyl state of histone 3 lysine 36 (H3K36me3) non-concurrent with G9a's additional activity on H3K27. Once specific tails are modified, the modifications are read by yet another set of enzymes called readers, which are most commonly bromodomains. (**Figure 1.4**) In cancer and other diseases, DNA promoter hypermethylation in combination with abnormal histone modifications have been associated with the aberrant silencing of genes.[126-128] Epigenetic gene silencing, in combination with gene mutations, are critical mechanisms involved in the etiology and progression of virtually all cancers.[126] Aberrant regulation of these processes can lead to silencing of tumor suppressor genes important in the development of cancer, and thus multiple chromatin remodeling enzymes have been targeted for the discovery of novel antitumor agents.[129-131] More recently, dysregulated epigenetic modulation has been shown to be a factor in diseases other than cancer. The focus of this dissertation is the histone demethylase enzyme class and its relation to the immune response in periodontal disease. The histone demethylases can be further broken down into FAD dependent (KDM1) and independent enzymes (KDM2-6). The FAD-independent histone demethylases have a jumonji C domain responsible for their catalytic activity whereas the FAD-dependent use FAD as a cofactor and commonly form complexes to enhance their catalytic activity.[132]

1.2.c. KDM1A

The first discovered and most extensively studied FAD-dependent histone demethylase enzyme is KDM1A, also known as lysine-specific demethylase 1 (LSD1) The primary function of KDM1A is to remove methyl groups from the activating chromatin mark

histone 3 lysine 4 (H3K4). KDM1A is specific for the substrates monomethyl histone 3 lysine 4 (H3K4me) and dimethyl histone 3 lysine 4 (H3K4me2). H3K4 methylation states are generally correlated with active transcription, where higher methylation (trimethylation) is found on highly active genes.[133] KDM1A is also known to demethylate histone 3 lysine 9 (H3K9) when co-localized with the androgen receptor in prostate tumors,[134] and also has

non-histone protein substrates such as p53 and deoxynucleic acid methyltransferase 1 (Dnmt1).[135] A number of effective KDM1A inhibitors have been identified, and include tranylcypromine-based irreversible inhibitors such as GSK2879552[136] and ORY-1001,[137-139] oligoamines such as verlindamycin[140] and related isosteric ureas and thioureas,[141-142] reversible benzohydrazide inhibitors such as SP-2509,[139] reversible 1,2,4-triazoles,[143] and dithiocarbamate-urea hybrid KDM1A inactivators.[144] KDM1A is now regarded as an emerging drug target for diseases other than cancer, such as neurological disease,[145-146] blood disorders,[147-148] viral infection,[149] diabetes[150-151] and fibrosis.[152]. The primary process KDM1A controls is cell proliferation and cell cycle regulation, and thus it has primarily been studied as a regulator in cancer cell progression and growth. It is clear that while KDM1A has several important regulatory functions, the potential of targeting this enzyme for treating human disease is in its infancy, and as time progresses it is certain that there will be development of further uses of inhibiting KDM1A as well as more and more potent KDM1A inhibitors.

Relevant to the current discussion, KDM1A has more recently been linked to the host immune response. For example, KDM1A expression is reduced upon TLR activation and subsequent inflammation, leading to endotoxin shock.[153] In the absence of KDM1A,

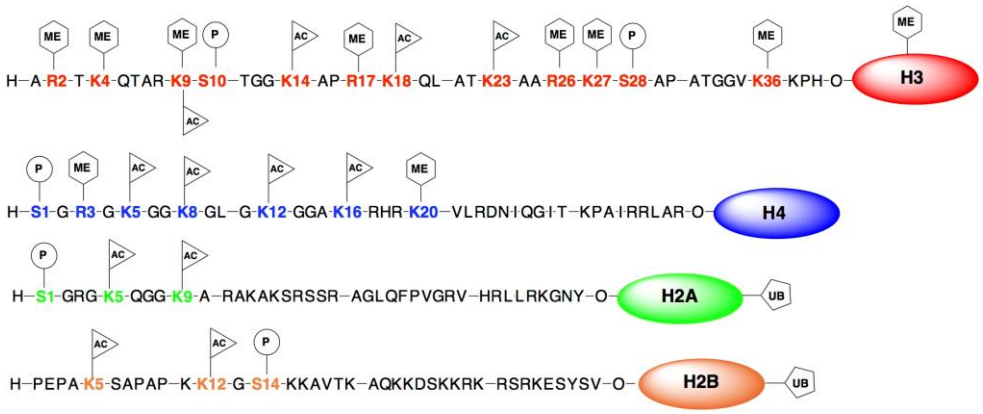

Figure 1.3. Modifiable sites on histones.

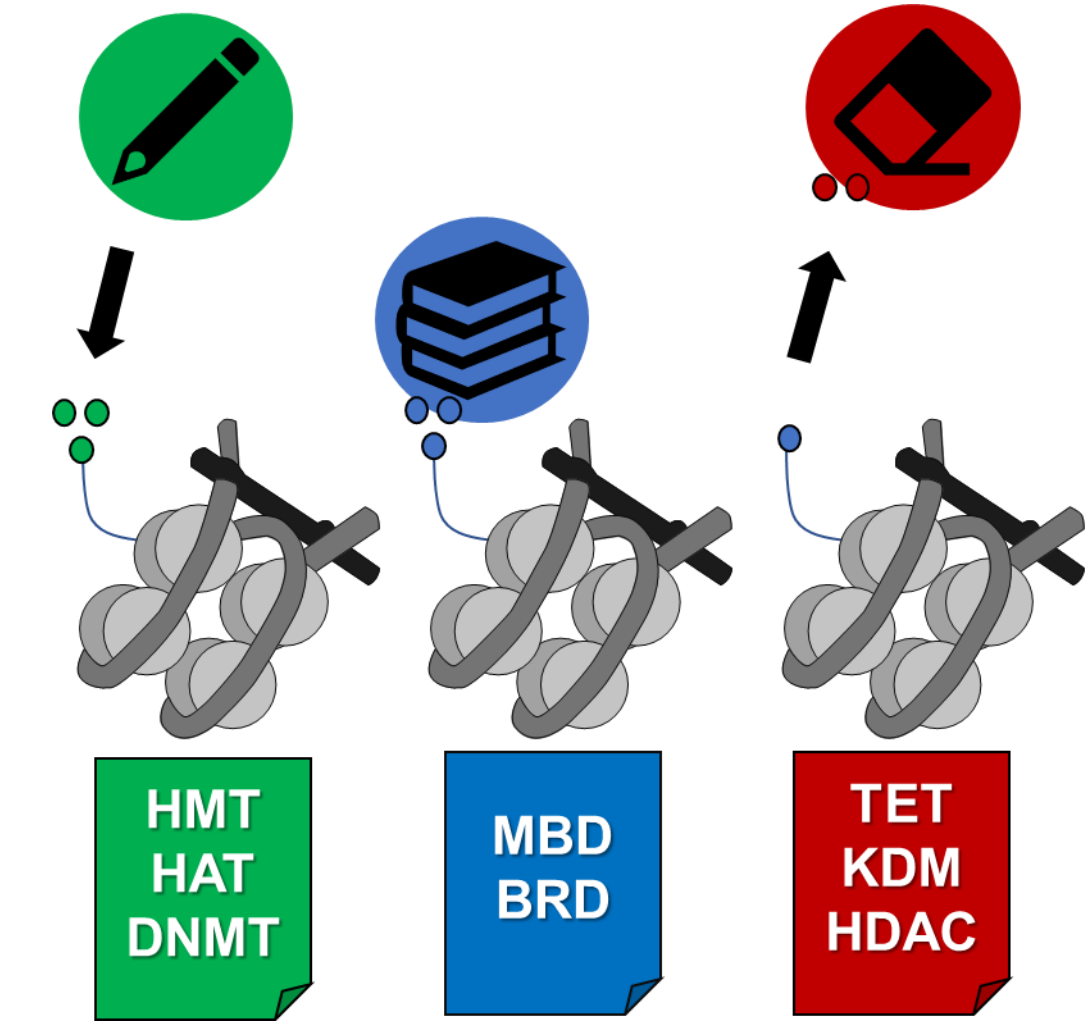

Figure 1.4. Writers, readers and erasers: some common examples and their main function.

hyperinflammation ensues causing host damage.[153] Also, KDM1A is critical for activation

of B cells, and when KDM1A is ablated in these cells, immune response genes are overactivated.[154] Agonizing histone demethylases is very difficult, and since the activity of KDM1A is correlated with immune suppression, we sought to determine a druggable target that would keep KDM1A active. More recently, Boulding et. Al showed that introduction of a KDM1A inhibitor promotes expression of M1 markers and decreases M2 markers.[46]

1.2.d. KDM4B: Introduction

The KDM4 family of epigenetic modifiers target the demethylation of histone 3 lysine 9 and 36, as well as histone1.4 lysine 26. Each member contains a jumonji C (jmjC) domain responsible for the demethylation activity, and uses Fe^{2+}, 2-oxoglutarate and O_2 for this activity.[155] (**Figure 1.5**) Only family members KDM4A-C contain double PHD and Tudor domains, and these differences are thought to attribute to the variable specificity between A-C compared to isozymes D-F. KDM4A-C have a 5-fold specificity for H3K9 over that of H3K36 and H1.4K26. KDM4B exhibits the lowest rate of demethylation within the family, for reasons that are not clear. KDM4D-F are half the size of other family members and are unable to demethylate H3K36.[156] As shown above, demethylation of histone lysines occurs through a well-defined mechanism that is conserved among enzyme superfamily. First, ferrous iron binds to the active site by coordinating with one aspartic/glutamic acid and two histidines as well as water. 2-oxoglutarate (2-OG) then binds displacing some water, followed by binding of the histone lysine which displaces the remaining water that is bound to iron. This activates iron to undergo an oxidative decarboxylation reaction, generating Fe(IV) and CO_2. Fe(IV) is then able to demethylate

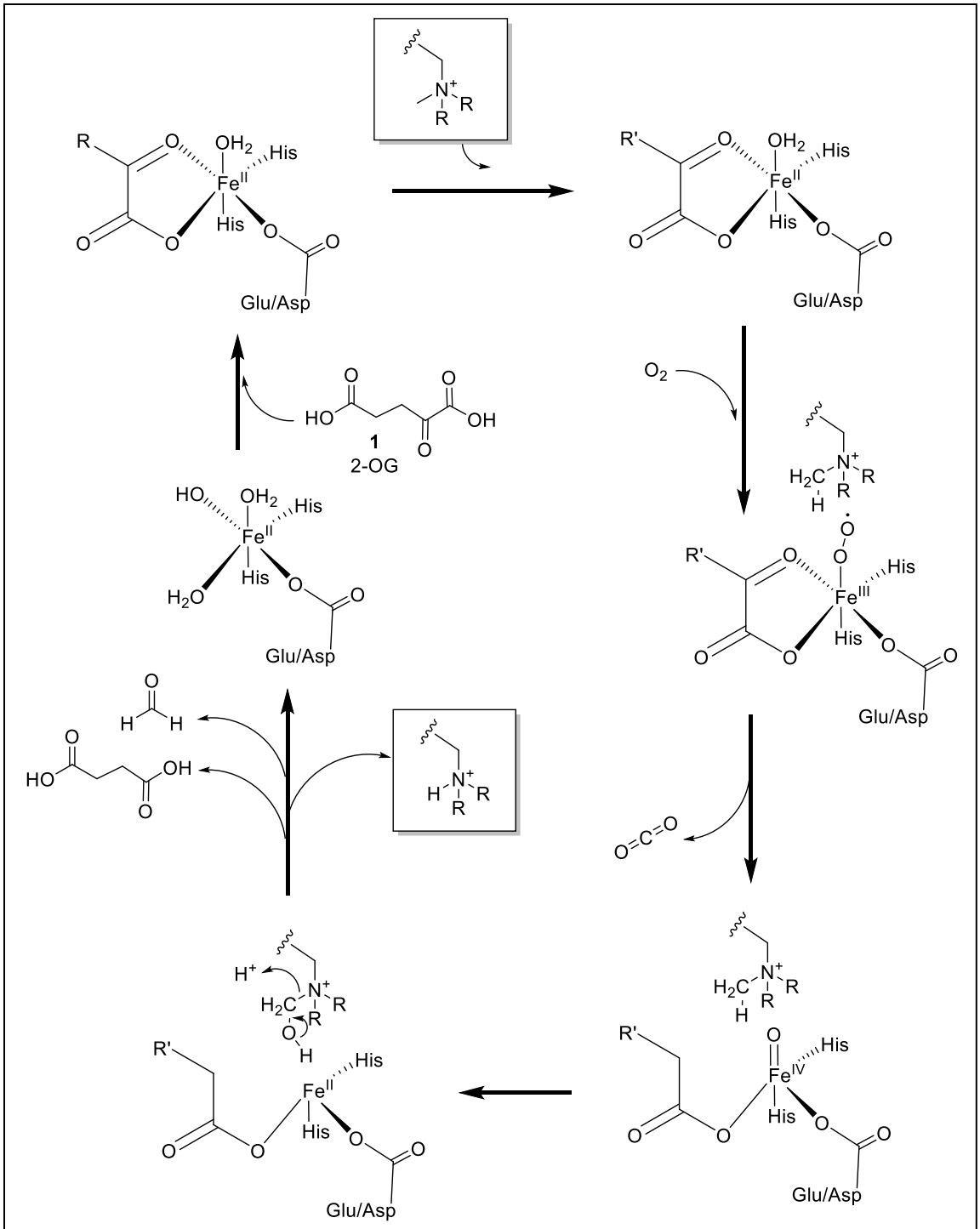

Figure 1.5. Mechanism of KDM4B-mediated demethylation.

the histone lysine, producing formaldehyde through a hemiaminal intermediate. The 2-OG

is converted to succinate through this process and once it is released, ferrous iron is regenerated, allowing for further demethylation.[132]

Trimethylation of H3K9 and H1.4K26 are classically thought to be repressive heterochromatin marks. This contrasts with H3K36 methylation which generally correlates with active expression.[156] The mechanisms underlying various histone methylation patterns and the enzymes involved in repressing or activating genes are yet to be understood, but there is substantial evidence supporting the idea that histone modifying enzymes exhibit crosstalk behavior, and also influence DNA methylation activity. Additionally, the activity of an epigenetic enzyme can have an influence on more than just histone lysines. These enzymes have been implicated in processes such as cytosolic and nuclear protein modifications, alternative splicing, as well as recruitment of other proteins for complex formation.

1.2.e. KDM4B: Immune Response

KDM4B and its primary substrate, histone 3 lysine 9 (H3K9), have been implicated in numerous immunological processes. For example, trimethylation at H3K9 has been shown to contribute to the repression of TLR4 expression.[157] In addition, TNFα transcription is repressed through H3K9 methylation during the process of endotoxin tolerance.[158] Also, H3K9me3 levels are decreased in macrophages through exposure to high glucose, accompanied by a simultaneous increase in inflammatory cytokine production.[159] H3K9me3 levels are also found to be increased in response to hypoxia, which downregulates mRNA expression of the chemokine Ccl2 and the chemokine receptors Ccr1 and Ccr5.[160] Additionally, decreased levels of H3K9me3 is associated with increased TLR4-mediated expression of pro-inflammatory cytokines through recruitment

of NF-κB p65 to their proximal promoters.[161] Dulal Das et al reports that KDM4B knockdown recruits repressive methylation marks to the promoters of IL-1β and IL-2 genes among others in neural stem cells.[162] IL-1β is an extremely important cytokine in the regulation of periodontal disease pathogenesis, and its transcription is prolonged by the bacterial challenge present in the plaque of diseased patients.[163] KDM4B has also been shown to promote osteogenic over adipogenic differentiation of mesenchymal stem cells.[164] *Helicobacter pylori* is the major etiological factor for development of gastric cancer, and a recent study found that *H. pylori* induces KDM4B overexpression in gastric tissues. The chronic inflammation seen in these tissues that leads from gastritis to gastric cancer is through NF-κB and COX-2, and this action is directly dependent on KDM4B demethylation activity.[165] Although this data supports the idea that KDM4B activity is correlated to hyper-inflammation, further studies are needed to fully define the immunomodulatory mechanism of KDM4B in the context of periodontal disease.

The KDM4 family is said to be able to demethylate H3K23me3, an underexplored chromatin mark. This allows for H3K36 demethylation activity to occur, which is an important epigenetic control point for meiosis and spermatogenesis. In relation to immunity, H3K36me2 expression results in expression of genes that promote plasma cell transformation.[166] H3K36 methylation has also been associated with macrophage polarization, and increased methylation at this mark results in suppressed production of IL-6 and TNF-α by macrophages.[167]

In addition to the traditional epigenetic mechanisms at play, KDM4B may functionally be linked to the immune response through immunometabolism. KDM4B is a target for hypoxia inducible factor 1 alpha (HIF-1α) in response to hypoxia.[168] HIF-1α-

dependent transcription is induced upon lipopolysaccharide pro-inflammatory stimulus and results in an increased glycolytic metabolic program in macrophages.[169] The M1 macrophage is a major immune cell responsible for inflammation. The expression of isocitrate dehydrogenase is decreased 7-fold in M1 macrophages compared to M0 macrophages.[170] This is the enzyme that converts citrate to alpha ketoglutarate (α-KG, also known as 2-oxoglutarate, 2-OG), which is a cofactor for KDM4 family of enzymes. In addition, α-KG is a source of glutamine and glutamate, and therefore plays a role in immunity through increases in immune cells and their respective activity.[171] If less α-KG is available to contribute to these protective immune responses secondary to depletion by KDM4, it can be said that KDM4 contributes to the loss of the protective immune response provided by glutamine and glutamate through competition for α-KG.

1.2.f. KDM4B: Drug Discovery

The focus of epigenetic-based drug discovery research has been mainly directed towards histone deacetylases (HDACs) in the treatment of various cancers. More recently, the KDM4 family of epigenetic modifying enzymes have been found to be linked to positive regulation of many immunological processes, and therefore serve as an interesting target for development of hyperinflammatory or autoimmune disorders. Unfortunately, drug development in the realm of immunity has not been initiated, though development of KDM4 inhibitors for treatment of prostate and breast cancer continue to progress. The first series of inhibitors of the KDM4 family were based on 2-oxoglutarate (2-OG) **1** because of it's critical role in the catalytic activity of the enzyme. N-oxalylglycine (NOG) **2** and 2-4-pyridine dicarboxylic acid (2-4-PDCA) **3** have been shown to inhibit various KDM4 family members by chelating iron, but are not selective and target many additionally related and

unrelated enzymes.[172] JIB-04 **4** was the first KDM4 inhibitor that was not a 2-OG competitive inhibitor, and although it is a pan JmjC KDM inhibitor, it has no activity toward KDM1A or other epigenetic enzymes, proving useful for mechanistic studies.[173] More recently, the 8-hydroxyquinoline (8-HQ) scaffold was identified as a hit through high-throughput screening.[174] These studies identified IOX1 **5** as a potent KDM4 inhibitor but this drug has poor cell permeability and has to be used as a prodrug methyl ester.[175] Based on this scaffold, several groups developed successful drugs, including the NIH Molecular Libraries program, which developed an extremely potent inhibitor, ML324 **6**.[176] Selective targeting of specific KDM4 family enzymes has yet to be successful, and the structure activity relationships that govern selective binding are yet to be understood. Additional analogues of ML324 were developed that have variable selectivity within the KDM4 family.[177] Other groups have identified additional compounds able to inhibit the KDM4 family such as NSC636819 **7**, a dinitrobenzene,[178] circuminoids,[179] pyridinyl thiazoles[180] and others, highlighting the diversity in available inhibitors and consequently the infancy in which KDM4 drug discovery exists. Studies describing development of KDM4 inhibitors rarely test the compounds for all of the KDM4 family members, and none have evaluated their inhibitors in both male and female samples, despite the association of these enzymes with sex-specific hormonal signaling pathways.[181-182] (**Figure 1.5**)

1.2.g. Epigenetic Coordination Mechanisms

As new epigenetic enzymes are discovered that possess different targets for regulating cellular processes, finding a definition of the epigenetic landscape, which encompasses all chromatin remodeling processes as well as crosstalk between epigenetic enzymes and marks, will be attempted. It has been known for some time that epigenetic enzymes themselves can be epigenetically modified, which suggests a checks and balance system or a compensatory mechanism by which our cells can maintain homeostasis. On the other hand, when epigenetically-controlled cellular processes are dysregulated to a degree that is beyond repair, small molecule therapeutics may be indicated to revert cells into a homeostatic state. Uncovering the entirety of this landscape will allow for understanding of how the histone modification system within our cells is responsible for making the changes necessary to drive an undifferentiated stem cell into a fully differentiated state.

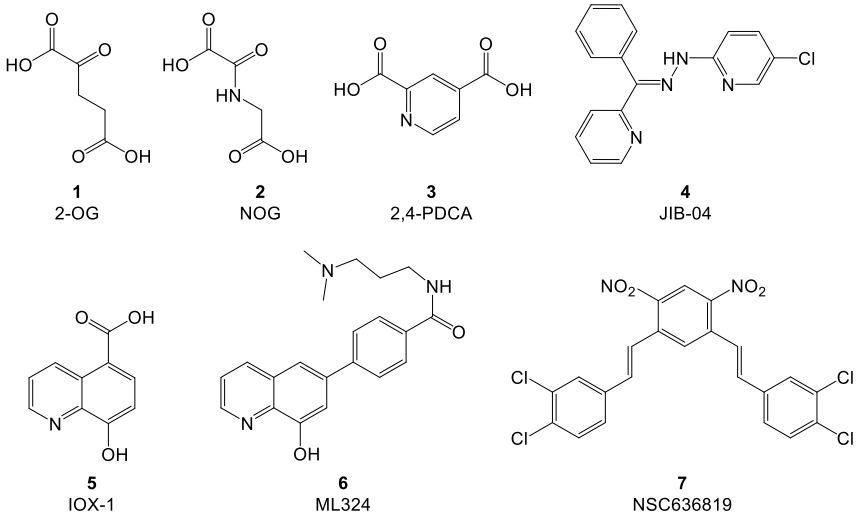

Figure 1.6. Compounds known to interact with KDM4B. Compounds **1-3** are previously published KDM4B inhibitors. Compound **4** is a KDM1A inhibitor.

Histone demethylase enzymes conserved among diverse species, but these enzymes are commonly redundant, sharing substrate specificity among different classes and families, as well as coordinated in their activity. For example, the demethylation activity of KDM1A on H3K4 leads to repression of pro-inflammatory cytokine gene

transcription.[183] Interestingly, previous data has shown that cross talk between KDM4B and KDM1A enzymes leads to a balanced system wherein lysine 9 methylation serves as

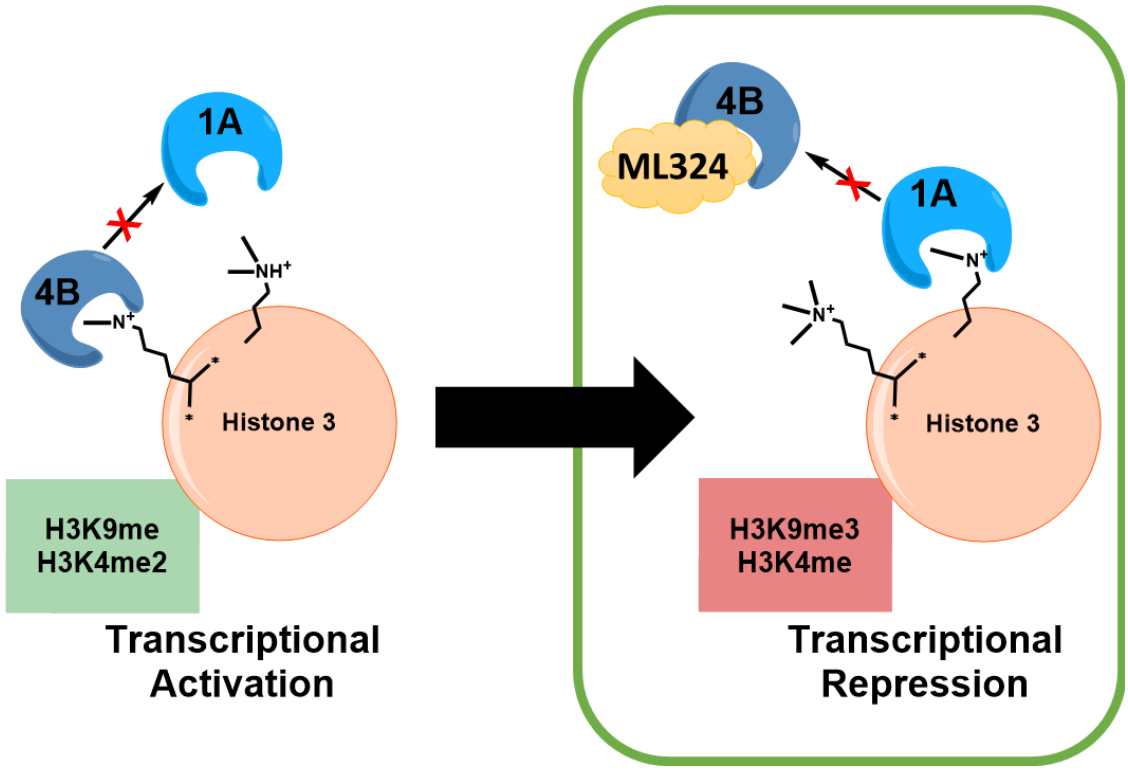

Figure 1.7. Proposed KDM4B-mediated immunomodulation mechanism. Coordination between KDM1A and KDM4B results in compensation between the two to ensure either active or repressed transcription.

a prerequisite to lysine 4 demethylation by KDM1A.[184] In other words, when KDM4B is active at the H3K9me3 mark, KDM1A cannot be concurrently active at H3K4me2, and vice versa.[184] KDM4B is then a positive regulator of the pro- inflammatory cytokine response through an indirect mechanism by inhibiting KDM1A. The link between these two histone marks is coupled to H3K9Ac levels, as has been additionally demonstrated in human CD4+ T cells. In this situation, T cell receptor stimulation induces pathologic FasL production proportional to the amount of H3K9 demethylation, H3K9 acetylation and H3K4 methylation.[185] Therefore, we are able to use coordination between mutually exclusive histone demethylases to antagonize one and indirectly agonize another.

1.3. Sex Differences

It is well known that sex plays a key role in the acquisition and progression of immune diseases. More specifically for periodontal disease, 56% of men have the disease compared to only 38% of females. Furthermore, 16.5% of male patients manifest with severe disease compared to 7.6% of females.[186] In general, females are thought to have superior functioning immune systems with responses more appropriate to clear the antigens and cause no further damage. For example, males are known to produce more damaging TNF-α in response to LPS, while females are known to be more efficient at antigen presentation. Additionally, circulating sex hormones may influence immune signaling, as there are estrogen and androgen response elements on the promoters of many acute inflammatory genes. Testosterone is generally immunosuppressive and is found in higher amounts in post-pubertal males than females. On the other hand, estrogen has an immune activating effect, increasing production of IL-1, IL-6 and TNF-α by macrophages.[187]

KDM4B regulates sex hormone signaling events. Current literature suggests that KDM4B can modulate cell signaling during androgen receptor (AR) mediated cancer growth and suppression, suggesting that KDM4B inhibition affects androgen receptor signaling leading to cancer cell death. More specifically, Coffey et al concluded that AR is depleted in response to KDM4B knockdown, and in turn KDM4B is required for the transcriptional activity of AR.[188] Additionally, while KDM1A is overexpressed in breast cancer and its activity upregulates ER transcription,[189] KDM4B has been identified as an estrogen receptor co-regulator and its inhibition limits breast cancer growth via GATA-3 co-activation.[190] KDM4B is also required for mammary gland development as well as

estrogen dependent cell proliferation and growth.[191] Despite these facts, ongoing research does not address the differential effects of sex on KDM4B signaling and immune processing. Wang et al. recently reported that KDM4A is required for M1 macrophage polarization in RAW264.7 macrophages, and that pharmacologic inhibition of the KDM4 family induces apoptosis in these cells.[47] Unfortunately, RAW264.7 macrophages are a male murine cancer cell line and therefore this data cannot be generalized to males and females. Additionally, Choi et al. demonstrated that ML324 treatment blocks TNF-α mediated neutrophil adhesion, a process critical for immune response propagation, but only conducted the experiment in male mice.[192] Thus, in addition to the importance of studying sex differences in periodontal disease, KDM4B also likely has sexual dimorphic characteristics; therefore, the work presented in this dissertation has been done in both sexes wherever possible, to account for these potential factors.

1.4. Systemic disease

Periodontal disease has been linked to several systemic diseases, which may have an underlying epigenetic component driving their correlation. One systemic disease which has been extensively linked to periodontal disease is diabetes mellitus (DM), a disease where the body's insulin is improperly managed, resulting in excessive blood glucose levels. This link has been attributed to several factors, but the most prominent is that both PD and DM patients exhibit a hyper-inflammatory state. For example, diabetic and obese patients exhibit higher serum levels of IL-6 and TNFa.[193] Additionally, diabetic patients have higher IL-1b and PGE2 in their gingival crevicular fluid.[194] Interestingly, monocytes from diabetic patients exhibit a hyper-inflammatory state, secreting higher concentrations of pro-inflammatory cytokines that drive PD in response to LPS than

monocytes from non-diabetic individuals.[195] KDM4B inhibition results in methylation of H3K9 and is required for deacetylation at H3 and H4.[196] This switch from methylation to acetylation at H3K9 is activated by p38 MAPK, by phosphorylating lysine methyltransferase 1A (KMT1A) and disabling its interaction with target genes.[197] P38 MAPK has long been known to positively regulate the immune response, but only more recently has the role of H3K9ac been characterized as a contributor to this activity. H3K9ac is increased in macrophages from diabetic mice, and this mark drives STAT1/MyD88 expression and subsequent sterile inflammation found in diabetes.[198] following hyperglycemic treatment, expression of SUV39H1, one of the histone methyltransferases that acts on H3K9, is decreased. Alternatively, glucose treatment recruits KDM1A to the NF-κB p65 promoter, an observation that has previously been shown to induce inflammatory cytokine expression. Interestingly, hyperglycemia increases H3K4 methylation and decreases H3K9 methylation, a pattern consistent with what we believe initiates immune dysfunction seen in periodontal disease.[199] These data suggest that the underlying link observed between diabetes and periodontal disease may be due to a dysregulated histone code, specifically involving KDM4B and KDM1A.

In addition to diabetes, obesity has also been extensively linked to both periodontal disease as well as epigenetic modifications. Obesity increases a patients risk of both acquiring periodontal disease as well as more severe forms of the disease.[200] For example, systemic inflammation and periodontal disease parameters such as probing depth induced by obesity can be decreased with dietary management.[201] Additionally, oral administration of the periopathogen *P. gingivalis* has effects on the gut microbiota, which alters metabolism.[202] In fact, obese patients have a completely different salivary

microbiome than that of their healthy counterparts, including significantly increased levels of the keystone pathogen genus prevotella.[203] Simply feeding mice a high-fat diet results in alveolar bone loss and increased pro-inflammatory cytokine production as compared to feeding mice a normal diet.[204] With regards to epigenetics, KDM4C is able to control adipogenesis via repression of PPAR-gamma, and has consequently been identified as a potential therapeutic for obesity or type 2 diabetes mellitus [205]. KDM4B has also shown to promote osteogenic over adipogenic differentiation of mesenchymal stem cells. This potentially links the KDM4 family with both bone diseases as well as obesity [164]. Not surprisingly, two back-to-back 2009 studies demonstrated that KDM4B knockout mice spontaneously develop obesity.[206-207] When KDM4B is specifically knocked out in adipocytes, these cells exhibit decreased energy expenditure as well as decreased glucose and lipid metabolism.[208-209] These data suggest that KDM4B may be dysregulated in both periodontal disease and obesity, but cell-type specific activity of this enzyme may be an important consideration for treatment of either disease.

1.5. Rationale for dissertation

Goals of the Proposed Research: Periodontal diseases (PD) affect 42% of the adult American population and are characterized by bacterial-driven inflammatory bone loss. Present adjunctive therapies to manage PD have limited clinical value, and in some cases carry potential side effects that may outweigh their benefit. It is well known that histone demethylases can modulate the immune response, but their correlation with periodontal status is largely unknown [155, 183-184, 210]. The primary objective of this research is to define the epigenetic profile of periodontal disease, specifically in the context of histone demethylase 4B (KDM4B). Additionally, this proposal aims to develop KDM4B inhibitors

with a greater ability to modulate PD pathogenesis through targeting inflammation and bone loss.

1.5.a. Hypothesis. The demethylation activity of KDM1A on histone 3 lysine 4 results in a reduction of pro-inflammatory cytokine transcription [183]. The histone lysine demethylase KDM4B is a histone demethylase that specifically demethylates histone 3 trimethyllysine 9 (H3K9me3) [155], but this demethylation activity is mutually exclusive of demethylation of H3K4me2 by KDM1A [184]. This proposal will take advantage of this coordination to reduce pro-inflammatory cytokine transcription by promoting KDM1A activity through KDM4B inhibition. *The central hypothesis of this proposal is that promotion of KDM1A activity by introduction of a specific KDM4B inhibitor will alleviate PD inflammation and bone loss and that by controlling the overactive immune system in diseased areas, it will enable the host to better manage the disease and prevent its recurrence*. We will test this hypothesis through completion of the following Specific Aims:

1.5.b. Specific Aims

1.5.b.1. Specific Aim 1: *We will define the role of KDM4B in periodontal inflammation and explore the mechanism by which these changes are mediated.* KDM4B abundance will be assessed in perio-pathogen activated inflammatory bone loss tissue sections. *In vitro*, TNF-α and IL-6 response to *A. actinomycetemcomitans* LPS (Aa-LPS), a major immunodominate surface antigen of a common perio-pathogen will be measured following KDM4B inhibition with commercially available inhibitors. To further define the immunomodulatory role of KDM4B, osteoclastogenesis will be measured in the presence and absence of KDM4B inhibitors.

1.5.b.2. Specific Aim 2: *We will use structure-based design techniques to discover novel inhibitors of KDM4B for adjunctive treatment of PD inflammation*. We will dock compounds from large commercially available libraries to the crystal structure of KDM4B using a modification of previously described techniques.[211-212] As hits are identified, 2D orthogonal mathematical models will be used to correlate immunomodulatory activity to structural characteristics of compounds. Immune modulation will be phenotypically screened using a primary macrophage model of PD. Top candidates will be synthesized and analyzed for cytotoxicity and immunomodulatory potential *in vitro*. For effective compounds, IC_{50} values will be determined.

1.5.b.3. Specific Aim 3: *We will evaluate novel and known KDM4B inhibitors for immunomodulatory activity in vivo.* Promising KDM4B inhibitors, as well as the previously defined KDM4B inhibitor (ML324), will be evaluated in a murine calvarial inflammatory bone loss model of periodontal disease. Wild type C57BL/6 mice 12-14 weeks old will be injected subcutaneously with fixed *A. actinomycetemcomitans* following pre-treatment with drug or vehicle control in the mid-sagittal region of the calvarium every day for 5 days to induce inflammatory bone loss. Compounds will be evaluated over a 100-fold concentration range as defined by maximum tolerated dose, and bone loss will be evaluated by micro-computed tomography. Tissues overlying the calvarial bones will be analyzed for changes in histone methylation marks.

1.5.c. Impact on the Field. The proposed research will elucidate an underlying epigenetic mechanism of PD pathogenesis and validate KDM4B as a drug target, thereby opening new doors for drug development and allowing for an enhanced understanding of the inter-related functions of histone methylation and PD progression. This proposal may result in

the development of a novel immunomodulatory compounds, which could be used in future periodontal disease studies.

Chapter 2: Materials/Methods

2.1. Animal Care and Use

C57BL/6 mice were purchased from Jackson Laboratories and maintained in accordance with NIH guidelines. Animals subject to food and tap water *ad libitum* and maintained under normal 12-hour light cycles. Animals were euthanized via CO_2 asphyxiation and death verified by cervical dislocation. Experimental protocols were approved by the Institutional Animal Care and Use Committee (IACUC) at the Medical University of South Carolina under protocol number #2718.

2.2 Bacterial culture

Aggregatibacter actinomycetemcomitans strain Y4 was purchased from American Type Culture Collection (ATCC) and grown following manufacturer's protocols. A single colony was selected by plating the bacterial suspension onto brain heart infusion (BHI) agar and incubating for 3 days in a 5% CO2 incubator at 34 °C. A single colony was picked and expanded in 10mL BHI broth overnight on a shaker. A growth curve was generated by inoculating 10uL of this expanded solution into 20mL broth and monitoring the optical density at a wavelength of 450nm every hour. At the mid-logarithmic growth phase, bacteria were quantified using serial dilutions. Bacteria were expanded into 500mL and diluted to OD450 = 0.3. Bacteria were centrifuged at 1500 x g for 10 minutes, washed with PBS and fixed with 10% formalin for 30 minutes at room temperature. Formalin was

removed by pelleting the fixed bacteria at 1500 x g and rinsing twice with PBS. Bacteria were resuspended in PBS for *in vitro* experimentation and calvarial injections.

2.3 Murine Calvarial Model

Mice were anesthetized using isoflurane inhalation where fifteen uL of 12.5 or 20 μM of ML324, 20 μM **36** or DMSO vehicle control in a 15 μL volume. One hour later, mice were

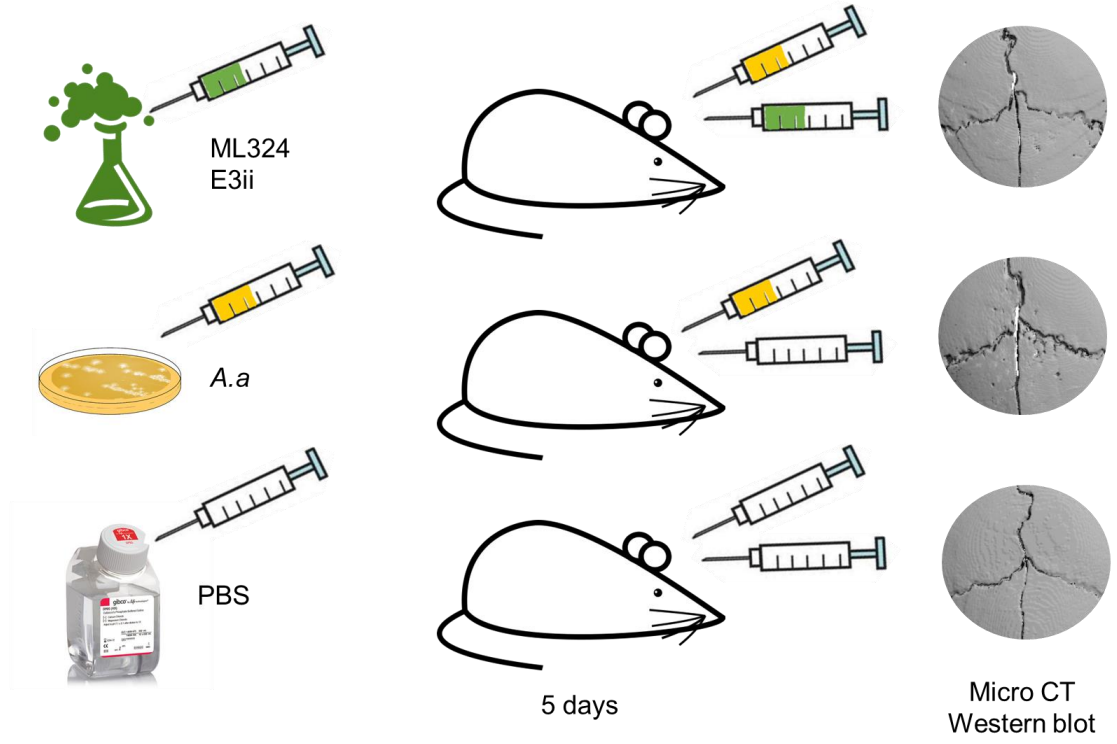

Figure 2.1. Murine calvarial model description.

anesthetized using isoflurane and $2x10^9$ CFU fixed *Aggregatibacter actinomycetemcoitans* strain Y4, serotype b or phosphate buffered saline (PBS) vehicle control was injected subcutaneously supraosteal to the mid-sagittal suture between the eyes and ears to approximate the bregma point into 12-week C57BL/6 male mice. Injections were repeated every 24 hours for 5 days. On day 6, 18 hours following the final

injection, mice were euthanized and connective tissue and skin overlying the calvarial bone was flash frozen, ground using a mortar and pestle and resuspended in M-PER protein isolation buffer. Calvarial bones were fixed in 10% formalin for 24h and then stored in ethanol for micro-computed tomographic analysis.

2.4 Protein Isolation and Immunoblotting

Protein was isolated from skin and connective tissue overlying the calvarial bone by flash freezing tissues upon collection and immediately resuspending the ground tissues in 500 µL of mammalian protein extraction reagent (M-PER, Thermo fisher). Solutions were sonicated at 4 °C for 60 seconds and centrifuged at 1500 x g. Pellets were discarded and supernatant solution containing protein was analyzed using a BCA assay. 25ug protein was run on a SDS-PAGE gel along with Precision Plus Protein Dual Color standards (Bio-Rad). Gels were transferred to a PVDF membrane using the trans-blot turbo transfer system (Bio-Rad) and blocked in 5% fat-free milk in TBS-T overnight at 4 °C. Blots were incubated with primary antibodies in TBS-T overnight at 4 °C. Blots were washed three times in TBS-T and were incubated for 1 hour at room temperature with secondary antibody in TBS-T. Blots were washed three times in TBS-T and developed using Azure Biosciences ECL reagent. Blots were imaged using the Azure c600 imaging system and densitometric analysis of protein was done using ImageJ software. Proteins of interest were normalized to GAPDH as a standard.

2.5 mRNA isolation and qRT-PCR

Media was rinsed with PBS and cells were lysed using TriZol Reagent (Invitrogen, Cat# 15596026). mRNA was isolated according to manufacturer's protocols and purity confirmed using a Nanodrop-1000 spectrophotometer (Thermo Fisher). Quantitative

reverse-transcription real time polymerase chain (qRT-PCR) reaction was run using a High-Capacity cDNA Reverse Transcription Kit (Applied Biosystems, Cat# 4368814) followed by TaqMan® Fast Advanced Master Mix (Applied Biosystems, Cat# 4444557) with TaqMan® Gene Expression Assay Primers (Applied biosystems, listed below) using a StepOne Plus instrument (Thermo Fisher). TNF-α, IL-6 and the internal control GAPDH were then quantitated for each sample in triplicate. Results are reported as fold change ($2^{-\Delta\Delta CT}$).

2.6 Cell Culture

All Cells were cultured at 37 °C in 5% CO_2.

2.6.a. RAW264.7. Cells were cultured in dulbecco's modified essential medium (DMEM) supplemented with 10% fetal bovine serum (FBS) and 1% penicillin/streptomycin. (P/S)

2.6.b. Primary Bone Marrow Macrophage Cell culture. Primary bone marrow was cultured into macrophages as described previously [213]. Briefly, bone marrow from left and right femurs and tibiae of 12-14-week old wild type C57BL/6 mice was flushed into α-MEM (Corning, Cat# 10-022-CV) supplemented with 10% fetal bovine serum (Hyclone, Cat# SH30071.03HI) and 1% penicillin streptomycin (Sigma, Cat# P4333) and plated overnight at 37 °C in 5% CO_2. Cells remaining in suspension were differentiated into experimental wells at a concentration of 2E6 cells/mL for 7 days or until 80% confluency and homogeneity was achieved using macrophage colony stimulating factor (R&D Systems, Cat# 416-ML-500), reconstituted in PBS + 1% BSA (Sigma, Cat# A8806) supplementation (10ng/mL/48h). Cells at this point are referred to as bone marrow derived macrophages (BMDMs).

BMDMs were pre-treated with experimental KDM4B inhibitors for 1 hour at various concentrations followed by incubation with *Aggregatibacter actinomycetemcomitans* lipopolysaccharide (*A.a* LPS) for various time points (generally 8, 16 or 24h).

2.6.c. Primary Bone Marrow Osteoclast Cell culture.

Bone marrow stem cells were isolated from C57BL/6 mice, and differentiated into osteoclasts as previously described [214-215]. In brief, bone marrow isolated from femurs and tibiae of 12 week-old wild-type C57BL/6 mice was plated overnight into phenol red free α-MEM (Gibco, Cat# 41061-029). Adherent cells were discarded and cells that remained in suspension were plated into the wells of a 96-well culture plate (Corning, Cat#3598) at a density of 15,000 cells/well. Cells were supplemented with macrophage colony stimulating factor (M-CSF, R&D Systems, Cat# 416-ML-500) (15ng/mL/48h) for 3 days followed by supplementing with M-CSF (15ng/mL/48h) and receptor activator of nuclear factor kappa b ligand (RANK-L) (R&D Systems, Cat# 462-TEC-010) (50ng/mL/48h) for 2 days. On day 5, wells were rinsed to remove RANK-L and replacement media was supplemented with M-CSF (15ng/mL) with or without *Aa*-LPS (100ng/mL) or RANK-L (R&D Systems, Cat# 462-TEC-010) (50ng/mL) and ML324 (SelleckChem, Cat# S7296, 10μM) or DMSO vehicle control for 72 hours.

2.7. TRAP staining and enumeration

Following osteoclast formation experiments, cells were rinsed twice, fixed with 10% glutaraldehyde (Fisher, Cat# O2957-1) and stained for tartrate resistant acid phosphatase (TRAP) as described in BD Bioscience Technical Bulletin No. 445 using a 10-minute incubation with TRAP buffer. Subsequently, 3 representative images per well were captured using an Eclipse TS100 microscope (Nikon) equipped with an Evolution MP

camera (Media Cybernetics). Osteoclasts were quantified as multinucleated, TRAP+ cells and statistically significant differences were computed using a paired one-way ANOVA with multiple comparisons with an alpha of 0.05.

2.8. Cycloheximide Treatment

RAW264.7 macrophages were grown to 80% confluence in α-MEM supplemented with 10% FBS (Hyclone, Cat# SH30071.03HI) and 1% penicillin/streptomycin (Sigma, Cat# P4333). Cells were then pre-treated with ML324 (SelleckChem, Cat# S7296, 50μM) or DMSO vehicle control with or without cycloheximide (Sigma, Cat# C7698, 10μg/mL) for 4h. DMSO remained constant in each group at a level of 0.1% to eliminate interference with the assay. Cells were challenged with *A.a* LPS (100 ng/mL) or PBS vehicle control for 24 hours and collected for qRT-PCR analysis.

2.9. Immunofluorescence

RAW264.7 macrophages were grown to 80% confluence in phenol red free α-MEM (Gibco, Cat# 41061-029) supplemented with 10% FBS (Hyclone, Cat# SH30071.03HI) and 1% penicillin/streptomycin (Sigma, Cat# P4333) on Sensoplate Plus glass bottom plates (Grenier Bio-One, Cat# 655892). Cells were pre-treated for 1 hour with test inhibitors (SelleckChem, Cat# S7296, 50 μM) or DMSO vehicle control followed by A.a LPS (100 ng/mL) for 24 hours. Cells were then rinsed with PBS and fixed using 4% paraformaldehyde (Sigma) at 37 °C for 10 minutes. Cells were permeablized using 0.1% Triton X-100 (Amresco, Cat# 0694) for 10 minutes and blocked using 3% Bovine Serum Albumin (Sigma, Cat# A8806) in PBS for 30 minutes. Cells were then incubated for 1 hour with rabbit anti-H3K4me (Active Motif, Cat# 39297, 1:750) in 3% BSA. Cells were rinsed and incubated with fluorescent goat anti-rabbit antibody (AbCam, Cat# ab150078, 1:500)

in 3% serum for 1 hour. Cells were counterstained with DAPI (VWR, Cat# 95059-474, 30μM) and AlexaFluor Phalloidin 488 (Invitrogen, A12379). Images were captured using a Wiscan imaging system (Hermes). 32-36 Images per well were used for analysis (n = 3 wells/group).

2.10. Human Periodontal Tissue Procurement

This study was approved by the Institutional Review Board for the Health Sciences at the Medical University of South Carolina, USA. Samples used for the present study represent a subset of samples used for a larger study. Informed consent was obtained with all patients prior to initiating study. Prior to surgery, clinical parameters were measured at the same sites where tissues were harvested including: plaque Index (PI) on a scale of 0-3 (0-no plaque, 1-w/probe, 2-visible, 3-abundant) [216], gingival Index (GI) on a scale of 0-3 (0-no inflammation, 1-mild, 2-moderate w/BOP, 3-severe, spontaneous bleeding on probing (BOP), pocket depth (PD), BOP, gingival recession (REC) and clinical attachment level (CAL). Based on these parameters the inclusion criteria for the diseased group consisted of at least 1 site with PD>4mm, GI 1-3 and PI 1-3. For the healthy controls acceptable parameters were: PD≤4mm, GI≤1, and PI≤2. The exclusion criteria for both groups included: smokers, unstable systemic diseases or chronic disorders (diabetes, rheumatoid arthritis), patients using steroids, antibiotics, NSAIDS and/or other host modulators. The procured samples were from tissues that would have been otherwise discarded after periodontal surgery and or extraction sites. When clinically indicated, procured tissues included connective tissue near the sulcular epithelium.

2.11. Immunohistochemistry

Calvariae from mice with periodontal disease, collected as previously described [217] were formalin fixed, decalcified using 0.5 M EDTA, pH 8.0 for 2 weeks, paraffin embedded and cut into 7 µm sections following standard protocols. Human periodontal tissues were formalin fixed, paraffin embedded and cut into 7 µm sections following standard protocols. Sections were permeablized using 0.2 M boric acid (Sigma, Cat# B6768). Tartrate resistant acid phosphatase (TRAP) was measured as described in BD Bioscience Technical Bulletin No. 445 following a 30-minute incubation with TRAP buffer. KDM4B was visualized following blocking with 3% normal goat serum (SeraCare, Cat# 5560-0007) using rabbit anti-KDM4B (AbCam, Cat# ab191434, 1:125) or rabbit anti-KDM4E (Novus, Cat# NBP2-49124) overnight at 4°C. The sample was then incubated for 1 hour with biotinylated goat anti-rabbit (Vectorlabs, Cat# BA-1000, 1:500). VECTASTAIN Elite ABC HRP Kit (Vectorlabs, 1:500, Cat# PK-6100), and a DAB Peroxidase (HRP) Substrate Kit (Vectorlabs, Cat# SK-4100) was then used for development. 15% Hematoxylin (Sigma, Cat# H3136) was employed as a counterstain. Images were captured using a Nikon 80i Eclipse microscope equipped with a DS-Fi1 camera. Region of interest selection and subsequent quantification was performed using visiopharm software (n = 3) for calvarial tissues. Human periodontal tissues were analyzed using imagej (n = 5-9).

2.12. JMJD2B Enzyme Assay

Inhibition of JMJD2B was assayed by BPS Biosciences using an 11-point IC_{50} determination using the histone demethylase AlphaScreen (PerkinElmer) assay (BPS Bioscience, Cat# 50414). Briefly, enzymatic reactions were conducted in triplicate at room temperature for 60 minutes in a 10 µl mixture containing assay buffer (BPS Bioscience,

Cat# 52407), histone H3 peptide substrate, demethylase enzyme (BPS Bioscience, Cat# 50111), and ML324 or 2,4-pyridine dicarboxylic acid as a reference inhibitor. All wells had a final DMSO concentration of 1%. After the enzymatic reactions were complete, anti-Mouse Acceptor beads (PerkinElmer, Cat# AL105C, 1:500) and Primary H3K9me3 antibody (BPS Biosciences, Cat# 52140E, 1:200) were added and samples were mixed. The reactions were incubated for an additional 30 minutes followed by addition of AlphaScreen Streptavidin-conjugated donor beads (PerkinElmer,Cat# 6760002S, 1:125). 30 minutes later the samples were measured using an AlphaScreen microplate reader (EnSpire Alpha 2390 Multilabel Reader, PerkinElmer). In the absence of the compound, the intensity (C_e) in each data set was defined as 100% activity. In the absence of enzyme, the intensity (C_0) in each data set was defined as 0% activity. The percent activity in the presence of each compound was calculated according to the following equation: %activity = $(C-C_0)/(C_e-C_0)$, where C is the A-screen intensity in the presence of the compound. A plot of % activity versus concentration was then constructed using non-linear regression analysis of the sigmoidal dose-response curve generated with the equation $Y=B+(T-B)/1+10^{((LogIC50-X)\times Hill\ Slope)}$, where Y is percent activity, B is the minimum percent activity, T is the maximum percent activity, X is the logarithm of compound concentration and Hill Slope is the slope factor/Hill coefficient. The IC_{50} value was determined as the concentration causing half-maximal percent activity.

2.13. Enzyme-Linked Immunosorbent Assay (ELISA)

Following cell culture experiments, supernatant proteins were collected for analysis by ELISA. Standardization of samples was based on cell count at the initiation of experimentation, and samples were kept at -80 °C until use if not used immediately.

Samples were centrifuged at 1500 x g to remove insoluble contaminants. 96 well plates were coated with capture antibody overnight, washed three times and blocked with 1% BSA for 2 hours. After washing, samples were added to plates in a 100uL sample volume. Dilutions of samples were only done when necessary, in a subsequent assay if concentrations were not within the linear range of the standard curve. After a 2 hour incubation, plates were washed and a detection antibody was added and plates were incubated for 1 hour. Plates were washed and incubated with streptavidin:HRP for 20 minutes. Plates were washed and developed using proprietary color reagents from R&D Biosystems. Development was stopped by the addition of 2N H_2SO_4 and plates were read using a Spectramax plate reader at 560nm. Plates were normalized to a blank well when possible. A standard curve was fit using a log-log algorithm within the spectramax software and concentrations were determined for each sample. Significance was determined using either One-way or Two-way ANOVA with multiple comparisons, when applicable.

2.14. Micro-Computed Tomography

Calvariae were dissected from surrounding tissues upon sacrifice and immediately submerged in 10% formalin for fixation. Bones were incubated overnight at room temperature on a shaker to ensure complete fixation. Solutions were replaced with 70% ethanol to rinse and then stored for long-term analysis in a fresh solution of 70% ethanol. Samples were sent to Maria Johnson at University of Alabama Birmingham for scanning. Scans were run on a Scanco 40 instrument at a 15 μm resolution. A cylindrical region of interest was selected centered around the bregma point and samples were thresholded at a minimum intensity value of 3148HU based on control samples. Bone density was

determined using Analyze Pro software and statistical significance was determined using a Student's t-test.

2.15. Computational Chemistry

2.15.a. Docking Experiments

DOCK6.5: The KDM4B crystal structure (PDB: 4LXL) was prepared using UCSF Chimera following DOCK6.5 protocols.[218] Ligands and water molecules were removed from the crystal structure. The ZINC15 compound database was filtered using pre-defined subsets of compounds: those with predicted *in vitro* activity in combination with compounds that were purchasable.[219] This library was further refined by generating descriptors in Molecular Operating Environment (CGS) software in a high-throughput manner and eliminating large numbers of compounds based on these unfavorable descriptors: violation of one or more of Lipinski's rules, molecular weight less than 250 and greater than 500 g/mol, greater than 12 rotatable bonds, compounds with a formal charge <-2 or >2 and the library was charged and energy pre-minimized for each structure based on standard protocols. The compound library was docked using DOCK6.5 in an unbiased manner by using the entire enzyme as the active site for docking in flexible mode with 1000 maximum orientations per computation. The compound library was concurrently docked using Molecular Operating Environment in a rigid receptor dock constrained to the active site identified by the site finder tool in MOE. Hits from both programs were ranked based on the percentage of the maximum binding energy of each hit. Compounds that ranked independently within the top 70% of both docking experiments were selected for physicochemical clustering. OpenBabel descriptors were generated for the top 70%

consensus hits using Chemmine cheminformatics online tools.[220] Compounds were clustered by similarity and hits clustered in the smallest clade containing ML324, JIB-04 and NSC636819 were selected for *in vitro* evaluation. This consensus docking strategy was performed on a combinatorial library of novel compounds as needed to prioritize synthetic efforts.

2.15.b. Quantitative structure activity relationship (QSAR) development

The phenotypic immunosuppressive screen data was converted into binary data using statistical significance ($P<0.05$) determined by One-Way ANOVA compared to DMSO controls as a cutoff. A contingency analysis was run on the tested compounds to identify the 2D descriptors defined by MOE that were most highly correlated with activity. The top 12 descriptors from this analysis were used to map a quantitative structure activity relationship algorithm and cross-validation was conducted using a leave one out method following standard protocols. The model was applied to our combinatorial library to predict activity.[221-222]

2.16. Synthetic Chemistry

2.16.a. General Procedures: All solvents and chemicals were reagent grade. Anhydrous dichloromethane (DCM) and dichloroethane (DCE) were purchased from VWR. All solutions were dried over anhydrous magnesium sulfate or sodium sulfate, solvents were removed by rotary evaporation under reduced pressure. Solids used in dry reactions were additionally freeze dried before use. Microwave reactions were run in a Biotage Initiator. Flash column chromatography was carried out using pre-packed silica columns from RediSep or SiliCycle and mixtures adsorbed onto ISOLUTE for elution. Purity of compounds was >95% as determined by ultra-pure liquid chromatography analysis. NMR

spectra were recorded on a Bruker 400 MHz instrument using $CDCl_3$, MeOD or $DMSOd_6$ as solvents. Chemical shifts are reported in ppm relative to TMS (0.00 ppm) or solvent peaks as an internal reference. Splitting patterns are indicated as follows: s, singlet; d, doublet; t, triplet; q, quartet; m, multiplet.

All data are represented as geometric mean ± standard error of the mean (SEM) and statistical significance was determined using One-Way ANOVA with multiple comparisons ($p<0.05$).

2.16.b. Compound 2: 5-Chloro-2-[(E)-2-[phenyl(pyridin-2-yl)methylidene]hydrazin-1-yl]pyridine (JIB-04). Hydrazine hydrate (5.48 g, 171 mmol, 5.34 mL) was added to a solution of 2,5-dichloropyridine **1** (0.21 g, 1.42 mmol) in pyridine (10 mL) and the reaction mixture was refluxed for 6 h. The resulting suspension was dried in vacuo (rotary evaporator), dissolved in dichloromethane and washed with a 50 mL portion of 1.0 N NaOH and three 50 mL portions of water. The organic layer was dried over anhydrous magnesium sulfate, filtered, and the solvent was removed in vacuo to yield 5-chloro-2-hydrazinylpyridine **2** as a white crystalline solid (0.097 g, 47%)

A 20 mg portion of **2** (20 mg, 1.4 mmol) and benzoyl pyridine **3** (25.5 mg, 1.4 mmol) were refluxed overnight in methanol (10 mL) with a traces of acetic acid. The resulting solution was dried via rotary evaporator and crystallized from ethyl acetate to yield 5-Chloro-2-[(E)-2-[phenyl(pyridin-2-yl)methylidene]hydrazin-1-yl]pyridine (JIB-04) **4** as fine yellow needles (0.099 g, 23%).

2.16.c. Compound 16, 23-28: Biphenyl benzoyl chloride (3.6 mmol) was added to aminobenzoate derivatives **17** (3 mmol) under reflux in toluene (25 mL) as previously described.[223] Reaction was refluxed for 4h and product was evaporated under reduced

pressure by adding water continually until all toluene was removed. Product was extracted from ethyl acetate rinsing with brine. The remaining organic layer was loaded onto a 25g silica column and purified using flash chromatography with a solvent gradient from 0-100% ethyl acetate in hexanes over 25 minutes. Fractions containing product **18** were combined and identity of products were confirmed using UPLC and NMR.

The resulting ester **18** (1 mmol) was added to a microwave vial with LiOH (.5 mmol) and dissolved in methanol and water (3:1, 10mL). The reaction was microwave irradiated at 100 °C for 1-2 hours until the ester starting material was consumed. The reaction was acidified, evaporated under reduced pressure, and vacuum filtered rinsing with cold HCl to yield product **16, 23-28** as a white to off-white solid.

Final products were lyophilized and analyzed using UPLC for >95% purity and ^{1}H NMR for identification.

2.16.d. Compound 29-46 were synthesized using a modification of a previously described technique.[224] Derivatized trifluoroborates (0.25 mmol), derivatized bromobenzenes (0.25 mmol), and cesium carbonate (0.756 mmol) was combined with catalytic [1,1′-Bis(diphenylphosphino)ferrocene]dichloropalladium(II), complex with dichloromethane (0.023 mmol) and the mixture was suspended in a degassed solution of THF and water (1:10, 5mL) in a 20mL microwave vial. The reaction was vortexed briefly and irradiated in a biotage initiator at 100 °C for 1-2 hours until the starting material was consumed as determined by TLC as previously described. The reaction mixture was evaporated under reduced pressure, acidified using HCl and extracted 3x from DCM. The organic was dried over sodium sulfate and adsorbed onto isolute for separation using flash chromatography to yield an off-white solid. The resulting ester (1 mmol) was added to a microwave vial with

LiOH (0.5 mmol) and dissolved in methanol and water (3:1, 10mL). The reaction was microwave irradiated at 100 °C for 1-2 hours until the ester starting material was consumed. The reaction was acidified, evaporated under reduced pressure, and vacuum filtered rinsing with cold HCl to yield a white solid **15**.

Carboxylic acid **15** (2 mmol) was lyophilized and resuspended in dry DCE (10 mL) under nitrogen in a flame dried flask. Oxalyl chloride (3.6 mmol) and catalytic DMF (5 drops) were added to the reaction on ice and the solution was allowed to stir at room temperature for 1-24 h until gas was no longer produced. The reaction generally turned yellow upon formation of the carbonyl chloride in solution. DCE was removed under reduced pressure using rotary evaporation to yield a bright yellow residue. The residue was resuspended in dry DCM (10mL) and in a separate flask, Aminobenzoate derivatives **17** were dissolved in dry DCM (10 mL) with TEA (8.2 equiv.). The basic aminobenzoate solution was added to the benzoyl chloride under nitrogen via cannula transfer and the reaction was stirred at room temperature under nitrogen for 1-24h until the amine starting material was consumed as confirmed by UPLC. The reaction mixture was filtered to remove the TEA salt, and the remaining liquid was extracted from ethyl acetate, rinsing sequentially with citric acid, NaOH and brine. The remaining organic layer was loaded onto a 25g silica column and purified using flash chromatography with a solvent gradient from 0-100% ethyl acetate in hexanes over 25 minutes. Fractions containing product **18** were combined and identity of products were confirmed using UPLC and NMR.

The resulting ester **18** (1 mmol) was added to a microwave vial with LiOH (0.5 mmol) and dissolved in methanol and water (3:1, 10mL). The reaction was microwave irradiated at 100 °C for 1-2 hours until the ester starting material was consumed. The reaction was

acidified, evaporated under reduced pressure, and vacuum filtered rinsing with cold HCl to yield product **29-46** as a white to off-white solid.

Final products were lyophilized and analyzed using UPLC for >95% purity and ^{1}H NMR for identification.

2.16.d. Spectroscopy for Synthesized compounds:

2:

Intermediate: ^{1}H NMR ($CDCl_3$) δ: 3.795 (s, 2H), 5.797 (s, 1H), 6.697 (d, 1H, *J* = 8.8 Hz), 7.422 - 7.450 (dd, 1H, *J* = 2.5, 8.8 Hz), 8.058 (d, 1H, *J* = 2.3 Hz). MS calcd for $C_5H_6ClN_3$ 144.03 [M + H^+], found 144.02 [M + H^+].

Final product: ^{1}H NMR ($CDCl_3$) δ: 7.260-7.356 (m, 2H), 7.397-7.466 (m, 3H), 7.536-7.587 (m, 4H), 7.506 (td, 1H, *J* = 1.6, 7.8 Hz), 8.136 (d, 1H, *J* = 2.2 Hz), 8.823 (dd, 1H, *J* = 4.9, 0.7 Hz), 13.301 (s, 1H). MS calcd for $C_{17}H_{13}ClN_4$ 309.09 [M + H^+], found 309.41 [M + H^+]

16:

Intermediate: ^{1}H NMR (400 MHz, $CDCl_3$) δ3.90 (s, 3H), 7.25 (m, 1H), 7.42 (t, 1H), 7.51 (t, 2H), 7.69 (m, 1H), 7.77 (t, 2H), 8.04 (m, 3H), 8.59 (d, 1H), 11.68 (s, 1H)

Final Product: ^{1}H NMR (400 MHz, $CDCl_3$)δ7.19-7.23 (t, 3H), 7.59-7.64 (t, 3H), 8.09-8.13 (m, 3H), 8.74, 8.76 (d, 1H), 8.87, 8.89 (d, 2H), 12.61 (s, 1H), 12.91 (s, 2H)

23:

Intermediate 1: ^{1}H NMR (400 MHz, $(CD_3)_2SO$)δ 2.11 (s, 3H), 2.34 (t, 3H), 3.53 (s, 3H), 7.16 (t, 1H), 7.26 (t, 1H), 7.35 (m, 3H), 7.50 (q, 1H), 7.59 (q, 2H), 7.68 (t, 2H), 7.91 (d, 2H), 9.87 (s, 1H)

Final product: ^{1}H NMR (400 MHz, $(CD_3)_2SO$)δ 2.07 (s, 3H), 7.12 (t, 1H), 7.26 (q, 1H), 7.35 (q, 3H), 7.52 (q, 1H), 7.60 (t, 2H), 7.68 (d, 2H), 9.95 (s, 1H), 12.62 (s, 1H)

24:

Intermediate 1: ^{1}H NMR (400 MHz, $CDCl_3$)δ 3.92 (s, 3H), 7.44 (d, 1H), 7.53 (t, 2H), 7.62 (d, 1H), 7.78 (m, 3H), 7.92 (d, 2H), 8.06 (d, 2H), 8.50 (q, 1H), 11.41 (s, 1H)

UPLC R_t: 7.022 minutes

Final product: ^{1}H NMR (400 MHz, $(CD_3)_2SO$)δ 7.26(t, 1H), 7.40 (m, 3H), 7.60 (m, 3H), 7.73 (d, 2H), 7.88 (d, 2H), 8.54 (q, 1H), 11.85 (s, 1H), 13.99 (s, 1H)

25:

Final product: ^{1}H NMR (400 MHz, $(CD_3)_2SO$)δ 7.25 (m, 2H), 7.37 (m, 3H), 7.54 (d, 1H), 7.61 (t, 2H), 7.69 (d, 2H), 7.91 (d, 2H), 10.04 (s, 1H), 13.01 (s, 1H)

26:

Final product: ^{1}H NMR (600 MHz, $CDCl_3$)δ 3.98 (d, 4H), 6.87 (q, 1H), 7.42 (t, 1H), 7.52 (q, 3H), 7.66 (m, 4H), 7.78 (t, 2H), 8.14 (q, 4H), 8.82 (q, 1H)

27:

Intermediate 1: ^{1}H NMR (400 MHz, $CDCl_3$)δ3.74 (s, 3H), 7.25 (m, 1H), 7.37 (m, 3H), 7.52 (m, 1H), 7.61 (t, 2H), 7.70 (d, 2H), 7.95 (m, 2H), 8.34 (t, 1H), 10.37 (s, 1H)

Final product: ^{1}H NMR (600 MHz, $(CD_3)_2SO$)δ 7.39 (d, 1H), 7.53 (m, 3H), 7.69 (m, 1h), 7.79 (t, 2H), 7.87 (t, 2H), 8.10 (m, 3H), 8.47 (d, 1H), 10.48 (s, 1H), 12.94 (s, 1H)

28:

Intermediate 1: ^{1}H NMR (400 MHz, $CDCl_3$)δ 3.67 (s, 3H), 7.24 (d, 1H), 7.34 (t, 2H), 7.59(d, 3H), 7.69 (d, 2H), 7.81 (s, 4H), 7.92 (d, 2H), 10.45 (s, 1H)

Final product: ^{1}H NMR (600 MHz, $(CD_3)_2SO$)δ 7.42 (m, 2H), 7.54 (q, 2H), 7.68 (q, 1H), 7.78 (d, 2H), 7.84 (d, 2H), 7.89 (d, 2H), 7.93 (d, 2H), 7.99 (d, 1H), 8.09 (d, 2H), 10.44 (s, 1H)

29:

Intermediate 1: ^{1}H NMR (400 MHz, $CDCl_3$)δ 3.84 (s, 3H), 7.19 (m, 1H), 7.26 (d, 1H), 7.34 (q, 2H), 7.45 (t, 2H), 7.54 (t, 2H), 7.63 (m, 2H), 7.82 (d, 1H), 8.17 (t, 1H), 8.85 (q, 1H), 11.71 (s, 1H)

Final product: ^{1}H NMR (400 MHz, $CDCl_3$)δ 7.24 (q, 2H), 7.35 (q, 2H), 7.44 (t, 1H), 7.54 (d, 2H), 7.66 (m, 2H), 7.83 (d, 1H), 8.06 (s, 1H), 8.82 (q, 1H), 11.71 (s, 1H)

30:

Final product: ^{1}H NMR (400 MHz, $CDCl_3$)δ 6.88 (q, 1H), 7.41 (d, 1H), 7.51 (t, 2H), 7.61 (t, 1H), 7.71 (d, 2H), 7.84 (d, 1H), 8.01 (d, 1H), 8.20 (q, 1H), 8.31 (s, 1H), 8.80 (q, 1H), 12.13 (s, 1H)

31:

Intermediate 1: ^{1}H NMR (400 MHz, $CDCl_3$)δ 3.62 (s, 3H), 6.89 (m, 1H), 7.10 (q, 2H), 7.31 (q, 4H), 7.38 (m, 2H), 7.59 (t, 1H), 7.77 (q, 1H), 8.53 (d, 1H), 10.85 (s, 1H)

Final product: ^{1}H NMR (400 MHz, $CDCl_3$)δ 6.93 (t, 1H), 7.14 (m, 3H), 7.30 (m, 4H), 7.46 (m, 2H), 7.62 (d, 1H), 7.88 (d, 1H), 8.60 (d, 1H), 10.47 (s, 1H)

32:

Intermediate 1: ^{1}H NMR (400 MHz, $CDCl_3$)δ 2.00 (s, 3H), 3.71 (s, 3H), 6.98 (t 1H), 7.21 (m, 3H), 7.29 (q, 1H), 7.35 (m ,4H), 7.57 (q, 1H), 7.66 (q, 1H), 8.93 (s, 1H)

Final product: ^{1}H NMR (400 MHz, $CDCl_3$)δ 2.03 (s, 3H), 7.01 (d, 1H), 7.15 (d, 1H), 7.20 (t, 2H), 7.27 (t, 2H), 7.32 (d, 2H), 7.38 (t, 1H), 7.67 (t, 2H), 8.70 (s, 1H)

33:

Intermediate 1: ^{1}H NMR (400 MHz, $CDCl_3$)δ3.65 (s, 3H), 7.08 (m, 2H), 7.18 (t, 2H), 7.30 (m, 4H), 7.37 (t, 1H), 7.44 (q, 1H), 7.58 (t, 1H), 8.54 (q, 1H), 10.66 (s, 1H)

Final product: ^{1}H NMR (400 MHz, $CDCl_3$)δ 7.14 (m, 4H), 7.28 (d, 1H), 7.34 (m, 2H), 7.43 (m ,1H), 7.53 (q, 1H), 7.63 (m, 1H), 8.61 (q, 1H), 10.33 (s, 1H)

34:

Intermediate 1: ^{1}H NMR (400 MHz, $CDCl_3$)δ3.68 (s, 3H), 7.02 (m, 1H), 7.12 (m, 1H), 7.23 (t, 2H), 7.35 (m, 5H), 7.51 (d, 1H), 7.65 (t, 1H), 8.67 (s, 1H)

Final product: ^{1}H NMR (400 MHz, $CDCl_3$)δ 7.18 (m, 4H), 7.30 (q, 4H), 7.40 (t, 1H), 7.56 (d, 1H), 7.69 (d, 1H), 8.48 (s, 1H)

35:

Intermediate 1: ^{1}H NMR (400 MHz, $CDCl_3$)δ 3.67 (s, 3H), 7.12 (m, 2H), 7.23 (m, 5H) 7.31 (t, 1H), 7.37 (m, 2H), 7.50 (s, 1H), 7.55 (d, 1H), 7.66 (t, 1H)

Final product: ^{1}H NMR (400 MHz, $CDCl_3$)δ 7.13 (q, 1H), 7.21 (q, 3H), 7.27 (t, 2H), 7.33 (m, 2H), 7.43 (m, 3H), 7.54 (t, 1H), 8.02 (s, 1H), 10.29 (s, 1H), 12,49 (s, 1H)

36:

Intermediate 1: ^{1}H NMR (400 MHz, $CDCl_3$)δ 2.38 (s, 3H), 3.64 (s, 3H), 7.19 (s, 4H), 7.36 (t, 2H), 7.49 (m, 1H), 7.79 (d, 1H)

Intermediate 2: ^{1}H NMR (400 MHz, $CDCl_3$)δ 2.26 (s, 3H), 7.04(d, 2H), 7.13 (t, 2H), 7.25(m, 2H), 7.42 (m, 1H), 7.81 (m, 1H), 10.55 (s, 1H)

Intermediate 3: ^{1}H NMR (400 MHz, $CDCl_3$)δ 2.01 (s, 3H), 2.19 (s, 3H), 3.69 (s, 3H), 7.01 (m, 4H), 7.24 (m, 3H), 7.36 (q, 1H), 7.59 (d, 1H), 7.65 (d, 1H), 8.94 (s, 1H)

Final product: ^{1}H NMR (600 MHz, $CDCl_3$)δ 2.355 (s, 3H), 7.19 (m, 4H), 7.37 (m, 3H), 7.45 (m, 4H), 7.54 (m, 1H), 7.81 (m, 2H), 8.93 (s, 1H)

37:

Intermediate 1: ^{1}H NMR (400 MHz, $CDCl_3$)δ 3.63 (s, 3H), 3.81 (s, 3H), 6.91 (d, 2H), 7.28 (d, 1H), 7.34 (t, 2H), 7.62 (t, 1H), 7.76 (m, 2H)

Intermediate 2: ^{1}H NMR (400 MHz, $CDCl_3$)δ3.84 (s, 3H), 6.93 (t, 2H), 7.28 (q, 2H), 7.38 (q, 2H), 7.54 (m, 1H), 7.92 (t, 1H)

Intermediate 3: ^{1}H NMR (400 MHz, $CDCl_3$)δ 3.61 (s, 3H), 3.66 (s, 3H), 6.67 (d, 2H), 6.93 (t, 1H), 7.33 (m, 6H), 7.59 (d, 1H), 7.77 (d, 1H), 8.63 (d, 1H), 10.77 (s, 1H)

Final product: ^{1}H NMR (400 MHz, $CDCl_3$)δ 3.58 (s, 3H), 6.68 (d, 2H), 6.96 (m, 1H), 7.11 (s, 1H), 7.20 (d, 2H), 7.29 (m, 2H), 7.37 (m, 1H), 7.46 (t, 1H), 7.59 (t, 1H), 7.86 (q, 1H), 8.67 (d, 1H), 10.51 (s, 1H)

38:

Intermediate 1: ^{1}H NMR (400 MHz, $CDCl_3$)δ 2.24 (s, 3H), 3.74 (s, 3H), 7.09 (q, 1H), 7.24 (m, 1H), 7.34 (m, 3H), 7.44 (t, 1H), 7.52 (q, 2H), 7.64 (m, 1H), 7.71 (q, 1H), 7.84 (m, 1H), 8.12 (t, 1H), 10.01 (s, 1H)

Final product: ^{1}H NMR (400 MHz, $CDCl_3$)δ 2.27 (s, 3H), 7.14 (t, 1H), 7.23 (t, 1H), 7.34 (t, 3H), 7.46 (t, 1H), 7.54 (t, 1H), 7.61 (d, 2H), 7.72 (d, 1H), 7.78 (d, 1H), 8.15 (s, 1H), 9.90 (s, 1H), 12.69 (s, 1H)

39:

Intermediate 1: ^{1}H NMR (400 MHz, $CDCl_3$)δ3.72 (s, 3H), 3.75 (s, 3H), 7.09 (m, 1H), 7.43 (m, 3H), 7.52 (t, 2H), 7.63 (q, 4H), 7.77 (d, 1H), 7.86 (q, 3H), 8.13 (t, 1H), 9.87 (s, 1H)

Final product: ^{1}H NMR (600 MHz, $CDCl_3$)δ 7.41 (m, 3H), 7.58 (m, 3H), 7.81 (d, 1H), 7.88 (m, 2H), 7.94 (d, 1H), 8.00 (d, 1H), 8.11 (m, 2H), 8.37 (t, 2H), 9.88 (s, 1H)

40:

Intermediate 1: ^{1}H NMR (400 MHz, $CDCl_3$)δ 2.00 (s, 3H), 3.71 (s, 3H), 6.98 (t, 1H), 7.21 (m, 3H), 7.27 (q, 1H), 7.34 (m, 4H), 7.57 (q, 1H), 7.66 (q, 1H), 8.93 (s, 1H)

Final product: ^{1}H NMR (400 MHz, $CDCl_3$)δ 2.02 (s, 3H), 7.02 (t, 1H), 7.18 (m, 3H), 7.27 (t, 3H), 7.32 (d, 2H), 7.38 (q, 1H), 7.66 (t, 2H), 8.71 (s, 1H)

41:

Intermediate 1: ^{1}H NMR (400 MHz, $CDCl_3$)δ 3.62 (s, 3H), 6.59 (m, 1H), 7.38 (m, 7H), 7.61 (d, 1H), 7.81 (q, 1H), 8.46 (d, 1H), 11.02 (s, 1H)

Final product: ^{1}H NMR (400 MHz, $CDCl_3$)δ 6.72 (m, 1H), 7.19 (m, 5H), 7.36 (m ,2H), 7.44 (m, 2H), 7.54 (m, 1H), 7.71 (q, 1H), 7.95 (q, 1H), 8.60 (q, 1H), 10.73 (s, 1H)

42:

Intermediate 1: ^{1}H NMR (400 MHz, $CDCl_3$)δ 2.38 (s, 3H), 3.92 (d, 3H), 7.24 (d, 2H), 7.51 (q, 2H), 7.68 (d, 2H), 8.10 (t, 2H)

Intermediate 3: ^{1}H NMR (400 MHz, $CDCl_3$)δ2.36 (s, 3H), 3.96 (s, 3H), 7.24 (m, 3H), 7.49 (d, 3H), 7.70 (m, 3H), 8.01 (d, 2H), 8.88 (q, 1H), 11.89 (s, 1H)

Final product: ^{1}H NMR (600 MHz, $(CD_3)_2SO$)δ 2.36 (s, 4H), 7.28 (d, 2H), 7.56 (m, 1H), 7.67 (d, 2H), 7.77 (q, 1H), 7.88 (d, 2H), 8.04 (d, 2H), 8.72 (q, 1H), 11.83 (s, 1H)

43:

Intermediate 1: ^{1}H NMR (400 MHz, $CDCl_3$)δ 2.38 (s, 3H), 3.64 (s, 3H), 7.19 (s, 4H), 7.36 (t, 2H), 7.49 (m, 1H), 7.79 (d, 1H)

Intermediate 2: ^{1}H NMR (400 MHz, $CDCl_3$)δ 2.26 (s, 3H), 7.04(d, 2H), 7.13 (t, 2H), 7.25(m, 2H), 7.42 (m, 1H), 7.81 (m, 1H), 10.55 (s, 1H)

Intermediate 3: ^{1}H NMR (400 MHz, $CDCl_3$)δ2.65 (s, 3H), 3.62 (s, 3H), 6.92 (d, 2H), 7.02 (m, 3H), 7.14 (m, 4H), 7.24 (m, 3H), 7.33 (m, 1H), 7.41 (q, 1H), 7.51 (d, 1H), 7.79 (s, 1H), 8.51 (q, 1H), 10.66 (s, 1H)

Final product: ^{1}H NMR (400 MHz, MeOD)δ 2.30 (s, 3H), 7.15 (d, 2H), 7.32 (m, 3H), 7.50 (t, 2H), 7.60 (t, 1H), 7.68 (q, 1H), 8.63 (q, 1H)

44:

Intermediate 1: ^{1}H NMR (400 MHz, $CDCl_3$)δ3.62 (s, 3H), 3.68 (s, 3H), 6.95 (m, 3H), 7.22 (d, 1H), 7.37 (m, 1H), 7.63 (m, 1H), 7.85 (q, 1H)

Intermediate 2: ^{1}H NMR (400 MHz, $CDCl_3$)δ 3.55 (s, 3H), 6.72 (d, 1H), 6.89 (q, 1H), 6.98 (d, 2H), 7.11 (t, 1H), 7.18 (m, 2H), 7.29 (m ,3H), 7.41 (q, 1H), 7.78 (q, 1H)

Intermediate 3: ^{1}H NMR (400 MHz, $CDCl_3$)δ 2.97 (s, 3H), 3.59 (s, 3H), 3.82 (s, 3H), 6.76 (d, 1H), 6.90 (q, 1H), 7.00 (m, 2H), 7.30 (m, 2H), 7.46 (q, 1H), 7.53 (m, 2H), 7.62 (q, 2H), 8.05 (s, 1H), 8.77 (q, 1H), 10.86 (s, 1H)

Final product: ^{1}H NMR (400 MHz, $CDCl_3$) 1.69 (s, 3H), 3.69 (s, 3H), 7.00 (t, 2H), 7.17 (m, 3H), 7.31 (m, 3H), 7.60 (m, 2H), 9.52 (s, 1H)

45:

Intermediate 1: ^{1}H NMR (400 MHz, $CDCl_3$)δ2.41 (s, 3H), 3.94 (s, 3H), 7.27 (t, 1H), 7.48 (d, 1H), 7.52 (d, 2H), 8.00 (q, 1H), 8.27 (d, 1H)

Intermediate 2: ^{1}H NMR (400 MHz, $CDCl_3$)δ 2.19 (s, 3H), 7.13 (d, 2H), 7.42 (t, 3H), 7.73 (t, 2H), 7.99 (s, 1H)

^{13}C NMR (400 MHz, D_2O)δ167.7, 140.87, 136.80, 131.87, 131.34, 130.18, 129.79, 128.43, 127.47, 127.06, 21.13

Intermediate 3: ^{1}H NMR (400 MHz, $CDCl_3$)δ2.42 (s, 3H), 3.96 (s, 3H), 7.28 (d, 2H), 7.34 (m, 1H), 7.57 (t, 3H), 7.75 (m, 2H), 7.97 (t, 1H), 8.92 (q, 1H), 11.96 (s, 1H)

Final product: ^{1}H NMR (400 MHz, $CDCl_3$)δ2.34 (s, 3H), 7.26 (s, 2H), 7.42(s, 1H), 7.57 (s, 3H), 7.81, 7.90 (d, 3H), 8.21 (s, 1H), 8.95 (s, 1H), 12.16 (s, 1H)

46:

Intermediate 1: ^{1}H NMR (400 MHz, $CDCl_3$)δ 3.79 (s, 3H), 6.99 (m ,1H), 7.25 (m, 2H), 7.54 (m, 2H), 7.65 (m, 1H), 7.76 (m, 1H), 7.86 (m, 1H), 7.94 (q, 1H), 8.00 (m, 1H), 8.14 (t, 1H), 8.23 (t, 1H), 8.77 (q, 1H), 12.07 (s, 1H)

Final product: ^{1}H NMR (400 MHz, $CDCl_3$)δ 7.11 (m ,1H), 7.34 (m ,1H), 7.43 (q, 2H), 7.54 (t, 1H), 7.65 (m, 3H), 7.76 (m, 1H), 7.98 (m, 1H), 8.12 (q, 1H), 8.22 (t, 1H), 8.90 (q, 1H), 11.96 (s, 1H)

2.17. Antibodies

KDM4B: AbCam, Cat# ab191434

KDM4E: Novus, Cat# NBP2-49124

H3K9me3: Abcam, Cat# ab176916

H3K4me: Active Motif, Cat# 39297

H3K4me2: Abcam, Cat# ab32356

GAPDH: Abgent, Cat# AP7873b

Goat anti-rabbit: Vectorlabs, Cat# BA-1000

Fluorescent secondaries:

Goat anti-rabbit: AbCam, Cat# ab150078

2.18. Primers

TaqMan® Gene Expression Assay Primers (ThermoFisher)

GAPDH: Mm99999915_g1

IL-6: Mm00446190_m1

TNF-α: Mm00443258_m1

IL-10: Mm01288386_m1

KDM4B: Mm01236310_m1

IL-1b: Mm00434228_m1

Era: Mm00469669_m1

Chapter Three: Inhibition of the Histone Demethylase KDM4B Leads to Activation of KDM1A, Attenuates Bacterial-Induced Pro-Inflammatory Cytokine Release and Reduces Osteoclastogenesis.

3.1. Rationale and Hypothesis

Periodontal disease (PD) causes irreversible tissue damage and bone loss and affects 46% of adult Americans. PD is a common chronic inflammatory disease characterized by destruction of the supporting structures of the teeth.[50, 186] This chapter describes a novel approach that targets epigenetic control of gene expression in the host to resolve the pro-inflammatory immune response driving PD.

The pro-inflammatory cytokines TNF-α and IL-6 are classically upregulated in gingival connective tissues of PD patients, [36] and these cytokines are secreted from perio-pathogen activated macrophages through toll like receptor (TLR) signaling.[225] TLR4 binding by periopathogenic LPS activates a signaling cascade that drives both cytokine and chemokine production. KDM4B and its major substrate, H3K9, have been linked to this process by several research groups. [157-159, 192] Because of this, we hypothesize that KDM4B is a mediator of PD progression, and demonstrate that its demethylation activity is a signature of several pro-inflammatory processes.

It is well known that histone demethylase enzymes are conserved throughout species, and that these enzymes are commonly redundant, share substrate specificity

among different classes and families, and are coordinated in their activity. Multiple studies support the idea that H3K4 and H3K9 methylation are mutually exclusive states.[184, 226] For example, cross talk between KDM4B and KDM1A enzymes leads to a balanced system wherein lysine 9 methylation serves as a prerequisite to lysine 4 demethylation by KDM1A.[184] Because it is known that the demethylation activity of KDM1A on Histone 3 lysine 4 leads to repression of pro-inflammatory cytokine gene transcription,[183] we postulate that KDM4B is a positive regulator of the pro-inflammatory cytokine response through an indirect mechanism by inhibiting KDM1A.

The current study aims to interrogate the activity of KDM4B as it relates to the immune response in periodontal disease through the use of the JMJD2 demethylase inhibitor ML324.[212] We hypothesize that KDM4B inhibition using this inhibitor will result in a reduced immune response to bacterial LPS, and that ML324 could prove useful as a chemical tool and lead compound for future studies on PD or other hyper-inflammatory or autoimmune diseases.

3.2. Results

3.2.a. KDM4B and KDM4E protein abundance is increased in areas of periodontal inflammatory infiltrate.

To test the hypothesis that KDM4B is overexpressed upon LPS stimulation, histological sections from the calvariae of mice that had been injected daily for 5 days with fixed *Aggregatibacter actinomycetemcomitans (A.a)* or PBS were stained for KDM4B protein. An increase in resorption pits due to osteoclast activity was observed in calvariae treated with A.a, confirming this as a viable model for periodontal disease.[217] Staining for tartrate resistant acid phosphatase (TRAP) and F4/80 marked the area in the calvarial

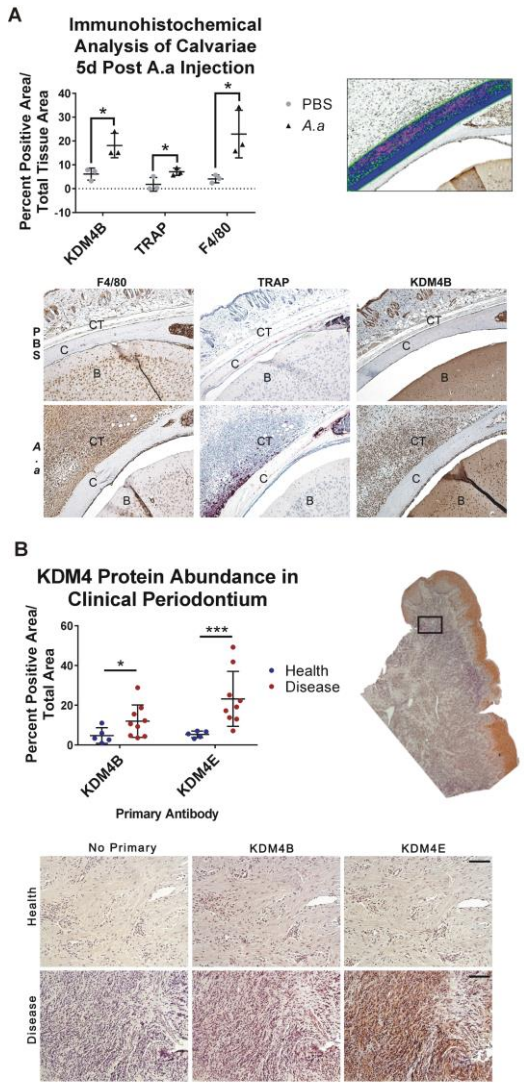

Figure 3.1. KDM4B abundance is significantly increased in periodontal diseased versus healthy tissues. Live *A.a* was injected subcutaneously into 12-week old C57BL/6 mice at the mid-sagittal region of the calvarium every day for 5d. Paraffin embedded sections were stained for F4/80, TRAP and KDM4B using immunohistochemistry, all of which were significantly upregulated in diseased versus healthy calvariae. 10x Images presented are representative of the data set. (A) In clinical periodontal specimens, the region of interest was defined as the connective tissue underlying the oral epithelium. Paraffin embedded sections were stained for KDM4E and KDM4B using immunohistochemistry, both of which were upregulated in diseased versus healthy patient tissues. 20x images are representative of the data set. (B) positive pixels quantified using color thresholding in ImageJ. Data are presented as mean ± SD. Significance was determined using a one-tailed Wilcoxon ranked sum test. Epithelium (E) Calvarial Bone (C) Brain (B) *p<0.05, ***p<0.001. Scale bars, 100 μm

sections most active with inflammatory infiltration. This region of interest showed a significantly higher concentration of KDM4B protein (**Figure 3.1A**), indicating that KDM4B protein levels correlate with immune activation in periodontal disease. The experimental inhibitor ML324 has also been shown to inhibit the related demethylase KDM4E,[212] but this protein is not found in mice. Therefore, tissue sections from periodontally diseased human patients and healthy controls were stained for both KDM4E and KDM4B using immunohistochemistry. The connective tissue underlying the oral epithelium was chosen as the region of interest for analysis. A statistically significant increase in both KDM4B and KDM4E abundance was observed in diseased versus healthy tissues (**Figure 3.1B**), demonstrating that KDM4 enzymes are implicated in periodontal disease status.

3.2.b. ML324, previously defined as a KDM4E inhibitor, shows inhibitory activity against KDM4B.

ML324 was docked into the active site of the KDM4A-E family in flexible mode, and was found to have high computational selectivity for the KDM4B active site (**Figure 3.2A**). ML324 exhibited a lower average binding energy to the KDM4B active site (-53.04 kcal/mol) for the top 30 conformers versus KDM4E (-42.52 kcal/mol). Additionally, we used an Alphascreen® assay to determine the effect of ML324 on the demethylation activity of KDM4B. Here we show that ML324 has inhibitory activity towards KDM4B, with an IC_{50} value of 4.9 μM (**Figure 3.2B**). Additionally, we have defined the EC_{50} of ML324 for translational immunosuppression in primary macrophages to be 31 μM (**Figure 3.2C**). IL-6 production drives periodontal disease pathogenesis, therefore the ability of ML324 to effectively reduce the production of this cytokine emphasizes the potential of KDM4B inhibitors as therapeutics for PD treatment.

3.2.c. KDM4B inhibition using ML324 results in a significantly reduced cytokine immune response to Aa-LPS in macrophages.

After a 1-hour pre-tr eatment with ML324 (50 μM) followed by an inflammatory *Aa*-LPS challenge (100 ng/mL), ELISA and PCR analysis revealed that the KDM4B inhibitor ML324 significantly reduced the levels of inflammatory cytokines in primary murine macrophages (**Figure 3.3A-D**). At 8- and 24-hour time points and in both male and female cells, ML324 was able to significantly reduce IL-6 and TNF-α transcription and translation compared to LPS treatment with vehicle control (DMSO). A pan-selective KDM4 family inhibitor, JIB-04, was also able to produce this effect in most groups, but with a more variable response. As expected, GSK-LSD1, a KDM1A inhibitor, produced either no

change or a significant increase compared to vehicle controls in the majority of groups. These data demonstrate not only that KDM4B inhibition reduces inflammatory cytokine production but also that this effect is specific to KDM4B over the KDM4 family as a whole. It is important to note, however, that enzyme kinetics and mode of binding of ML324 to KDM4B have not been described, although the *in vivo* pharmacokinetics and ADME properties of this compound are extremely favorable.[212] Additionally, this data shows that as hypothesized, the activity of KDM4B and KDM1A are negatively correlated; and that inhibiting KDM1A via GSK-LSD1 gives an opposing effect on inflammatory cytokine production compared to KDM4B inhibition using ML324.

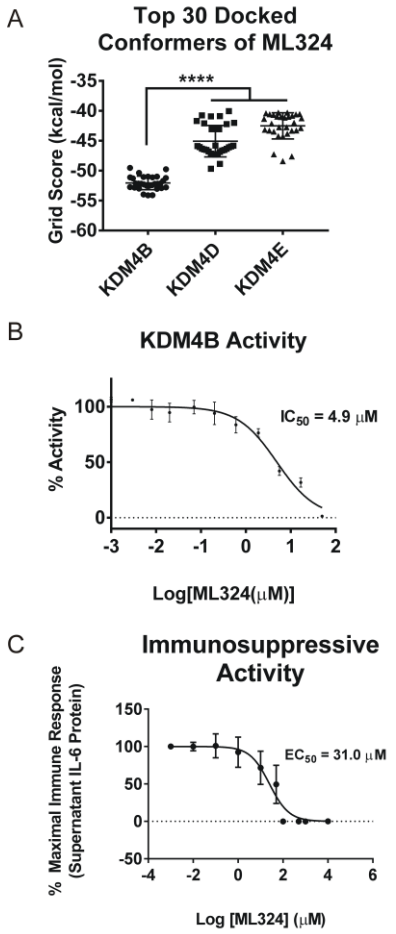

Figure 3.2. ML324 demonstrates inhibitory activity towards KDM4B and causes dose dependent immunosuppression. The KDM4A-E protein crystal structures were subjected to unbiased docking of ML324 where the top 30 conformers in the active site were used for analysis (A). KDM4A and C had no poses of ML324 dock into the active site of these enzymes, therefore this data is not displayed. Inhibition of KDM4B was assessed using an 11-point IC_{50} determination using the histone demethylase AlphaScreen (PerkinElmer) assay in triplicate resulting in an IC_{50} of 4.9 μM (B). The EC_{50} for immunosuppression using ML324 was determined to be 31 μM by measuring supernatant IL-6 protein following a 24h *Aa*-LPS stimulation with variable concentrations of ML324 in primary BMDM cells (C). Cells were treated for 1h with each indicated concentration of ML324, followed by Aa-LPS challenge for 24h. The data were normalized as a percentage of the maximal IL-6 response in response to LPS. Data for all panels are represented as mean ± SD. N=4

3.2.d. KDM4B inhibition using ML324 results in a significant reduction in osteoclastogenesis.

After 5 days of priming bone marrow-derived hematopoietic stem cells into pre-osteoclasts using macrophage colony stimulating factor (M-CSF) and receptor activator of nuclear factor kappa β ligand (RANK-L), osteoclastogenesis was significantly increased in cells treated with RANK-L or Aa-LPS for 3 days compared to PBS treated cells, and this effect was lost in cells pre-treated with ML324 (10 μM). TRAP+, multinucleated cells were significantly increased in both cells treated with Aa-LPS as well as RANK-L compared to PBS treated control cells. By contrast, in cells that were pre-treated with ML324, there was

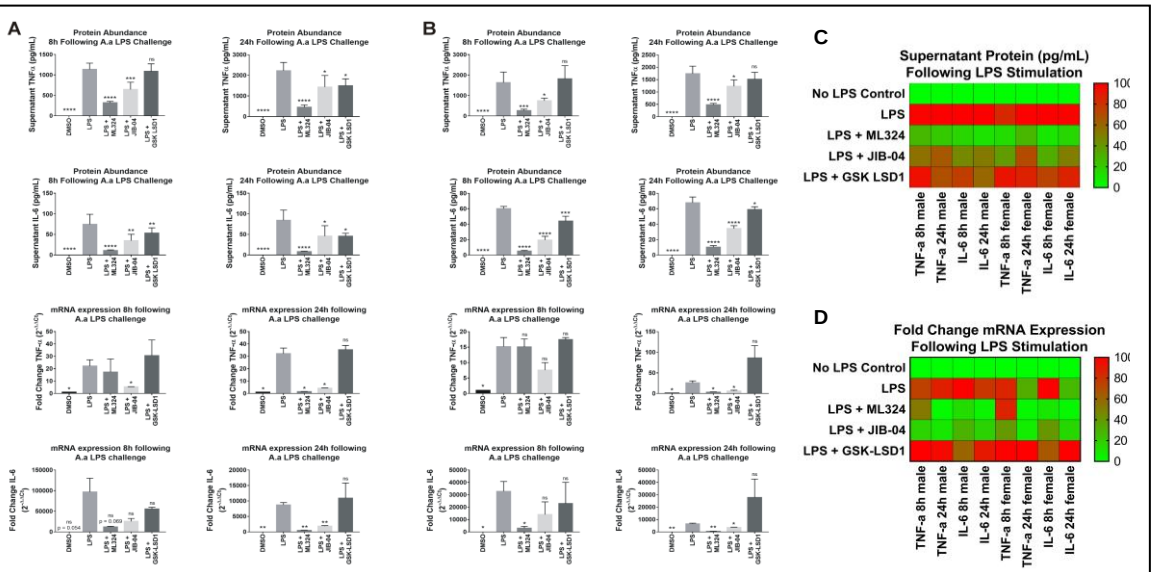

Figure 3.3. KDM4B inhibition significantly reduces the *A.a* LPS-induced immune response in primary macrophages. Male (A) and female (B) murine bone marrow derived macrophages were pre-treated for 1h with the selective KDM4B inhibitor, ML324, a family-wide KDM4 inhibitor, JIB-04, and a KDM1A inhibitor, GSK-LSD1 or DMSO vehicle. Following drug treatment, cells were challenged with *Aa*-LPS for 8 and 24h, where gene expression and supernatant protein concentration were measured via rt-qPCR relative to GAPDH and ELISA relative to a standard curve. Data was normalized as a percentage of the maximal response (red) in each group for display. (C,D). N=4 per experiment, data is representative of 3 experiments. Data are presented as mean ± SD. Statistical significance was determined using a repeated measures ANOVA with multiple comparisons. ***p<0.001, **p<0.01, *p<0.05 compared to same sex LPS controls. N=4 per experiment, data is representative of 3 experiments.

no significant difference in osteoclast formation compared to control groups, regardless of

whether cells were stimulated with Aa-LPS or RANK-L. Additionally, formed osteoclasts appeared smaller, and had less intense TRAP staining **(Figure 3.4).**

3.2.e. Immunosuppressive effects of KDM4B inhibition act indirectly, through demethylation of H3K4 by KDM1A.

To understand the mechanism for KDM4B inhibition induced immunosuppression, we used the RAW264.7 macrophage cell line, which is the best representation of primary

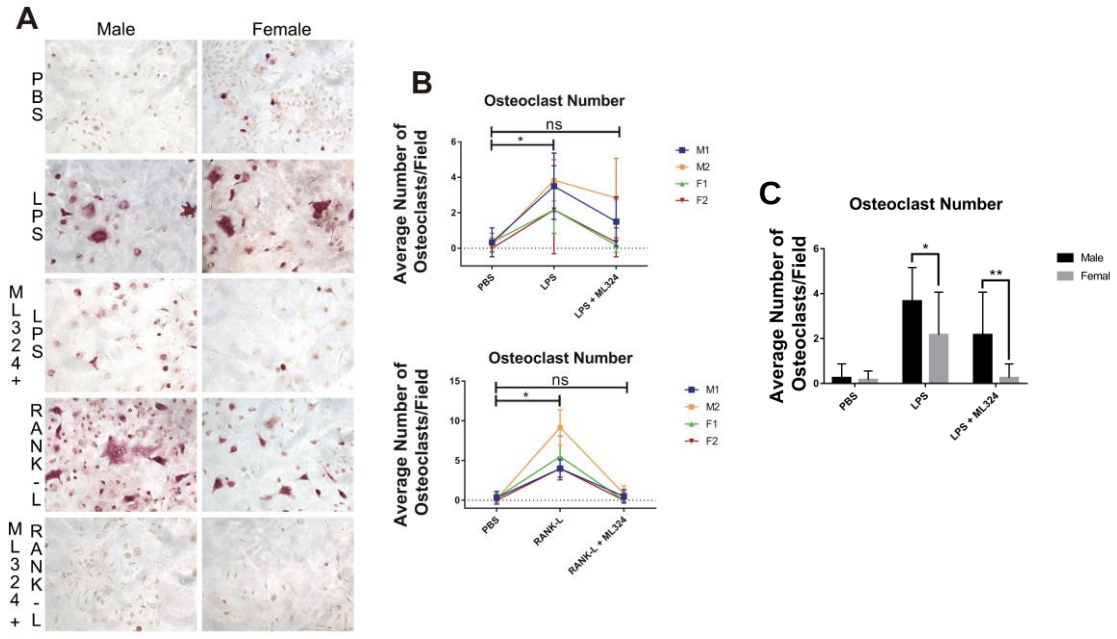

Figure 3.4. KDM4B inhibition via ML324 prevents osteoclast formation induced by either *A.a* LPS or RANK-L. Murine bone marrow was differentiated into osteoclasts by supplementation of the hematopoietic compartment with M-CSF for 3 days and RANK-L + M-CSF for 2 days, where cells were rinsed and pre-treated for 1h with M-CSF and ML324 or DMSO vehicle followed by supplementation with RANK-L or *A.a* LPS. After 72 hours, cells were fixed and stained for tartrate resistant acid phosphatase. 3 representative images were taken of each well, and TRAP+, multinucleated cells were counted in each field. 10x representative images of M1 and F2 are displayed. (**A**) Each mouse (M1, M2 = male; F1, F2 = female) independently showed a significant increase in osteoclast formation in response to LPS or RANK-L alone compared to PBS controls, but no significant difference in osteoclast formation was observed between PBS and ML324 + LPS or ML324 + RANK-L treated cells (**B**). Male cells exhibit increased osteoclastogenesis in response to RANK-L or *A.a* LPS compared to female cells. (**C**) Data is presented as the mean number of osteoclasts in each field ± SD. Statistical significance was determined using a paired Friedman test or two-way ANOVA with multiple comparisons at an α = 0.05. *p<0.05, **p<0.01 n = 3 fields per well, 2 wells per group, per mouse.

bone marrow derived macrophages.[227] Interestingly, when cycloheximide (5 µg/mL) was co-administered with ML324 (50 µM) prior to Aa-LPS challenge in these cells, the ability

of ML324 to reduce LPS-induced cytokine production is lost (**Figure 3.5A**). Because cycloheximide inhibits eukaryotic translation, this data indicates that ML324-induced immunosuppression relies on new protein synthesis, and that the reduced cytokine response to LPS is not a direct effect of KDM4B inhibition, but rather requires intracellular signaling.

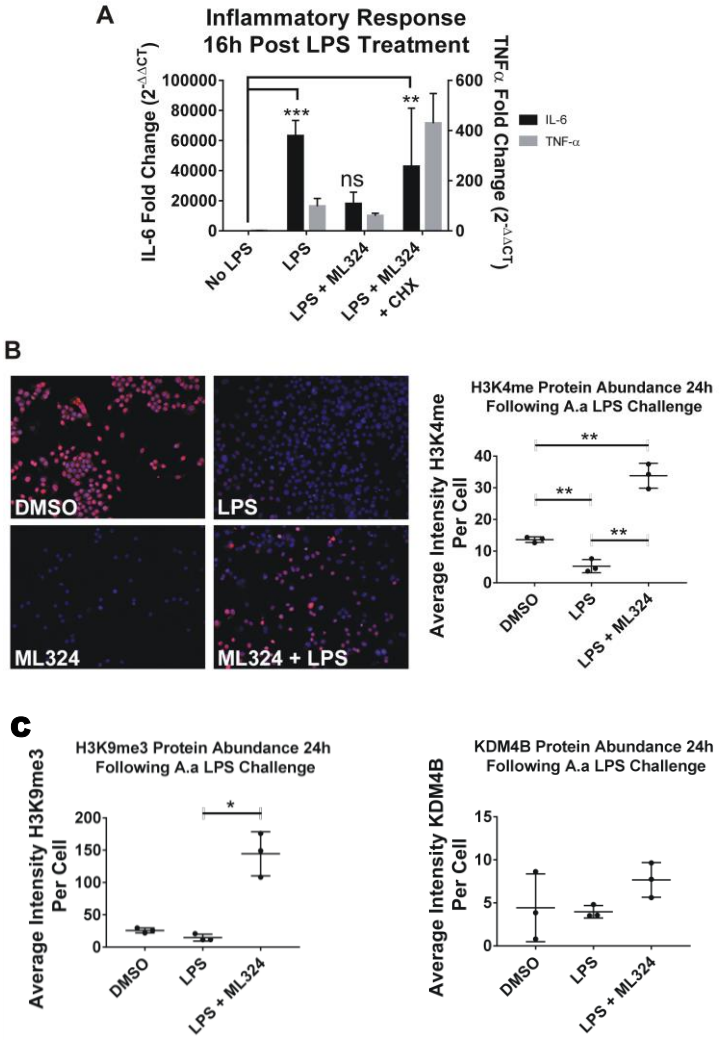

Figure 3.5. KDM4B inhibition mediated immunosuppressive effect is indirect, requiring new protein synthesis and increased KDM1A activity. New protein synthesis is required for the immunosuppressive effects of ML324 on the LPS-induced immune response (A). Cells were pre-treated with cycloheximide (5ug/mL) for 4 h with or without ML324 (50 μM) followed by *Aa*-LPS challenge (100ng/mL) for 16h where RNA was collected and analyzed using qRT-PCR to measure IL-6 expression compared to GAPDH as an endogenous control. Statistical significance was determined using a repeated measures ANOVA with multiple comparisons. Demethylation at H3K4 is significantly decreased in cells following LPS treatment, but the effect is reversed upon addition of ML324. (B) ML324 treatment causes a significant increase in H3K9me3 but not KDM4B, and these marks are not affected by LPS treatment alone. (C) RAW264.7 cells were pre-treated for 1h with ML324 followed by *Aa*-LPS challenge for 24h where H3K4 mono-methylation was measured in fixed cells using immunofluorescent antibody to H3K4me at 10x. KDM1A activity is significantly decreased following *Aa*-LPS treatment alone, but in combination with ML324 pretreatment, KDM1A activity is increased. n = 3 wells, 48 fields/well, **p<0.01. Data are represented as mean ± SD. Statistical significance was determined using one-way ANOVA with multiple comparisons where the outcome was log transformed.

To determine if the cellular response to LPS altered KDM4B expression levels, we used a bioinformatics database (NCBI Gene Expression

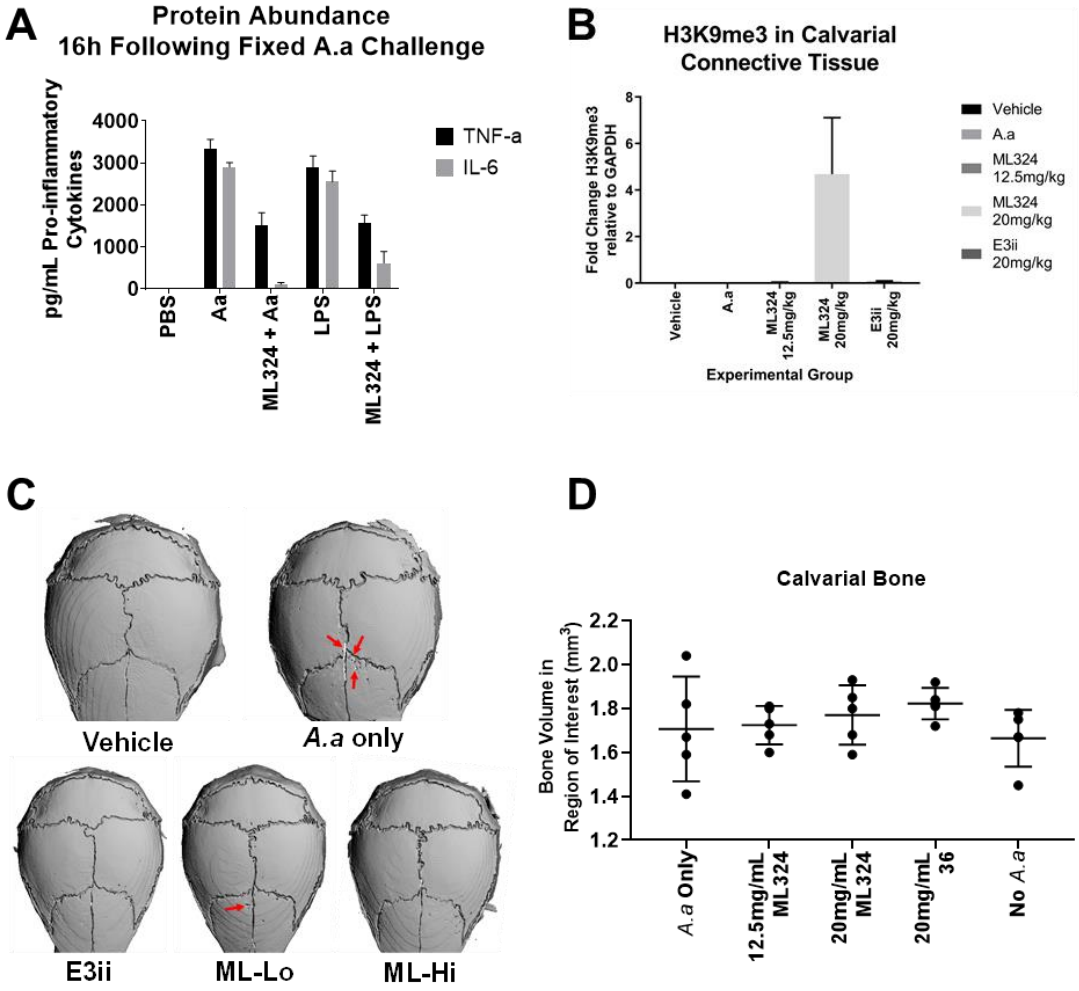

Figure 3.7. KDM4B inhibition reduces *A.a.*-induced inflammation *in vitro* and modifies calvarial bone loss pattern *in vivo*. ML324 reduced fixed *A.a* induced inflammatory cytokine production in bone marrow derived macrophages. (A) 12-week old C57BL/6 were injected subcutaneously and supraperiosteally at the mid-sagittal suture daily for 5d with either *A.a* alone, *A.a* + drug or DMSO as a negative control. Mice were sacrificed on day 6, where calvarial tissue was homogenized and protein isolated for western blot analysis of H3K9me3 compared to GAPDH as internal control. (B) Calvarial bones were dissected and micro-computed tomography was run using a Scanco40 instrument at a 15µm resolution.(**C**) A region of interest was defined as a 150 mm^3 cylinder centered at the bregma point (intersection of the frontal and parietal bones at the midline). Total bone volume at this area was quantified using AnalyzePro software. (**D**) Significance was determined using one-way ANOVA with multiple comparisons.

Omnibus (GEO) profiles). There was no change in mRNA expression of KDM4B in response to LPS, suggesting that the activity of KDM4B as opposed to its expression level drives the immune response to LPS. Further, KDM4A, KDM4C, and KDM4D also show no significant differences in expression in response to LPS. To confirm that the activity of

KDM4B was altered in response to LPS, the histone methylation marks H3K4me and H3K9me3 were monitored by immunofluorescence following ML324 pre-treatment (50 μM) and Aa-LPS challenge. Concurrent with the absence of change in mRNA levels of KDM4B, there was no significant difference in KDM4B protein levels between groups (**Figure 3.6**). In contrast, the activity of KDM4B was decreased following ML324 pre-treatment as evidenced by a significant increase in H3K9me3. Interestingly, there was not a significant difference between control and LPS treated cells (**Figure 3.5B**). Conversely, H3K4me levels significantly decreased following *A.a*.LPS challenge, but ML324 pre-treatment not only reversed this effect, but caused a significant increase in H3K4me levels compared to PBS controls (**Figure 3.5B**). These data together suggest that H3K4 methylation is differentially regulated by inflammatory stimuli in macrophages, and this activity can be modulated indirectly through pharmacological inhibition of KDM4B.

3.2.f. KDM4B inhibition using ML324 and Experimental Inhibitor 36 Results in Altered *A.a*-Induced Bone Loss Phenotype

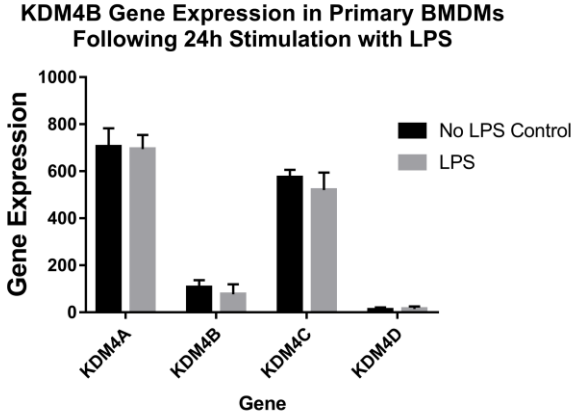

Figure 3.6. KDM4 family gene expression is unaltered in response to LPS treatment. KDM4A-D mRNA expression in primary bone marrow derived macrophages following lipopolysaccharide stimulation for 24h. Data were obtained from NCBI Gene Expression Omnibus profiles (http://www.ncbi.nlm.nih.gov/geoprofiles; Reporter: GPL1261; Record: GDS5196)

To recapitulate the anti-inflammatory effects of ML324 treatment *in vitro*, we used a 5-day murine calvarial model of periodontal disease using Aggregatibacter actinomycetemcomitans induced bone loss to probe the *in vivo* efficacy of KDM4B inhibition. First, we verified

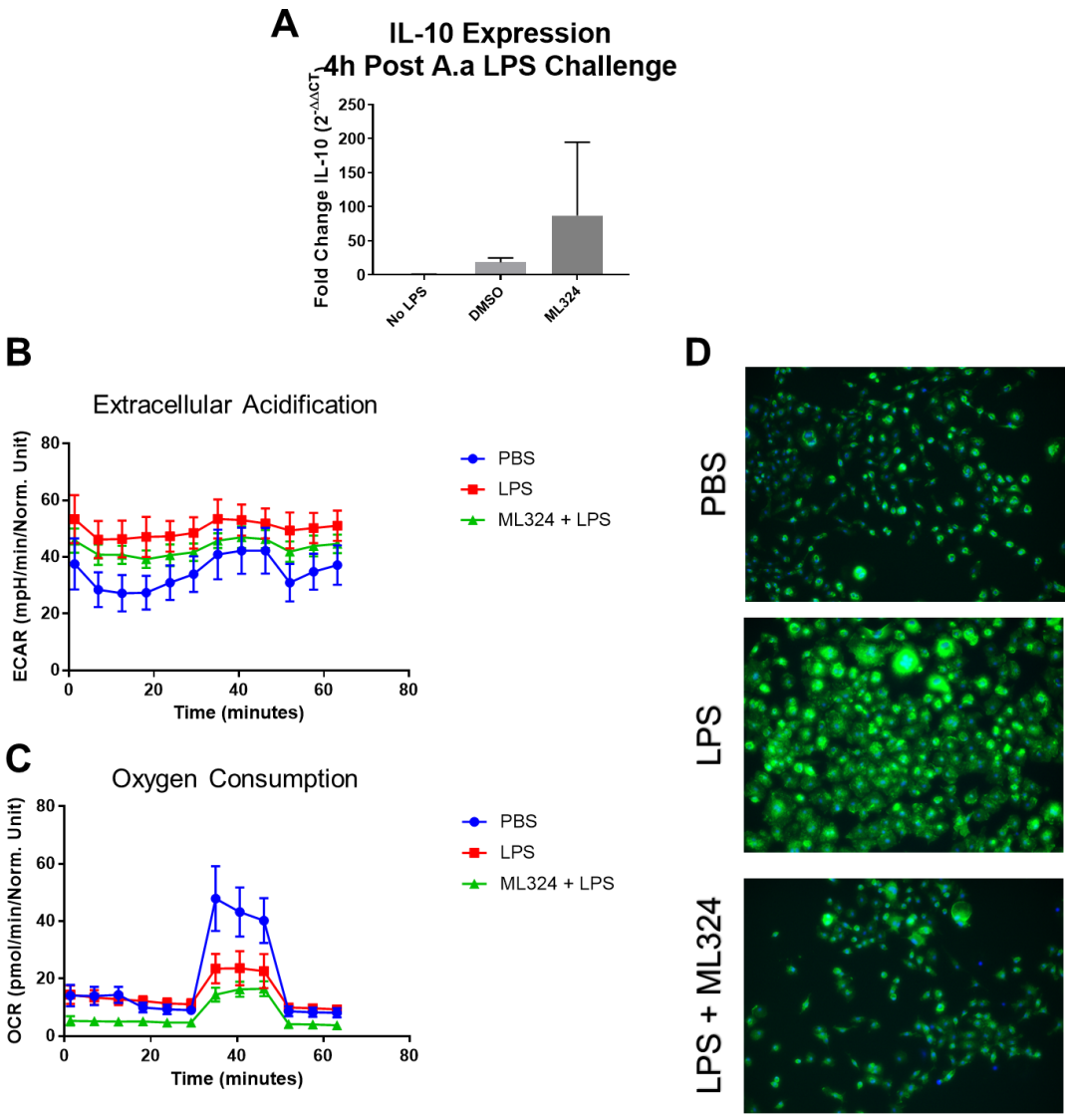

Figure 3.8. ML324 alters macrophage polarization. KDM4B inhibition alters macrophage metabolism in response to A.a LPS. Primary BMDMs were isolated and differentiated as previously described and were pre-treated with ML324 at 50uM for 1 hour followed by A.a LPS (100ng/mL). 24 hours later, extracellular flux was analyzed using a seahorse XFe96 instrument and following metabolic analysis, cells were incubated with phalloidin 488 and DAPI. Representative images were acquired using the Hermes Wiscan system at 10x for morphological analysis. N=4.

that ML324 was able to reduce fixed *A.a* induced cytokine production, as all previous experimentation was done using isolated LPS from *A.a.* We found that ML324 significantly reduced *A.a*-induced inflammatory cytokine production to the same degree that it was

previously shown to inhibit *A.a* LPS-induced inflammatory cytokine production. (**Figure 3.7A**) Mice were injected subcutaneously supraperiosteal to the calvarial bone with both fixed whole *A.a* or PBS control and ML324, **36** or DMSO control for 5 days, and calvariae and tissues overlying the calvarial bone were collected following sacrifice. We found that in ML324 treated animals, H3K9me3 protein abundance was higher on average although insignificant, suggesting the effect was on target and that KDM4B was indeed inhibited *in vivo*. (**Figure 3.7A**) Unfortunately, we didn't observe this effect with the experimental inhibitor we tested, **36.** This could be due to absorbance or metabolism issues, as neither of these things were tested in our experimentation. Using micro-computed tomography, we analyzed total bone volume for a specific region of interest that spans 10mm x 10mm centered over the mid sagittal suture between the anterior and posterior calvarial bone. (**Figure 3.7C**) Unfortunately, there was a highly variable and not robust enough response to *A.a* treatment to discern any significant differences in our treatment groups. (**Figure 3.7D**) We did, however, observe a very consistently high average bone volume within our region of interest for both ML324 and **36** treated animals. (**Figure 3.7B**) Overall, these data suggest that KDM4B inhibition may serve as a useful therapeutic intervention for prevention of periopathogen-induced bone resorption *in vivo*, but further experimentation is needed.

3.2.g. ML324 alters *A.a* LPS-induced macrophage polarization

As previously mentioned, literature suggests that KDM4B may be involved in macrophage polarization,[46, 228-229] therefore we wanted to test whether ML324-induced immunosuppression was due to M2 polarization or de-differentiation of macrophages. Primary BMDMs were isolated and differentiated as previously described and were pre-

treated with ML324 at 50 μM for 1 hour followed by *A.a* LPS (100ng/mL). 24 hours later, mRNA was isolated and IL-10 expression was quantified using qRT-PCR and ML324 pre-treated cells were found to have significantly higher IL-10 expression. (**Figure 3.8A**) To determine if macrophages were M2 polarized, Extracellular flux was analyzed using a seahorse XFe96 instrument as previously described.[230] We found that LPS treated cells are more glycolytic than PBS control cells, and ML324 pre-treatment rescued this effect. (**Figure 3.8B**) Additionally, cells treated with LPS, with or without ML324 exhibit a reduced spare respiratory capacity compared to PBS control treated cells. (**Figure 3.8C**) These data suggest that ML324 pre-treatment alters macrophage metabolism with an overall reduction in metabolic activity. To further probe macrophage polarization, we fluorescently stained both the cytoplasm and nuclei of cells to visualize cell morphology, as clear morphological differences are known to exist between M0 (un- or de- differentiated macrophages), M1 (pro-inflammatory) or M2 (anti-inflammatory) macrophages.[231] We found that LPS treated macrophages exhibited an M1 phenotype, and ML324 pre-treatment was able to rescue this effect, appearing very similar to PBS control treated cells. (**Figure 3.8D**)

Chapter 4: Discovery of anti-periodontitis biphenyl-carboxamido-benzoic acids via Phenotypic Screening Guided QSAR.

4.1. Rationale and Hypothesis

Previous data from the project laboratory implicates KDM4B as a regulatory enzyme in periodontal disease progression through its role in suppressing both osteoclastogenesis and inflammatory cytokine production in primary macrophages.[232] The exacerbated immune response of the periodontally diseased host is well known in the

literature to be the source of the tissue damage and bone loss characteristic of the disease.[50] Still, therapeutic development has been aimed towards local antimicrobials such as chlorhexidine (PerioChip), doxycycline (Periostat) and minocycline (Arestin). Nevertheless, these therapies provide a moderate clinical benefit at best,[7] and require strict patient compliance with visits required as often as every three months, which is rarely covered by insurance premiums. While the microbial component of periodontal disease is indeed critical to disease pathogenesis,[50, 64, 233] these therapies are applied by clinicians following standard of care treatment – which is to remove plaque biofilms through scaling and root planning (SRP), effectively leaving little to no microbial load immediately following treatment.[233] Disease recurrence is driven rather by a continuation of immune activation and an inability for the periodontal wounds to heal.[234-235] Given this information, one can imagine that a local immunosuppressive drug would afford some benefit, allowing the host immune system to resolve, wounds to heal, and ultimately preventing disease recurrence. The failure of previously explored anti-inflammatory agents is likely due to their surface level targets such as secreted effector proteins that do not cause heritable changes beyond single cell divisions. Epigenetic therapeutics offer an advantage in this regard as they seek to reverse detrimental environmental changes that have the ability to propagate harmful disease processes.

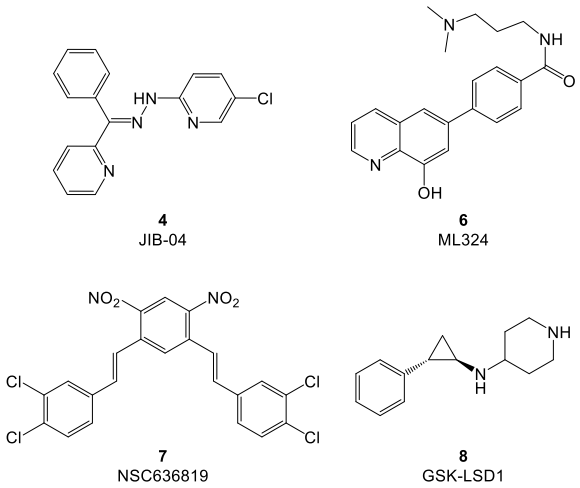

Figure 4.1. Compounds used to physicochemically cluster screening data. Compounds **4,6 and 7** are previously published KDM4B inhibitors. Compounds **8** is a KDM1A inhibitor.

In 2012, the NIH molecular libraries program reported the discovery of *N*-(3-(dimethyamino)propyl-4-(8-hydroxyquinolin-6-yl)benzamide(**1**), a small molecule inhibitor specifically targeting KDM4E.[212] While this compound was shown to inhibit viral replication of herpes simplex virus and cytomegalovirus, and later shown to induce depression in mice at high doses,[236] the compound was not probed for additional activity. We recently reported that ML324**, 8,** is active toward a closely related enzyme, KDM4B, and has immunosuppressive action in murine macrophages.[232] While this compound exhibits good

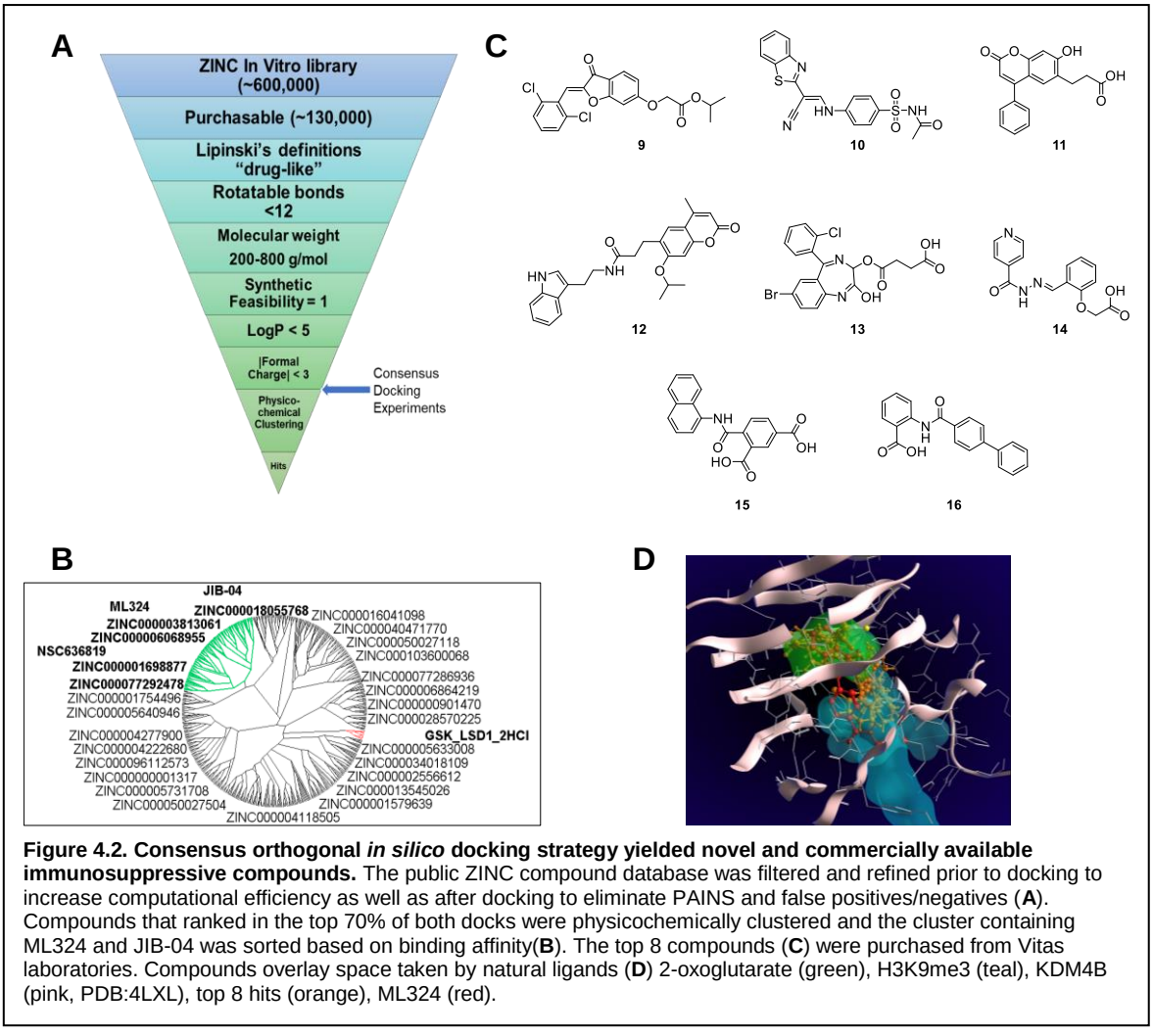

Figure 4.2. Consensus orthogonal *in silico* docking strategy yielded novel and commercially available immunosuppressive compounds. The public ZINC compound database was filtered and refined prior to docking to increase computational efficiency as well as after docking to eliminate PAINS and false positives/negatives (**A**). Compounds that ranked in the top 70% of both docks were physicochemically clustered and the cluster containing ML324 and JIB-04 was sorted based on binding affinity(**B**). The top 8 compounds (**C**) were purchased from Vitas laboratories. Compounds overlay space taken by natural ligands (**D**) 2-oxoglutarate (green), H3K9me3 (teal), KDM4B (pink, PDB:4LXL), top 8 hits (orange), ML324 (red).

cell permeability, it is highly insoluble at effective doses and requires a 14-step synthesis

for development of new derivatives.[212] Because of this, we sought to determine novel scaffolds with the potential to inhibit KDM4B, cause immunosuppressive effects, and potentially serve as optimizable compounds for localized treatment of periodontal disease.

The current study utilized a multidisciplinary approach that combined consensus computational docking data with phenotypic screens using primary murine macrophages

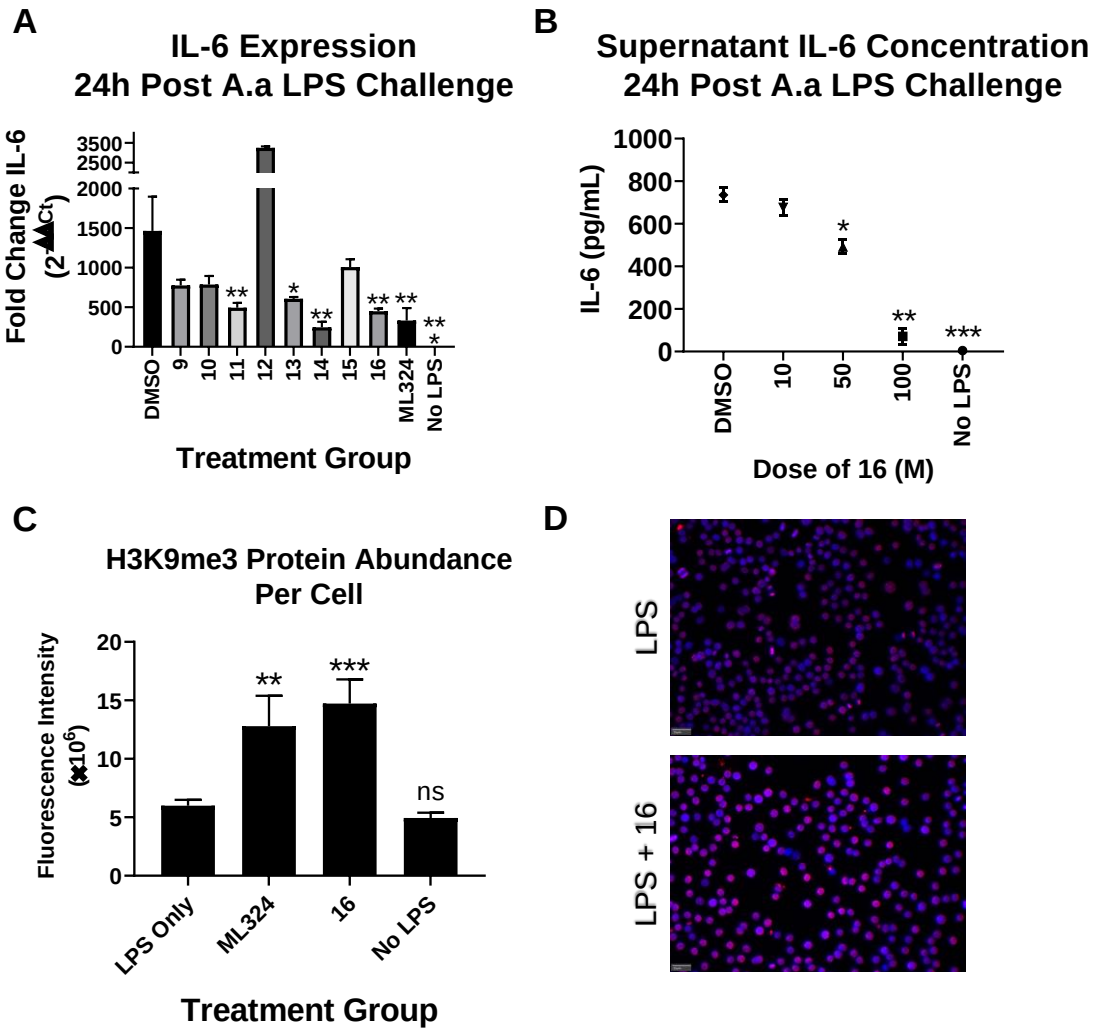

Figure 4.3. Phenotypic screening data for compounds identified by in silico docking suggests compound 16 is a promising hit for further development. Several initial hits caused suppressed the immune response to *A.a* LPS *in vitro*. (A) n=2 Compound 16 was further evaluated for dose-dependent immunosuppression, N = 4 (B) as well as for KDM4B inhibitory activity through measurement of H3K9me3 using fluorescent immunostaining, N = 3. (C,D) *p<0.05, **p<0.01, ***p<0.001 compared to DMSO control via one-way ANOVA with multiple comparisons.

to identify a derivatizable scaffold with KDM4B inhibitory action. We further used this strategy to optimize our lead compounds and ultimately identified compound **46** as a

Table 4.1. Novel compounds synthesized.

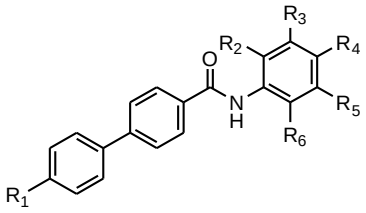

Scaffold 1

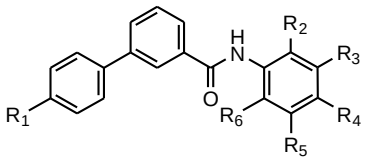

Scaffold 2

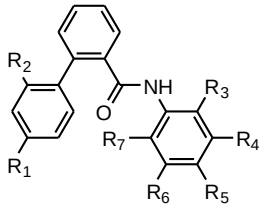

Scaffold 3

Compound	Scaffold	R_1	R_2	R_3	R_4	R_5	R_6	R_7
16	1	H	COOH	H	H	H	H	H
23	1	H	COOH	H	H	H	CH3	H
24	1	H	COOH	H	F	H	H	H
25	1	H	COOH	H	H	H	F	H
26	1	H	COOH	H	H	F	H	H
27	1	H	H	COOH	H	H	H	H
28	1	H	H	H	COOH	H	H	H
29	2	H	COOH	H	F	H	H	H
30	2	H	COOH	H	H	F	H	H
31	3	H	H	COOH	H	H	H	H
32	3	H	H	COOH	H	H	H	CH3
33	3	H	H	COOH	H	F	H	H
34	3	H	H	COOH	H	H	H	H
35	3	H	H	H	COOH	H	H	H
36	3	CH3	H	COOH	H	H	H	CH3
37	3	O-Me	H	COOH	H	H	H	H
38	2	H	COOH	H	H	F	CH3	H
39	2	H	COOH	H	H	H	F	H
40	3	H	H	COOH	H	H	H	CH3
41	3	H	H	COOH	H	H	H	H
42	1	CH3	COOH	H	F	H	H	H
43	3	CH3	H	COOH	H	F	H	H
44	3	H	O-Me	COOH	H	H	H	CH3
45	2	CH3	COOH	H	H	H	CH3	H
46	2	H	COOH	H	H	H	H	H

potent immunosuppressive compound that could be used to treat periodontal disease

4.2. Results

4.2.a. Consensus computational docking followed by physicochemical clustering yields commercially available immunosuppressive compounds

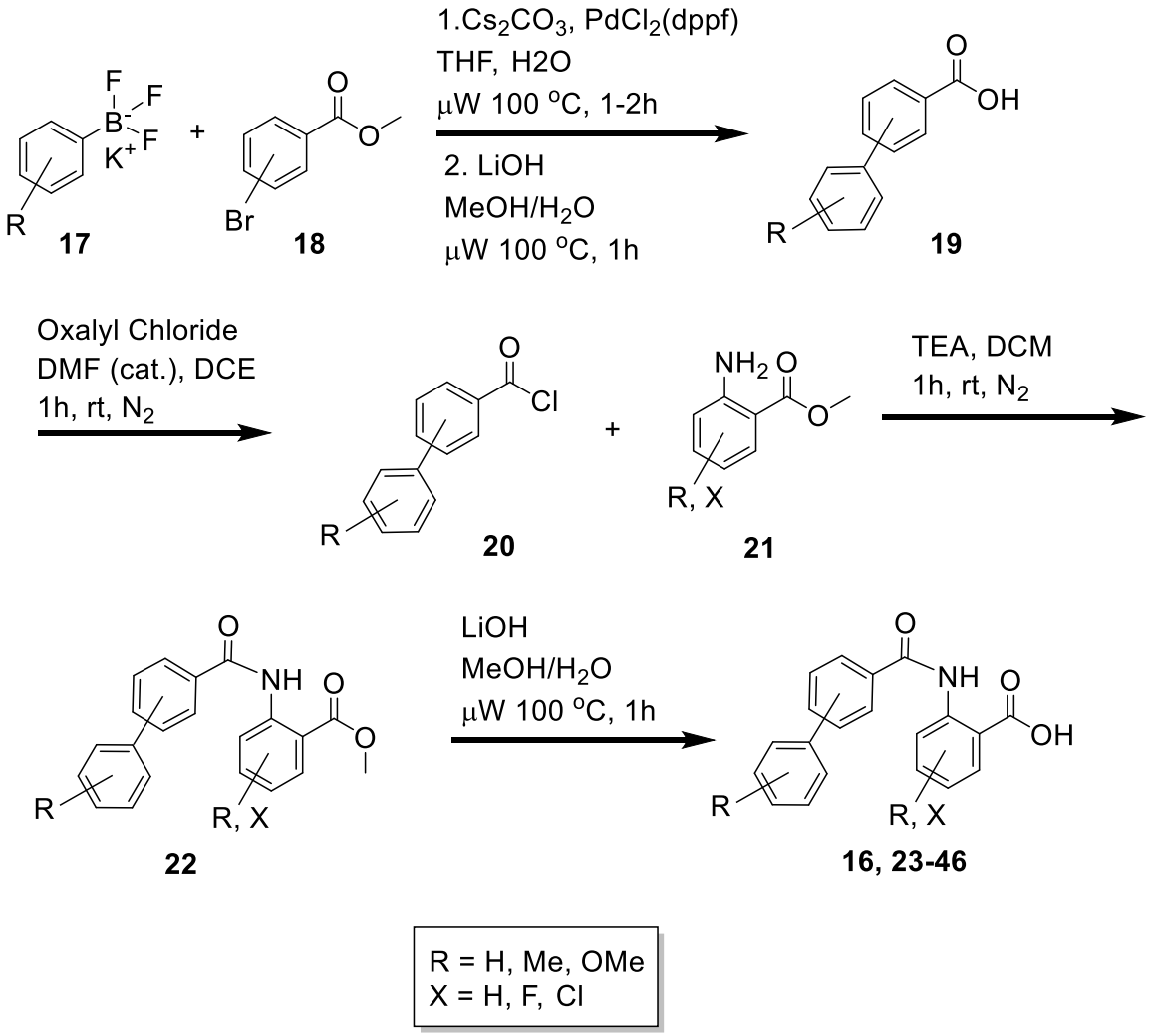

Scheme 4.1. Synthetic method for development of biphenyl carboxamido benzoic acids.

The ZINC database of molecules[237] was filtered to retrieve compounds that were proposed to have *in vitro* activity as well as compounds that could be purchased. This library was further filtered to remove any potential pan-assay interference compounds (PAINS)[238] as

well as compounds with Lipinski violations, cytotoxic or unfavorable features[239] (**Figure 4.2A**). The remaining compounds were subjected to high throughput screening for activity towards the KDM4B active site using two separate software programs (DOCK6.5,

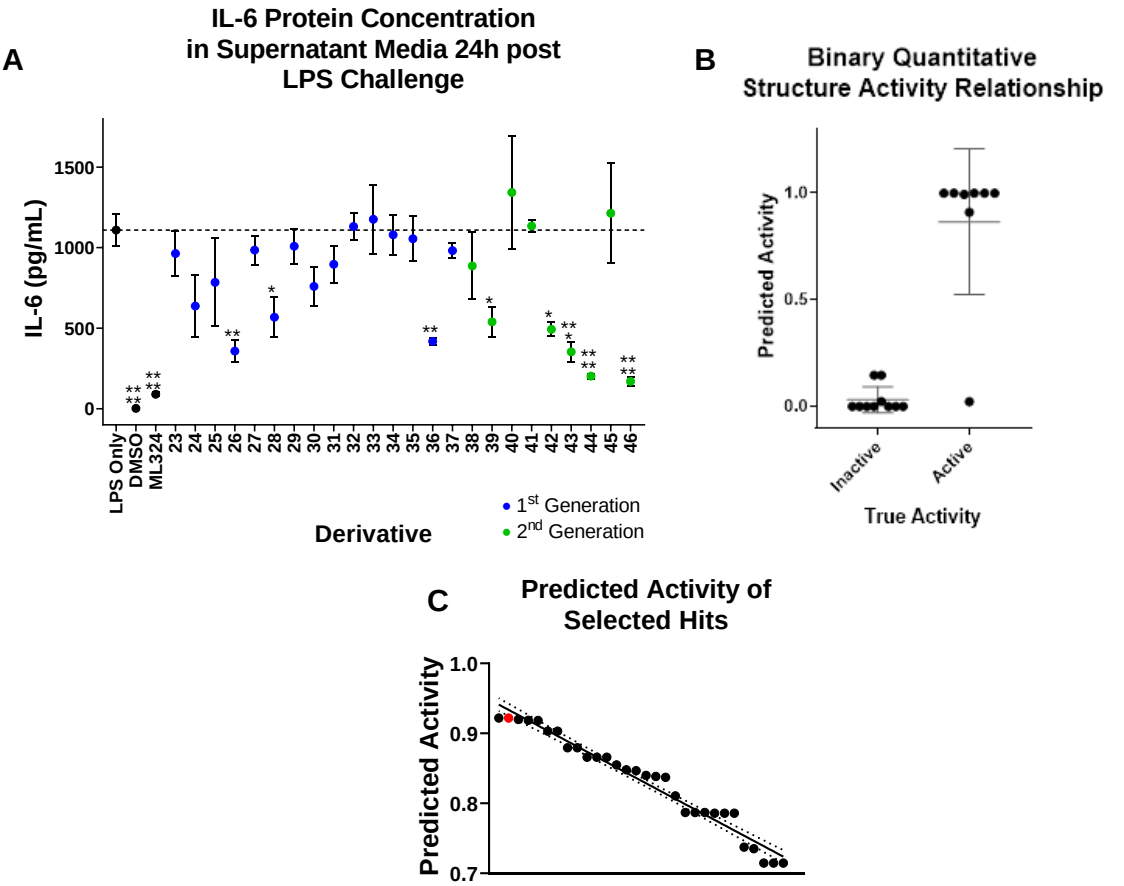

Figure 4.4. Derivatives of 16 cause immunosuppression and were used to develop a binary QSAR model. The phenotypic immunosuppressive screen data (**A**) was converted into binary data using statistical significance ($P<0.05$) as a cutoff. A contingency analysis was run on the tested compounds to identify the physicochemical descriptors that were most highly correlated with activity. The top 12 descriptors from this analysis were used (**Table 4.2**) to map a quantitative structure activity relationship using Molecular Operating Environment software that had accuracy to predict actives of 100% and inactives of 100% (**B**). 30 compounds were predicted to have activity with >70% confidence, and this subset included our current lead compound 42 (red). (**C**) *p<0.05, **p<0.01, ****p<0.0001 compared to DMSO control via one-way ANOVA with multiple comparisons.

Molecular Operating Environment). The consensus activity data[240] was consolidated into 8,000 top compounds that were clustered based on similarity of their physicochemical properties[241] (**Figure 4.2B**) and the top compounds that were physicochemically similar to

previously identified KDM4B inhibitors[212, 242-243] were purchased for *in vitro* evaluation (**Figure 4.2C,D**).

4.2.b. 2-([1,1'-biphenyl]-4-carboxamido)benzoic acid causes dose-dependent immunosuppression and increased H3K9me3

Several compounds from this initial clustered data set were active and suppressed the immune response to *A.a* LPS at 50 μM (**Figure 4.3A**). We decided to move forward with **11** because of its three membered structure and multiple routes of straight forward combinatorial chemistry-based synthesis. Before investing significant time in development of derivatives of **12**, we confirmed a dose-dependent immunosuppressive response to *A.a* LPS (**Figure 4.3B**) with a concurrent increase in H3K9me3 (**4.3C, D**), suggesting the effect was on target.

4.2.c. Development of efficient synthetic methods for 2-([1,1'-biphenyl]-4-carboxamido)benzoic acid derivatives

Sixteen derivates (**Table 4.1**; **13-28**) were synthesized using a 5-step microwave assisted synthesis from derivatized bromobenzenes, phenyltrifluorborates and 2-amino benzoates (**Scheme 4.1**). Potential compounds were developed *in silico*, using commercially available and economical starting materials. This library was docked to the active site of KDM4B using consensus screening and hits were ranked based on binding affinity. Top derivatives predicted by consensus scores as well as easy to synthesize derivatives were synthesized. The first step of synthesis was a microwave assisted Suzuki coupling of a bromobenzene and trifluoroborate to yield a two-ringed ester. The second

step was microwave-assisted saponification to cleave the ester into a reactive carboxylic acid. The third step was further activated the carbonyl into a carbonyl chloride followed by addition of an aminobenzoate under basic conditions to yield the final three-membered ester. The resulting ester was cleaved in the final step using the same microwave-assisted saponification reaction to increase solubility of the final compounds.

Table 4.2. QSAR model descriptors and classes.

Physicochemical Descriptor	Descriptor Class
balabanJ	Adjacency and distance matrix
BCUT_SLOGP_2	
diameter	
GCUT_PEOE_1	
radius	
VDistEq	
wienerPath	
wienerPol	
Kier2	Kier and Hall connectivity and kappa shape
Kier3	
KierA3	
PEOE_VSA+0	Partial charge

4.2.d. 2-([1,1'-biphenyl]-4-carboxamido)benzoic acid derivatives prevent inflammatory cytokine production in primary macrophages stimulated with *A.a* LPS

Derivatives were monitored for *in vitro* immunosuppressive activity using the previously described periodontal disease inflammation model[232] using primary murine macrophages. **22, 24, 32** caused a significantly reduced secretion of the pro-inflammatory cytokine, IL-6, in response to *A.a* LPS. (**Figure 4.4A**) resulting in an overall hit rate of 20%. Compounds that significantly reduced inflammatory cytokine production compared to DMSO controls as determined by one-way ANOVA with multiple comparisons were set as actives while those that did not were set as inactives. These data were consolidated into a binary quantitative structure activity relationship, where descriptors were chosen based on contingency analysis (**Table 4.2**). Overall the model had an accuracy of 100% with a

60% chance value. This model had an 100% accuracy to predict active hits with a 28% chance value and a 100% accuracy to predict inactive compounds with a 72% chance value (**Figure 4.4B**). The *in silico* library of derivatives was fit to this model and yielded 30 potential hits with greater than 70% chance of being active, one of which was one of our current leads, compound **42.** (**Figure 4.4C**) More importantly, several hits were eliminated

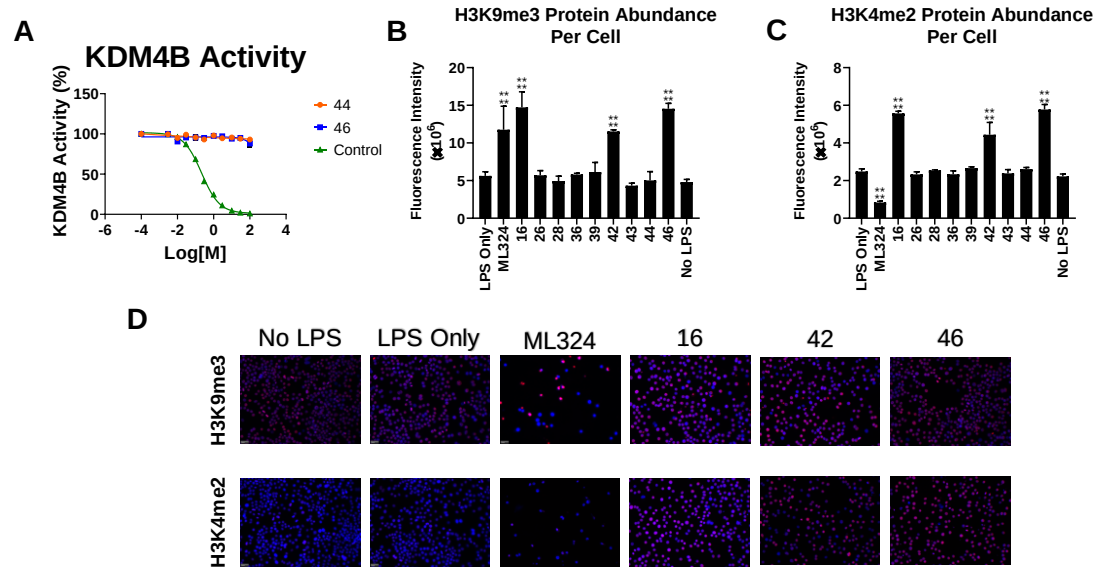

Figure 4.5. Potent immunosuppressive compounds do not inhibit KDM4B in biochemical assays, but show functional suppression of KDM4B activity *in vitro*. KDM4B activity was measured using an AlphaLISA® assay with experimental inhibitors 44 and 46, exhibiting an IC_{50} >100 μM. (A) H3K9me3 (B) and H3K4me2 (C) protein abundance was quantified in RAW264.7 macrophages 24h following *A.a* LPS challenge. Cells were fluorescently stained and 36 images per well were captured using a Hermes Wiscan imaging system. Total fluorescence intensity was normalized to cell number and statistical significance was determined using a one-way ANOVA with multiple comparisons. N=3, 36 images per well. *p<0.05, **p<0.01, ***p<0.001.

from the pool of potential hits with high confidence.

4.2.e. A binary quantitative structure activity relationship guided synthesis of potent immunosuppressors using phenotypic screening data

Our second generation (**34-42**) of inhibitors was synthesized (**Table 4.1**) and compound **35, 38-40 and 42** significantly reduced the secretion of IL-6 in response to *A.a* LPS *in vitro*. (**Figure 4.4**) The current lead compounds **44** and **46** were further evaluated

because of their potent immunosuppressive action rivaling that of the control compound, **1**. Surprisingly, using an AlphaLISA® KDM4B assay, we found that these compounds had no inhibitory activity for KDM4B at concentrations as high as 100μM. (**Figure 4.5A**) On the other hand, when we measured histone methylation marks as functional readouts in response to inhibitor treatment *in vitro*, we found that **42** and **46** were able to significantly increase H3K9me3 protein expression *in vitro*. (**Figure 4.5B. D)** Interestingly, while ML324 pre-treatment resulted in the expected decrease in H3K4me2, **16**, **42** and **46** all caused a significant increase in this mark. (**Figure 4.5C, D**) This suggests that these inhibitors may target a similar enzyme with additional activity at H3K4me2 or may indirectly cause inhibition of KDM4B through a process that is poorly recapitulated in biochemical assays using recombinant protein.

Chapter 5: General Discussion and Future Directions:

5.1. General Discussion

To date, there is limited mechanistic data concerning the epigenetic modulation of periodontal inflammation. A 2014 study by Meng et al. used a novel BET bromodomain inhibitor, JQ1, in an experimental periodontal disease model and found that a decrease in BRD4 recruitment led to a reduction in periodontal inflammation and subsequent bone loss.[244] Importantly, there have been no studies that suggest that any of the histone demethylases play a direct role in the progression or persistence of periodontal disease, despite the fact that numerous links between the KDM4 family of epigenetic modifiers and inflammation have been published. The study described herein demonstrates that inhibition of KDM4B reduces the pro-inflammatory cytokine immune response to bacterial

lipopolysaccharide in macrophages. This effect occurs through new protein synthesis and a subsequent overactivation of KDM1A. In the absence of KDM4B, macrophages do not produce these inflammatory signals, and thus modulation of KDM4B activity could be utilized to locally suppress the immune response to plaque and microbial biofilms in PD patients for the resolution of inflammatory disease states.

To determine whether KDM4B inhibition could be used as a therapeutic strategy to manage periodontal disease, we first demonstrated that the abundance of KDM4B protein is significantly increased in areas of inflammatory infiltrate marked by increased F4/80+ macrophage cells and increased tartrate resistant acid phosphatase (TRAP)+ osteoclastic cells following live A.a. subcutaneous injection into murine calvariae (**Figure 3.1A**).[245] The murine genome does not express KDM4E,[246] leading us to believe that the ML324-induced immunomodulatory effect is entirely dependent on KDM4B. However, it is likely that ML324 would also interact with KDM4E when administered in humans. Thus, we sought to determine whether one or both of these enzymes were overproduced in periopathogen-activated immune cells using human clinical PD tissues. Our results demonstrate that the abundance of both KDM4B and KDM4E protein is significantly increased in the oral epithelium of patients with periodontal disease, compared to healthy controls. (**Figure 3.1B**).

Based on computational studies, ML324 demonstrated promising selectivity for KDM4B (**Figure 3.2A**). Additionally, within the first 500 least energy docked poses, ML324 did not enter the active site of either KDM4A or KDM4C. ML324 is a methyl derivative of the 8-hydroxyquinoline compounds developed as selective KDM4B inhibitors, yet thus far the drug has only been published as an inhibitor of KDM4E with an IC_{50} of 920 nM. The synthetic route used to produce JIB-04 is depicted in **Scheme 3.1** and is described in

detail in the Experimental section. Herein we show that ML324 has additional inhibitory activity towards KDM4B, with an IC_{50} value of 4.9 μM (**Figure 3.2B**)[247] and an EC_{50} value for its immunosuppressive action *in vitro* of 31.0 μM (**Figure 3.2C**). JIB-04 is a pan Jumonji domain demethylase inhibitor that inhibits KDM4B with an IC_{50} of 435 nM, but is a more potent inhibitor of the related demethylases JARID1A and KDM4E. Another KDM4B inhibitor, NSC636819, has been identified with a substantially higher IC_{50} against KDM4B of 9.3 μM. These data identify ML324 as a potent inhibitor of KDM4B with moderate selectivity that can be used as a tool to study phenotypic changes resulting from KDM4B inhibition.

We thus reasoned that the periodontal immune response might be attenuated in the absence of KDM4B activity. Macrophages have been established as the primary mediator of the acute PD inflammatory response.[248-250] For this reason, murine bone marrow derived macrophages (BMDMs) have been utilized extensively to model oral inflammatory responses. The pro-inflammatory cytokines TNF-α and IL-6 are classically up regulated in gingival connective tissues of PD patients, [36] and these cytokines are secreted from periopathogen activated macrophages through toll like receptor (TLR) signaling.[225] Lipopolysaccharide (LPS) is a predominate surface antigen that activates this pathway; [251-252] therefore Aa-LPS, a well characterized periopathogen[251-252] was used to simulate the immune challenge present in PD. We anticipate that KDM4B inhibition will be useful clinically following standard of care treatment (scaling and root planing (SRP)), where cells are primed for responding to inflammatory stimuli but are temporarily halted due to the elimination of the plaque biofilm. Introduction of an adjuvant therapy directly after SRP allows for modulation of the host immune response that can prevent future episodes of hyper-inflammation that drives tissue damage and bone loss. Since most

patients resume building biofilms back almost immediately after clinical intervention, we felt that a 1 hour pre-treatment would recapitulate the clinical setting most likely encountered by PD patients. Our results show that ML324-induced inhibition of KDM4B significantly suppresses the inflammatory response to bacterial LPS (**Figure 3.3**). TNF-α mRNA at 8h after Aa-LPS challenge was the only time point tested that did not produce a statistically significant effect, and this was consistent between both male and female cells (**Figure 3.3**). This suggests that TNF-α and IL-6 are epigenetically regulated differently due to the differences seen between groups in these cytokines.

An additional component of the pathogenesis of periodontal disease is the imbalance in osteoimmunological mediators, resulting in a net loss of alveolar bone. KDM4B was recently shown to drive mesenchymal stem cells towards an osteogenic lineage preferentially over adipogenesis,[253] but it is unknown how KDM4B regulates osteoclastic cell types. Because we have seen a decrease in inflammatory mediators required for endogenous osteoclastogenesis, we hypothesized that inhibition of KDM4B would also reduce osteoclastogenesis. Our data demonstrates that osteoclastogenesis proceeds normally with supplementation of either Aa-LPS or RANK-L, but when KDM4B is inhibited in pre-osteoclasts using ML324, neither of these additives induce significant osteoclast formation compared to vehicle control (**Figure 3.4**). This effect is seen in cells from both sexes, although there is a significantly higher number of osteoclasts formed in male cells compared to female cells, consistent with previous literature[254] (**Figure 3.4C**).

The mechanism by which KDM4B inhibition promotes immunosuppression is unknown. A study by Whetstine et al. demonstrated that KDM4B is structurally distinct from its other family members, and has the lowest demethylase activity of the KDM4 family, for reasons that are not clear.[255] KDM4B has also been recognized for its ability to

demethylate non-histone proteins, many of which are transcriptional repressors.[256] We used the NCBI Gene Expression Omnibus databank to determine the differences in expression of the KDM4 family of enzymes following lipopolysaccharide treatment in primary BMDMs. We found that the expression level of these enzymes doesn't reflect their activity, as there are no significant differences in the expression of any KDM4 family gene between LPS treated cells and vehicle treated cells (**Figure 3.6**). Therefore, we probed methylation marks rather than expression of KDM4B itself to determine the mechanism of action of ML324. The RAW264.7 macrophage cell line is the best representation of primary bone marrow derived macrophages,[227] but exhibit increased resiliency for use with glass plates for fluorescent imaging and highly cytotoxic chemicals such as cycloheximide. Herein we used immunofluorescent staining for methylation marks as well as cycloheximide treatment to show that KDM4B-induced immunosuppression acts via an indirect mechanism.[257] After ML324 pre-treatment and Aa-LPS challenge in the presence of cycloheximide, the immunosuppressive effects of ML324 are completely abolished (**Figure 3.5A**). Additionally, it appears that when ML324 is added, even more IL-6 and TNF-α are being transcribed in response to Aa-LPS (**Figure 3.5A**). We postulate that because the cells are not able to effectively propagate intra- and inter-cellular signaling events, the transcripts are aberrantly abundant. Although the immunosuppressive activity of KDM4B inhibition requires new protein synthesis, an epigenetic mechanism is still at play, as evidenced by the increase in H3K9me3 and H3K4me levels that are reversed when KDM4B is inhibited (**Figure 3.5B, C**).

We were able to recapitulate our *in vitro* data *in vivo* using a murine calvarial model of periodontal disease. The calvarial model used is superior to other methods to simulate

PD: the ligature induced periodontal disease model is too acute for drug studies, while the alveolar LPS injection model is not as robust and has unavoidable experimentalist variability. Correlating with decreased osteoclastogenesis, we saw a decrease in bone loss following A.a injection with both ML324 and E3ii treatment as well as an increase between PBS vehicle and A.a treated mice. Tissues overlying the injection site were found to have increased amounts of H3K9me3 in ML324 treated animals, but this wasn't affected by A.a injection alone, as was previously seen *in vitro*.

These data together demonstrate that newly synthesized protein signals KDM1A following KDM4B inhibition, resulting in reduced transcriptional processing of pro-inflammatory cytokines as well as reduced osteoclast formation. This translates to reduced bone loss in vivo, which suggests that KDM4B inhibition could be a viable therapeutic option for treating periodontal disease induced bone loss.

Drug discovery in the field of periodontics currently lacks momentum, and the minimal drug discovery that does go on frequently recycles drugs used for other purposes such as NSAIDs and antibiotics. We sought to utilize the well-established interconnectedness of histone 3 lysine 9 methylation with the immune system to develop drugs that could prevent the aberrant immune response that drives periodontal damage.

ML324 was originally published as a KDM4E inhibitor,[212] and therefore exhibits poor selectivity. This compound also suffers from extremely poor solubility. To enhance both of these properties, we utilized an *in silico* docking approach to identify several hit compounds for optimization. Our strategy utilized the consensus hits between multiple docking algorithms within two different software programs (DOCK6.5 flexible dock and Molecular Operating Environment rigid receptor dock) to eliminate potential false

negatives. Prior to docking, we selected the ZINC library containing compounds with predicted *in vitro* activity that were also available for sale. We filtered this compound library by eliminating compounds that were not drug-like following Lipinski's rules, had many rotatable bonds and thus, had predicted cytotoxicity, and compounds that were not easy to synthesize in a high throughput manner (**Figure 4.1**). This refined library was docked into the active site of KDM4B and hits that ranked highly (>70th percentile) within both programs were subjected to physicochemical clustering.[220] We generated a set of OpenBabel descriptors for each compound and clustered them based on similarity to eachother as well as similarity to known KDM4B inhibitors (ML324[212] **1**, JIB-04[242] **2** and NSC636819[243] **3**). We selected the smallest grouping that contained all three of these inhibitors and made sure that this grouping did not contain the control compound, a KDM1A inhibitor. (**Figure 4.1**)

We screened the purchased hits using a previously published[232] periodontal disease immunosuppression model using primary murine macrophages challenged with *Aggregatebacter actinomycetemcomitans* lipopolysaccharide for 24 hours following 1 hour pre-treatment at 50 μM with each compound. It is of critical importance in these experiments to use primary cells from normal mice as KDM4B has been established as a therapeutic target for anti-cancer agents.[243, 258] Our experiments yielded several potential hits from our initial screen of several different chemotypes including anti-anxiolytic cinazepam[259] **13** and anti-tuberculosis drug aconiazide[260] **14**. We ultimately selected 2-([1,1'-biphenyl]-4-carboxamido)benzoic acid **16** due to its potency, solubility, ease of derivatization as well as ease of overall synthesis. We divided the scaffold into three units, each containing a benzene ring available for derivatization. We generated a combinatorial

library *in silico* based on commercially available and economical starting materials. Our initial library was subjected to consensus docking to prioritize our synthetic efforts. Despite our awareness of the power in using this tool, we ultimately synthesized both compounds with high binding affinity as well as compounds that we were able to synthesize efficiently. For example, the parent scaffold (scaffold 1) had a simplified synthetic scheme because of the purchasability of a two ringed starting material, eliminating the bulk of the synthetic difficulty.

The Suzuki coupling reaction resulted in homocoupling of the bromobenzene starting material, which had been previously reported.[261] Additionally, the third step sometimes generated an anyhydride product for selected diphenyl carboxylic acids. We hypothesize that the nucleophilic amine starting material was stabilized by the carboxylic acid hydroxy group, reducing its nucleophilicity and hydrophilicity making both the reaction and purification extremely difficult. Because of this, several hits were synthesized based on our ability to purchase starting materials that eliminated steps in our method (biphenyl carboxylic acids **19**, eliminating the Suzuki coupling and ester cleavage reactions) as well as compounds that were very reactive or could be used in heavy excess due to the high yield of the previous step.

Our synthetic method (**Scheme 4.1**) was relatively simple and utilized microwave assisted reactions to reduce the total time for synthesis. Purification of the three-ringed product **22** from the amine starting material **21** proved unexpectedly difficult, likely due to strong hydrogen bonding between the amine hydrogen and the lone pairs of the adjacent acetate oxygen. For this reason, reactions were crystallized rather than purified by column chromatography whenever possible. In the second step, we found that lyophilization of the

starting material **21** as well as removing the excess oxalyl chloride prior to adding the nucleophilic amine **21** were critical for the success of this step. To do this more efficiently, we used dry DCE rather than DCM as was previously published,[224] due to its higher boiling point. At this point, all reactions were bright yellow in color. For the next step we pre-stirred triethylamine with the amine **21**, and this solution was added via cannula transfer to the reaction under nitrogen. When using lower equivalents of TEA the reaction did not proceed, likely due to strong hydrogen bonding between the amine hydrogen and the lone pairs of the adjacent acetate oxygen which decreased the nucleophilicity of the amine. When successful, the reaction proceeded almost instantaneously, with a sharp color change and white gas occurring in almost every reaction. Unfortunately, the final step was critical to the solubility of our final compounds. Thus, the ester **22** of each drug could not be considered for *in vitro* testing due to poor solubility. Purity of our final compounds was confirmed using UPLC, and compounds were characterized by NMR. Final compounds were only utilized for biological evaluation if purity was >95% by UPLC.

We utilized the immunosuppressive action (**Figure 4.4A**) of the first 16 (**16, 23-37**) compounds synthesized to build a quantitative structure activity relationship (**Figure 4.4B**) utilizing 11 descriptors. We chose to use contingency analysis for selection of descriptors so that our methodology would be reproducible. We had a 20% hit rate with a 100% probability to predict negative hits but only a 88% probability to predict positive hits. This model was used to guide synthesis of 9 more compounds (**38-46**), several of which showed a significantly higher efficacy than the first series of inhibitors (**Figure 4.4A**), with a hit rate within our second generation of 56% yielding an overall hit rate of 29%. We tested our two final best compounds as predicted by docking, QSAR and phenotypic

screening (**44, 46**) for KDM4B inhibitory action and surprisingly found that they exhibited IC_{50} values >100 μM.

Conclusion

ML324 is an effective inhibitor of KDM4B, which acts through binding to KDM4B and initiating de novo protein synthesis, subsequent KDM1A activation followed by H3K4 demethylation. This results in a reduced cytokine inflammatory response and decreased osteoclastogenesis in primary bone marrow cells. These data together provide a novel mechanism of immunomodulation through epigenetic modification, which can be used for further development of therapeutics for treatment of hyper-inflammatory disorders such as periodontal disease.

We were able to use high-throughput computational chemical consensus screens coupled with *in vitro* phenotypic screening to identify novel compounds that cause immunosuppression coupled to epigenetic changes. We optimized these with our phenotypic screening data to identify multiple potent compounds. We conclude that novel scaffolds have been identified that could serve useful in treating periodontal disease through a unique epigenetic mechanism.

5.2. Future Directions

5.2.a. Further drug development

This dissertation describes the identification of a novel scaffold for immunosuppressive drugs that could be used to treat hyper inflammatory disorders including periodontal disease. Additionally, this dissertation validated KDM4B as an epigenetic enzyme that produces immunosuppressive effects when inhibited in vitro and in vivo. Unfortunately, the drug discovery strategy utilized in this dissertation did not combine these two aims –

and our immunosuppressive compounds do not work through inhibition of KDM4B. Further drug discovery research should be conducted using enzymatic assay-based QSAR that correlates IC_{50} with structural characteristics rather than phenotypic immunosuppression which can be vague and off-target.

5.2.b. Human samples

While human tissues were stained immunohistochemically for KDM4B protein abundance from periodontally diseased and healthy tissues in this dissertation, no further human data was acquired. While there are obvious benefits associated with using a murine system to study periodontal disease such as cost, simplicity, sentience and complete genetic control, there are equally obvious limitations. For example, mice do not develop periodontal disease and are not naturally colonized with periodontal pathogens such as *Porphyromonas gingivalis* or *Aggregatibacter actinomycetemcomitans*. Because of this, it would be more clinically relevant to measure the efficacy of KDM4B inhibition to cause immunosuppression in human tissues or cells. Future studies should incorporate the use of either an immortalized human cell line or even a human macrophage cancer cell line such as KG-1 cells.

5.2.c. Assay development

As mentioned previously, the quantitative structure activity relationship that was developed through completion of this dissertation is binary and is based on statistically significant phenotypic immunosuppression data. While this type of screening produces clinically applicable inhibitors, the potential for development of drugs that are off-target is very high. This strategy was utilized due to the limited options available for biochemically assaying the enzymatic activity of KDM4B. The main strategy used currently is an

alphalisa or AlphaScreen assay which is costly and requires an advanced alpha count reading plate reader. Future work should focus on development of a more economical enzyme assay, or at the very least the growth of KDM4B protein in *E. coli*.

5.2.d. CRISPR/Cas9

While we feel confident that KDM4B inhibition presents a valid therapeutic strategy for treatment of inflammatory diseases through the data presented within this dissertation, genetic deletion of KDM4B would be a worthwhile endeavor in the multitude of cell types involved in periodontal disease pathogenesis. As drug discovery toward KDM4B inhibitors gains momentum and more potent inhibitors are developed, it is prudent to understand the systemic effects of deletion of KDM4B in both health and disease states. Several groups have successfully deleted KDM4B through the use of CRISPR/Cas9 technology, but it has yet to be done in macrophages or in an inflammatory setting. These studies would help determine whether KDM4B inhibition is feasible, the extent of compensatory mechanisms among the KDM4 enzyme family, and potential positive or negative feedback mechanisms that may come into play with long-term KDM4B inhibition therapy.

5.2.e. Macrophage polarization

Initial studies were conducted within this dissertation towards understanding the polarization of macrophages following KDM4B inhibition. Unfortunately, these studies were contradictory, and no definitive conclusions could be made. Macrophages treated with KDM4B inhibitors secrete less pro-inflammatory cytokines, increased IL-10, an anti-inflammatory cytokine, do not morphologically look like M1 macrophages when stimulated with LPS, and have a metabolic profile consistent with depolarized M0 or M2 macrophages. Previous literature suggests that other KDM enzymes regulate

macrophage polarization, therefore it is entirely possible that KDM4B is also involved in this switch that is seen in periodontal disease pathogenesis. Future work should clearly delineate whether KDM4B inhibition depolarizes or de-differentiates macrophages or if it induces M2 macrophage polarization. This could be done using cell sorting experiments or immunofluorescent staining of M1 and M2 macrophage markers.

5.2.f. Optimization and expansion of calvarial model

The in vivo experimentation conducted in this dissertation was unfortunately limited to male mice only. This decision was made based on the lack of differences seen between male and female cells in their inflammatory response to LPS and whole bacteria following KDM4B inhibition. Differences were observed in osteoclastogenesis between male and female cells in response to KDM4B inhibitors. These differences were seen with and without KDM4B inhibition, and previous literature has described differences between male and female osteoclastogenesis. While these facts validate the use of a single sex for preliminary experimentation, testing should be done in both male and female mice prior to translation to clinical studies.

Additionally, the A.a induced bone loss observed in our experimentation was not robust enough to determine significant differences between groups. A pilot study should be conducted that includes a dose-response to fixed A.a and experiments should be repeated. The most potent immunosuppressor, compound **46,** should also be tested *in vivo*.

5.2.g. Additional Disease models

Because the general idea of KDM4B inhibitors as therapeutics for periodontal disease is based on the concept of immunosuppression, it is conceivable that these compounds

could be used for various additional hyper-inflammatory diseases. For example, rheumatoid arthritis is a common degenerative disease driven by the immune response and affects more than 21% of the adult American population and would thus present a potential candidate disease that could be treated using KDM4B inhibitors. Additionally, as mentioned previously, periodontal disease has been linked to even more prevalent systemic diseases such as diabetes and obesity, for which an epigenetic mechanism underlying their interconnectedness has not been explored. A challenge with treatment of other diseases is the issue of systemic administration – in fact, the major appeal of epigenetic therapy for periodontal disease is the ability to provide local treatment directly in the oral cavity. Therefore, future work should focus on the potential effects of systemic KDM4B inhibitor administration.

5.3. Impact on the field

This project has several important implications that will make a significant impact across several fields, including periodontics, immunology and epigenetics. First, the regulation of periodontal disease by the epigenetic histone demethylase KDM4B was entirely unknown prior to completion of this dissertation. This project demonstrated that KDM4B plays a regulatory role in both perio-pathogen induced inflammation as well as bone loss. Prior to this study, host modulation therapy for treating periodontal disease through histone demethylase inhibition has yet to be translated into a pre-clinical model of the disease. This project resulted in a series of small molecule epigenetic modulating drugs and ultimately these compounds were tested *in vivo*. The synthetic methodology described in this dissertation has been optimized for development of additional inhibitors, to enable extension of this compound library efficiently in future studies. In addition to the novel

series of inhibitors that was developed, this project defined ML324 as a KDM4B inhibitor for the first time and extended the therapeutic potential for this drug to include reduction of inflammation and bone loss. Also, this project further confirmed the mutual exclusivity of the epigenetic enzymes KDM1A and KDM4B. The epigenetic landscape is extremely complex and yet to be completely understood; therefore, studies that elucidate interactions between epigenetic mechanisms are critically important. Overall, this project was able to bridge the gap in understanding between multiple fields.

References:

1. Eke, P. I.; Thornton-Evans, G. O.; Wei, L.; Borgnakke, W. S.; Dye, B. A.; Genco, R. J., Periodontitis in US Adults: National Health and Nutrition Examination Survey 2009-2014. *Journal of the American Dental Association (1939)* **2018,** *149* (7), 576-588.e6.

2. Global, regional, and national incidence, prevalence, and years lived with disability for 328 diseases and injuries for 195 countries, 1990-2016: a systematic analysis for the Global Burden of Disease Study 2016. *Lancet (London, England)* **2017,** *390* (10100), 1211-1259.

3. OECD, *Health at a Glance 2017*. 2017.

4. Natto, Z. S.; Abu Ahmad, R. H.; Alsharif, L. T.; Alrowithi, H. F.; Alsini, D. A.; Salih, H. A.; Bissada, N. F., Chronic Periodontitis Case Definitions and Confounders in Periodontal Research: A Systematic Assessment. *BioMed research international* **2018,** *2018*, 4578782.

5. Page, R. C.; Eke, P. I., Case Definitions for Use in Population-Based Surveillance of Periodontitis. *Journal of periodontology* **2007,** *78* (Suppl 7S), 1387-1399.

6. López, R.; Baelum, V., Periodontal disease classifications revisited. *European Journal of Oral Sciences* **2015,** *123* (6), 385-389.

7. Smiley, C. J.; Tracy, S. L.; Abt, E.; Michalowicz, B. S.; John, M. T.; Gunsolley, J.; Cobb, C. M.; Rossmann, J.; Harrel, S. K.; Forrest, J. L.; Hujoel, P. P.; Noraian, K. W.; Greenwell, H.; Frantsve-Hawley, J.; Estrich, C.; Hanson, N., Evidence-based clinical practice guideline on the nonsurgical treatment of chronic periodontitis by means of scaling and root planing with or without adjuncts. *Journal of the American Dental Association (1939)* **2015,** *146* (7), 525-35.

8. Dutra, E. H.; Nanda, R.; Yadav, S., Bone Response of Loaded Periodontal Ligament. *Current osteoporosis reports* **2016,** *14* (6), 280-283.

9. Bosshardt, D. D.; Lang, N. P., The junctional epithelium: from health to disease. *J Dent Res* **2005,** *84* (1), 9-20.

10. Hormia, M.; Owaribe, K.; Virtanen, I., The Dento-Epithelial Junction: Cell Adhesion by Type I Hemidesmosomes in the Absence of a True Basal Lamina. *Journal of Periodontology* **2001,** *72* (6), 788-797.

11. Hefti, A., Periodontal Probing. *Critical Reviews in Oral Biology & Medicine* **1997,** *8* (3), 336-356.

12. Armitage, G. C., Development of a classification system for periodontal diseases and conditions. *Annals of periodontology* **1999,** *4* (1), 1-6.

13. American Academy of Periodontology Task Force Report on the Update to the 1999 Classification of Periodontal Diseases and Conditions. *J Periodontol* **2015,** *86* (7), 835-8.

14. Vieira, A. R.; Albandar, J. M., Role of genetic factors in the pathogenesis of aggressive periodontitis. *Periodontol 2000* **2014,** *65* (1), 92-106.

15. American Academy of Periodontology Task Force Report on the Update to the 1999 Classification of Periodontal Diseases and Conditions. *Journal of Periodontology* **2015,** *86* (7), 835-838.

16. Papapanou, P. N.; Sanz, M.; Buduneli, N.; Dietrich, T.; Feres, M.; Fine, D. H.; Flemmig, T. F.; Garcia, R.; Giannobile, W. V.; Graziani, F.; Greenwell, H.; Herrera, D.; Kao, R. T.; Kebschull, M.; Kinane, D. F.; Kirkwood, K. L.; Kocher, T.; Kornman, K. S.; Kumar, P. S.; Loos, B. G.; Machtei, E.; Meng, H.; Mombelli, A.; Needleman, I.; Offenbacher, S.; Seymour, G. J.; Teles, R.; Tonetti, M. S., Periodontitis: Consensus

report of workgroup 2 of the 2017 World Workshop on the Classification of Periodontal and Peri-Implant Diseases and Conditions. *Journal of Periodontology* **2018,** *89* (S1), S173-S182.

17. Meitner, S., Co-destructive factors of marginal periodontitis and repetitive mechanical injury. *J Dent Res* **1975,** *54 Spec no C*, C78-85.

18. Meitner, S., Co-Destructive Factors of Marginal Periodontitis and Repetitive Mechanical Injury. *Journal of Dental Research* **1975,** *54* (3_suppl), 78-85.

19. Polson, A. M.; Kennedy, J. E.; Zander, H. A., Trauma and progression of marginal periodontitis in squirrel monkeys. *Journal of Periodontal Research* **1974,** *9* (2), 100-107.

20. Polson, A. M., Interrelationship of inflammation and tooth mobility (trauma) in pathogenesis of periodontal disease. *Journal of clinical periodontology* **1980,** *7* (5), 351-60.

21. Polson, A. M.; Kennedy, J. E.; Zander, H. A., Effect of traumatic injury on the progression of marginal periodontitis. *J Periodontal Res* **1972,** (10), 17.

22. Polson, A. M.; Kennedy, J. E.; Zander, H. A., Trauma and progression of marginal periodontitis in squirrel monkeys. I. Co-destructive factors of periodontitis and thermally-produced injury. *J Periodontal Res* **1974,** *9* (2), 100-7.

23. Lindhe, J.; Svanberg, G., Influence of trauma from occlusion on progression of experimental periodontitis in the beagle dog. *Journal of clinical periodontology* **1974,** *1* (1), 3-14.

24. Goodson, J. M.; Tanner, A. C.; Haffajee, A. D.; Sornberger, G. C.; Socransky, S. S., Patterns of progression and regression of advanced destructive periodontal disease. *Journal of clinical periodontology* **1982,** *9* (6), 472-81.

25. Lindhe, J.; Haffajee, A. D.; Socransky, S. S., Progression of periodontal disease in adult subjects in the absence of periodontal therapy. *Journal of clinical periodontology* **1983,** *10* (4), 433-42.

26. Socransky, S. S.; Haffajee, A. D.; Goodson, J. M.; Lindhe, J., New concepts of destructive periodontal disease. *Journal of clinical periodontology* **1984,** *11* (1), 21-32.

27. Akcalı, A.; Lang, N. P., Dental calculus: the calcified biofilm and its role in disease development. *Periodontology 2000* **2018,** *76* (1), 109-115.

28. Jin, Y.; Yip, H. K., Supragingival calculus: formation and control. *Critical reviews in oral biology and medicine : an official publication of the American Association of Oral Biologists* **2002,** *13* (5), 426-41.

29. Swati Gupta, P. J., Madhumani Kumra, Shweta Rehani, Yulia Mathias, Ramakant Gupta, .; et al., Bacterial Viability within Dental Calculus: An Untrodden, Inquisitive Clinico-Patho- Microbiological Research. *Journal of Clinical and Diagnostic Research* **2016,** *10* (7), ZC71-ZC75.

30. Janeway, C.; National Center for Biotechnology, I.; National Institutes of Health, P., Immunobiology 5 : the immune system in health and disease. 5th ed. ed.; Garland Pub. ;

NCBI: New York

Bethsada, MD., 2001.

31. Palazon-Riquelme, P.; Lopez-Castejon, G., The inflammasomes, immune guardians at defence barriers. *Immunology* **2018,** *155* (3), 320-330.

32. Lotze, M. T.; Robinson, B. W. S.; June, C. H.; Whiteside, T. L., 77 - Tumor immunotherapy. In *Clinical Immunology (Fourth Edition)*, Rich, R. R.; Fleisher, T. A.;

Shearer, W. T.; Schroeder, H. W.; Frew, A. J.; Weyand, C. M., Eds. Content Repository Only!: London, 2013; pp 935-945.

33. Park, B. S.; Lee, J. O., Recognition of lipopolysaccharide pattern by TLR4 complexes. *Experimental & molecular medicine* **2013,** *45*, e66.

34. Ceccarelli, S.; Nobili, V.; Alisi, A., Toll-like receptor-mediated signaling cascade as a regulator of the inflammation network during alcoholic liver disease. *World journal of gastroenterology* **2014,** *20* (44), 16443-51.

35. Akira, S.; Takeda, K., Toll-like receptor signalling. *Nature Reviews Immunology* **2004,** *4*, 499.

36. Noh, M. K.; Jung, M.; Kim, S. H.; Lee, S. R.; Park, K. H.; Kim, D. H.; Kim, H. H.; Park, Y. G., Assessment of IL-6, IL-8 and TNF-α levels in the gingival tissue of patients with periodontitis. *Experimental and Therapeutic Medicine* **2013,** *6* (3), 847-51.

37. Almehmadi, A. H.; Alghamdi, F., Biomarkers of alveolar bone resorption in gingival crevicular fluid: A systematic review. *Archives of Oral Biology* **2018,** *93*, 12-21.

38. Nathan, C., Points of control in inflammation. *Nature* **2002,** *420*, 846.

39. Yu, T.; Zhao, L.; Huang, X.; Ma, C.; Wang, Y.; Zhang, J.; Xuan, D., Enhanced Activity of the Macrophage M1/M2 Phenotypes and Phenotypic Switch to M1 in Periodontal Infection. *J Periodontol* **2016,** *87* (9), 1092-102.

40. Martinez, F. O.; Sica, A.; Mantovani, A.; Locati, M., Macrophage activation and polarization. *Frontiers in bioscience : a journal and virtual library* **2008,** *13*, 453-61.

41. Yu, T.; Zhao, L.; Huang, X.; Ma, C.; Wang, Y.; Zhang, J.; Xuan, D., Enhanced Activity of the Macrophage M1/M2 Phenotypes and Phenotypic Switch to M1 in Periodontal Infection. *Journal of Periodontology* **2016,** *87* (9), 1092-1102.

42. Zhu, Y.; van Essen, D.; Saccani, S., Cell-Type-Specific Control of Enhancer Activity by H3K9 Trimethylation. *Molecular Cell 46* (4), 408-423.

43. Hsieh, C.; Macatonia, S.; Tripp, C.; Wolf, S.; O'Garra, A.; Murphy, K., Development of TH1 CD4+ T cells through IL-12 produced by Listeria-induced macrophages. *Science* **1993,** *260* (5107), 547-549.

44. Bergman, Y., Linking DNA methylation and histone modification: patterns and paradigms. *Nat Rev Genet* **2009,** *10*, 295-304.

45. Takeuchi, T., The Jmjd3Irf4 axis regulates M2 macrophage polarization and host responses against helminth infection. *Nat Immunol* **2010,** *11*, 936-944.

46. Boulding, T.; McCuaig, R. D.; Tan, A.; Hardy, K.; Wu, F.; Dunn, J.; Kalimutho, M.; Sutton, C. R.; Forwood, J. K.; Bert, A. G.; Goodall, G. J.; Malik, L.; Yip, D.; Dahlstrom, J. E.; Zafar, A.; Khanna, K. K.; Rao, S., LSD1 activation promotes inducible EMT programs and modulates the tumour microenvironment in breast cancer. *Sci Rep* **2018,** *8* (1), 73.

47. Wang, X.; Wang, S.; Yao, G.; Yu, D.; Chen, K.; Tong, Q.; Ye, L.; Wu, C.; Sun, Y.; Li, H.; Hermann, D. M.; Doeppner, T. R.; Jin, F.; Dai, Y.; Wu, J., Identification of the histone lysine demethylase KDM4A/JMJD2A as a novel epigenetic target in M1 macrophage polarization induced by oxidized LDL. *Oncotarget* **2017**.

48. Liew, P. X.; Kubes, P., The Neutrophil's Role During Health and Disease. *Physiological reviews* **2019,** *99* (2), 1223-1248.

49. Del Fabbro, M.; Francetti, L.; Pizzoni, L.; Rozza, R.; Weinstein, R. L., [Neutrophil physiology: role and mechanism of action in the immune response at gingival level]. *Minerva stomatologica* **2000,** *49* (5), 227-48.

50. Silva, N.; Abusleme, L.; Bravo, D.; Dutzan, N.; Garcia-Sesnich, J.; Vernal, R.; HernÁNdez, M.; Gamonal, J., Host response mechanisms in periodontal diseases. *Journal of Applied Oral Science* **2015,** *23* (3), 329-55.

51. Wilensky, A.; Segev, H.; Mizraji, G.; Shaul, Y.; Capucha, T.; Shacham, M.; Hovav, A. H., Dendritic cells and their role in periodontal disease. *Oral Dis* **2014,** *20* (2), 119-26.

52. Song, L.; Dong, G.; Guo, L.; Graves, D. T., The function of dendritic cells in modulating the host response. *Molecular oral microbiology* **2018,** *33* (1), 13-21.

53. Laperine, O.; Blin-Wakkach, C.; Guicheux, J.; Beck-Cormier, S.; Lesclous, P., Dendritic-cell-derived osteoclasts: a new game changer in bone-resorption-associated diseases. *Drug discovery today* **2016,** *21* (9), 1345-1354.

54. Zhu, J.; Paul, W. E., CD4 T cells: fates, functions, and faults. *Blood* **2008,** *112* (5), 1557-1569.

55. Konkel, J. E.; Moutsopoulos, N. M., Unique Tailoring of Th17 at the Gingival Oral Mucosal Barrier. *J Dent Res* **2018,** *97* (2), 128-131.

56. Dutzan, N.; Kajikawa, T.; Abusleme, L.; Greenwell-Wild, T.; Zuazo, C. E.; Ikeuchi, T.; Brenchley, L.; Abe, T.; Hurabielle, C.; Martin, D.; Morell, R. J.; Freeman, A. F.; Lazarevic, V.; Trinchieri, G.; Diaz, P. I.; Holland, S. M.; Belkaid, Y.; Hajishengallis, G.; Moutsopoulos, N. M., A dysbiotic microbiome triggers TH17 cells to mediate oral mucosal immunopathology in mice and humans. *Science translational medicine* **2018,** *10* (463).

57. Kawai, T.; Eisen-Lev, R.; Seki, M.; Eastcott, J. W.; Wilson, M. E.; Taubman, M. A., Requirement of B7 costimulation for Th1-mediated inflammatory bone resorption in

experimental periodontal disease. *Journal of immunology (Baltimore, Md. : 1950)* **2000,** *164* (4), 2102-9.

58. Zouali, M., The emerging roles of B cells as partners and targets in periodontitis. *Autoimmunity* **2017,** *50* (1), 61-70.

59. Oliver-Bell, J.; Butcher, J. P.; Malcolm, J.; MacLeod, M. K.; Adrados Planell, A.; Campbell, L.; Nibbs, R. J.; Garside, P.; McInnes, I. B.; Culshaw, S., Periodontitis in the absence of B cells and specific anti-bacterial antibody. *Molecular oral microbiology* **2015,** *30* (2), 160-9.

60. Wilensky, A.; Chaushu, S.; Shapira, L., The role of natural killer cells in periodontitis. *Periodontol 2000* **2015,** *69* (1), 128-41.

61. Mendes, R. T.; Nguyen, D.; Stephens, D.; Pamuk, F.; Fernandes, D.; Hasturk, H.; Van Dyke, T. E.; Kantarci, A., Hypoxia-induced endothelial cell responses - possible roles during periodontal disease. *Clinical and experimental dental research* **2018,** *4* (6), 241-248.

62. Meyle, J.; Dommisch, H.; Groeger, S.; Giacaman, R. A.; Costalonga, M.; Herzberg, M., The innate host response in caries and periodontitis. *Journal of clinical periodontology* **2017,** *44* (12), 1215-1225.

63. Valero-Monroy, O.; Garcia-Cervantes, G.; Marquez-Corrales, L. F.; Leija-Montoya, A. G.; Sandoval-Basilio, J.; Martinez-Coronilla, G.; Isiordia-Espinoza, M. A.; Serafin-Higuera, N., Myeloid derived suppressor cell: A new player in periodontal disease? *Medical hypotheses* **2016,** *95*, 35-38.

64. Socransky, S. S.; Haffajee, A. D.; Cugini, M. A.; Smith, C.; Kent, R. L., Jr., Microbial complexes in subgingival plaque. *Journal of clinical periodontology* **1998,** *25* (2), 134-44.

65. Hajishengallis, G.; Darveau, R. P.; Curtis, M. A., The keystone-pathogen hypothesis. *Nature reviews. Microbiology* **2012,** *10* (10), 717-25.

66. Hajishengallis, G.; Lamont, R. J., Beyond the red complex and into more complexity: the polymicrobial synergy and dysbiosis (PSD) model of periodontal disease etiology. *Molecular oral microbiology* **2012,** *27* (6), 409-19.

67. Eick, S.; Nydegger, J.; Bürgin, W.; Salvi, G. E.; Sculean, A.; Ramseier, C., Microbiological analysis and the outcomes of periodontal treatment with or without adjunctive systemic antibiotics—a retrospective study. *Clinical Oral Investigations* **2018,** *22* (9), 3031-3041.

68. Takayanagi, H., Osteoimmunology: shared mechanisms and crosstalk between the immune and bone systems. *Nature Reviews Immunology* **2007,** *7*, 292.

69. Hienz, S. A.; Paliwal, S.; Ivanovski, S., Mechanisms of Bone Resorption in Periodontitis. *Journal of immunology research* **2015,** *2015*, 615486.

70. Smolen, J. S.; Redlich, K.; Zwerina, J.; Aletaha, D.; Steiner, G.; Schett, G., Pro-inflammatory cytokines in rheumatoid arthritis. *Clinical Reviews in Allergy & Immunology* **2005,** *28* (3), 239-248.

71. Kumari, A.; Silakari, O.; Singh, R. K., Recent advances in colony stimulating factor-1 receptor/c-FMS as an emerging target for various therapeutic implications. *Biomedicine & Pharmacotherapy* **2018,** *103*, 662-679.

72. Popova, A.; Kzhyshkowska, J.; Nurgazieva, D.; Goerdt, S.; Gratchev, A., Pro- and anti-inflammatory control of M-CSF-mediated macrophage differentiation. *Immunobiology* **2011,** *216* (1), 164-172.

73. Han, Y.; You, X.; Xing, W.; Zhang, Z.; Zou, W., Paracrine and endocrine actions of bone—the functions of secretory proteins from osteoblasts, osteocytes, and osteoclasts. *Bone Research* **2018,** *6* (1), 16.

74. Caffesse, R. G.; Echeverría, J. J., Treatment trends in periodontics. *Periodontology 2000* **2019,** *79* (1), 7-14.

75. Periodontology, A. A. o. Non-Surgical Periodontal Treatment. https://www.perio.org/consumer/non-surgical-periodontal-treatment.

76. Drisko, C. H.; Lewis, L. H., Ultrasonic instruments and antimicrobial agents in supportive periodontal treatment and retreatment of recurrent or refractory periodontitis. *Periodontology 2000* **1996,** *12* (1), 90-115.

77. Zappa, U. E., Factors determining the outcome of scaling and root planing. *Probe (Ottawa, Ont.)* **1992,** *26* (4), 152-9.

78. Brogden, K. A.; Guthmiller, J. M., Polymicrobial diseases. ASM Press: [Washington, D.C.], 2006. http://www.ncbi.nlm.nih.gov/books/bv.fcgi?call=bv.View..ShowTOC&rid=pmd.TOC&depth=2

http://www.asmscience.org/content/book/10.1128/9781555817947.

79. Renatus, A.; Herrmann, J.; Schonfelder, A.; Schwarzenberger, F.; Jentsch, H., Clinical Efficacy of Azithromycin as an Adjunctive Therapy to Non-Surgical Periodontal Treatment of Periodontitis: A Systematic Review and Meta-Analysis. *Journal of clinical and diagnostic research : JCDR* **2016,** *10* (7), Ze01-7.

80. Kapoor, A.; Malhotra, R.; Grover, V.; Grover, D., Systemic antibiotic therapy in periodontics. *Dental research journal* **2012,** *9* (5), 505-15.

81. van Winkelhoff, A. J.; Winkel, E. G., Antibiotics in Periodontics: Right or Wrong? *Journal of Periodontology* **2009,** *80* (10), 1555-1558.

82. SLOTS, J.; TING, M., Systemic antibiotics in the treatment of periodontal disease. *Periodontology 2000* **2002,** *28* (1), 106-176.

83. Magnusson, I.; Low, S. B.; McArthur, W. P.; Marks, R. G.; Walker, C. B.; Maruniak, J.; Taylor, M.; Padgett, P.; Jung, J.; Clark, W. B., Treatment of subjects with refractory periodontal disease. *Journal of clinical periodontology* **1994,** *21* (9), 628-637.

84. Walker, C. B., The acquisition of antibiotic resistance in the periodontal microflora. *Periodontology 2000* **1996,** *10* (1), 79-88.

85. Quirynen, M.; Teughels, W.; Van Steenberghe, D., Microbial shifts after subgingival debridement and formation of bacterial resistance when combined with local or systemic antimicrobials. *Oral Diseases* **2003,** *9* (s1), 30-37.

86. Pretzl, B.; Salzer, S.; Ehmke, B.; Schlagenhauf, U.; Dannewitz, B.; Dommisch, H.; Eickholz, P.; Jockel-Schneider, Y., Administration of systemic antibiotics during non-surgical periodontal therapy-a consensus report. *Clin Oral Investig* **2019,** *23* (7), 3073-3085.

87. Jepsen, K.; Jepsen, S., Antibiotics/antimicrobials: systemic and local administration in the therapy of mild to moderately advanced periodontitis. *Periodontology 2000* **2016,** *71* (1), 82-112.

88. Salvi, G. E.; Mombelli, A.; Mayfield, L.; Rutar, A.; Suvan, J.; Garrett, S.; Lang, N. P., Local antimicrobial therapy after initial periodontal treatment. *Journal of clinical periodontology* **2002,** *29* (6), 540-50.

89. Williams, R. C.; Paquette, D. W.; Offenbacher, S.; Adams, D. F.; Armitage, G. C.; Bray, K.; Caton, J.; Cochran, D. L.; Drisko, C. H.; Fiorellini, J. P.; Giannobile, W. V.;

Grossi, S.; Guerrero, D. M.; Johnson, G. K.; Lamster, I. B.; Magnusson, I.; Oringer, R. J.; Persson, G. R.; Van Dyke, T. E.; Wolff, L. F.; Santucci, E. A.; Rodda, B. E.; Lessem, J., Treatment of periodontitis by local administration of minocycline microspheres: a controlled trial. *J Periodontol* **2001,** *72* (11), 1535-44.

90. Mlachkova, A. M.; Popova, C. L., Dental Investigations: Efficiency of Nonsurgical Periodontal Therapy in Moderate Chronic Periodontitis. **2014,** *56* (2), 109.

91. James, P.; Worthington, H. V.; Parnell, C.; Harding, M.; Lamont, T.; Cheung, A.; Whelton, H.; Riley, P., Chlorhexidine mouthrinse as an adjunctive treatment for gingival health. *The Cochrane database of systematic reviews* **2017,** *3*, Cd008676.

92. Vijayalakshmi, R.; Anitha, V.; Ramakrishnan, T.; Sudhakar, U., Evidence-based periodontal therapy: An overview. *Journal of Indian Society of Periodontology* **2008,** *12* (3), 62-6.

93. Offenbacher, S.; Odle, B. M.; Braswell, L. D.; Johnson, H. G.; Hall, C. M.; McClure, H.; Orkin, J. L.; Strobert, E. A.; Green, M. D., Changes in cyclooxygenase metabolites in experimental periodontitis in Macaca mulatta. *J Periodontal Res* **1989,** *24* (1), 63-74.

94. Vogel, R. I.; Schneider, L.; Goteiner, D., The effects of a topically-active non-steroidal anti-inflammatory drug on ligature-induced periodontal disease in the squirrel monkey. *Journal of clinical periodontology* **1986,** *13* (2), 139-44.

95. Feldman, R. S.; Szeto, B.; Chauncey, H. H.; Goldhaber, P., Non-steroidal anti-inflammatory drugs in the reduction of human alveolar bone loss. *Journal of clinical periodontology* **1983,** *10* (2), 131-6.

96. Howell, T. H., Blocking periodontal disease progression with anti-inflammatory agents. *J Periodontol* **1993,** *64* (8 Suppl), 828-33.

97. Harirforoosh, S.; Asghar, W.; Jamali, F., Adverse effects of nonsteroidal antiinflammatory drugs: an update of gastrointestinal, cardiovascular and renal complications. *Journal of pharmacy & pharmaceutical sciences : a publication of the Canadian Society for Pharmaceutical Sciences, Societe canadienne des sciences pharmaceutiques* **2013,** *16* (5), 821-47.

98. Oduncuoglu, B. F.; Kayar, N. A.; Haliloglu, S.; Serpek, B.; Ataoglu, T.; Alptekin, N. O., Effects of a cyclic NSAID regimen on levels of gingival crevicular fluid prostaglandin E2and Interleukin-1beta: A 6-month randomized controlled clinical trial. *Nigerian journal of clinical practice* **2018,** *21* (5), 658-666.

99. Preshaw, P. M.; Hefti, A. F.; Jepsen, S.; Etienne, D.; Walker, C.; Bradshaw, M. H., Subantimicrobial dose doxycycline as adjunctive treatment for periodontitis. *Journal of clinical periodontology* **2004,** *31* (9), 697-707.

100. Franco, C.; Patricia, H. R.; Timo, S.; Claudia, B.; Marcela, H., Matrix Metalloproteinases as Regulators of Periodontal Inflammation. *International journal of molecular sciences* **2017,** *18* (2).

101. Ghodpage, P. S.; Kolte, R. A.; Kolte, A. P.; Gupta, M., Influence of phase I periodontal therapy on levels of matrix metalloproteinase 1 and tissue inhibitor of metalloproteinase 1. *The Saudi dental journal* **2014,** *26* (4), 171-5.

102. Caton, J.; Ryan, M. E., Clinical studies on the management of periodontal diseases utilizing subantimicrobial dose doxycycline (SDD). *Pharmacological research* **2011,** *63* (2), 114-20.

103. Garrido-Mesa, N.; Zarzuelo, A.; Gálvez, J., Minocycline: far beyond an antibiotic. *British Journal of Pharmacology* **2013,** *169* (2), 337-52.

104. Yrjänheikki, J.; Tikka, T.; Keinänen, R.; Goldsteins, G.; Chan, P. H.; Koistinaho, J., A tetracycline derivative, minocycline, reduces inflammation and protects against focal cerebral ischemia with a wide therapeutic window. *Proc Natl Acad Sci U S A* **1999,** *96* (23), 13496-500.

105. Honibald, E. N.; Mathew, S.; Padmanaban, J.; Sundaram, E.; Ramamoorthy, R. D., Perioceutics: Matrix metalloproteinase inhibitors as an adjunctive therapy for inflammatory periodontal disease. *Journal of pharmacy & bioallied sciences* **2012,** *4* (Suppl 2), S417-21.

106. Juric, V.; O'Sullivan, C.; Stefanutti, E.; Kovalenko, M.; Greenstein, A.; Barry-Hamilton, V.; Mikaelian, I.; Degenhardt, J.; Yue, P.; Smith, V.; Mikels-Vigdal, A., MMP-9 inhibition promotes anti-tumor immunity through disruption of biochemical and physical barriers to T-cell trafficking to tumors. *PLoS ONE* **2018,** *13* (11), e0207255.

107. Remacle, A. G.; Cieplak, P.; Nam, D. H.; Shiryaev, S. A.; Ge, X.; Strongin, A. Y., Selective function-blocking monoclonal human antibody highlights the important role of membrane type-1 matrix metalloproteinase (MT1-MMP) in metastasis. *Oncotarget* **2017,** *8* (2), 2781-2799.

108. Russell, R. G. G.; Watts, N. B.; Ebetino, F. H.; Rogers, M. J., Mechanisms of action of bisphosphonates: similarities and differences and their potential influence on clinical efficacy. *Osteoporosis International* **2008,** *19* (6), 733-759.

109. Giannobile, W. V., Host-response therapeutics for periodontal diseases. *J Periodontol* **2008,** *79* (8 Suppl), 1592-600.

110. Tella, S. H.; Gallagher, J. C., Prevention and treatment of postmenopausal osteoporosis. *The Journal of steroid biochemistry and molecular biology* **2014,** *142*, 155-70.

111. Shapiro, J. R.; Sponsellor, P. D., Osteogenesis imperfecta: questions and answers. *Current opinion in pediatrics* **2009,** *21* (6), 709-16.

112. Akram, Z.; Abduljabbar, T.; Kellesarian, S. V.; Abu Hassan, M. I.; Javed, F.; Vohra, F., Efficacy of bisphosphonate as an adjunct to nonsurgical periodontal therapy in the management of periodontal disease: a systematic review. *British journal of clinical pharmacology* **2017,** *83* (3), 444-454.

113. Lipton, A., Emerging role of bisphosphonates in the clinic—Antitumor activity and prevention of metastasis to bone. *Cancer Treatment Reviews* **2008,** *34*, S25-S30.

114. Marx, R. E., Pamidronate (Aredia) and zoledronate (Zometa) induced avascular necrosis of the jaws: a growing epidemic. *Journal of Oral and Maxillofacial Surgery* **2003,** *61* (9), 1115-1117.

115. Reid, I. R., Osteonecrosis of the jaw — Who gets it, and why? *Bone* **2009,** *44* (1), 4-10.

116. Endo, Y.; Kumamoto, H.; Nakamura, M.; Sugawara, S.; Takano-Yamamoto, T.; Sasaki, K.; Takahashi, T., Underlying Mechanisms and Therapeutic Strategies for Bisphosphonate-Related Osteonecrosis of the Jaw (BRONJ). *Biological & pharmaceutical bulletin* **2017,** *40* (6), 739-750.

117. Rosella, D.; Papi, P.; Giardino, R.; Cicalini, E.; Piccoli, L.; Pompa, G., Medication-related osteonecrosis of the jaw: Clinical and practical guidelines. *Journal of International Society of Preventive & Community Dentistry* **2016,** *6* (2), 97-104.

118. Shibahara, T., Antiresorptive Agent-Related Osteonecrosis of the Jaw (ARONJ): A Twist of Fate in the Bone. *The Tohoku journal of experimental medicine* **2019,** *247* (2), 75-86.

119. King, R.; Tanna, N.; Patel, V., Medication-related osteonecrosis of the jaw unrelated to bisphosphonates and denosumab—a review. *Oral Surgery, Oral Medicine, Oral Pathology and Oral Radiology* **2018**.

120. Thumbigere-Math, V.; Michalowicz, B. S.; Hodges, J. S.; Tsai, M. L.; Swenson, K. K.; Rockwell, L.; Gopalakrishnan, R., Periodontal disease as a risk factor for bisphosphonate-related osteonecrosis of the jaw. *J Periodontol* **2014,** *85* (2), 226-33.

121. Aghaloo, T.; Hazboun, R.; Tetradis, S., Pathophysiology of Osteonecrosis of the Jaws. *Oral and maxillofacial surgery clinics of North America* **2015,** *27* (4), 489-96.

122. Yoneda, T.; Hagino, H.; Sugimoto, T.; Ohta, H.; Takahashi, S.; Soen, S.; Taguchi, A.; Nagata, T.; Urade, M.; Shibahara, T.; Toyosawa, S., Antiresorptive agent-related osteonecrosis of the jaw: Position Paper 2017 of the Japanese Allied Committee on Osteonecrosis of the Jaw. *Journal of bone and mineral metabolism* **2017,** *35* (1), 6-19.

123. Heerboth, S.; Lapinska, K.; Snyder, N.; Leary, M.; Rollinson, S.; Sarkar, S., Use of Epigenetic Drugs in Disease: An Overview. *Genetics & Epigenetics* **2014,** *6*, 9-19.

124. Shi, Y.; Lan, F.; Matson, C.; Mulligan, P.; Whetstine, J. R.; Cole, P. A.; Casero, R. A.; Shi, Y., Histone demethylation mediated by the nuclear amine oxidase homolog LSD1. *Cell* **2004,** *119* (7), 941-53.

125. Scheer, S.; Zaph, C., The Lysine Methyltransferase G9a in Immune Cell Differentiation and Function. *Frontiers in immunology* **2017,** *8*, 429.

126. Baylin, S. B.; Ohm, J. E., Epigenetic gene silencing in cancer - a mechanism for early oncogenic pathway addiction? *Nat Rev Cancer* **2006,** *6* (2), 107-16.

127. Baylin, S. B.; Jones, P. A., A decade of exploring the cancer epigenome - biological and translational implications. *Nat Rev Cancer* **2011,** *11* (10), 726-34.

128. Dawson, M. A.; Kouzarides, T., Cancer epigenetics: from mechanism to therapy. *Cell* **2012,** *150* (1), 12-27.

129. Copeland, R. A., Molecular pathways: protein methyltransferases in cancer. *Clin Cancer Res* **2013,** *19* (23), 6344-50.

130. Hojfeldt, J. W.; Agger, K.; Helin, K., Histone lysine demethylases as targets for anticancer therapy. *Nature reviews* **2013,** *12* (12), 917-30.

131. James, L. I.; Frye, S. V., Targeting Chromatin Readers. *Clin. Pharmacol. Ther.* **2014,** *93* (4), 312-314.

132. Kaniskan, H.; Martini, M. L.; Jin, J., Inhibitors of Protein Methyltransferases and Demethylases. *Chemical reviews* **2018,** *118* (3), 989-1068.

133. Araki, Y.; Mimura, T., The Histone Modification Code in the Pathogenesis of Autoimmune Diseases. *Mediators of Inflammation* **2017,** *2017*, 2608605.

134. Wang, M.; Liu, X.; Guo, J.; Weng, X.; Jiang, G.; Wang, Z.; He, L., Inhibition of LSD1 by Pargyline inhibited process of EMT and delayed progression of prostate cancer in vivo. *Biochem Biophys Res Commun* **2015,** *467* (2), 310-5.

135. Nicholson, T. B.; Chen, T., LSD1 demethylates histone and non-histone proteins. *Epigenetics* **2009,** *4* (3), 129-32.

136. Zheng, Y. C.; Yu, B.; Jiang, G. Z.; Feng, X. J.; He, P. X.; Chu, X. Y.; Zhao, W.; Liu, H. M., Irreversible LSD1 inhibitors: Application of tranylcypromine and its derivatives in cancer treatment. *Curr Top Med Chem* **2016**.

137. Guibourt, N.; Ortega-Munoz, A.; Castro-Palomino Laria, J. US Patent Application 20120004262: Phenylcyclopropylamine derivatives and their medical use. 2012.

138. Ortega-Munoz, A.; Castro-Palomino Laria, J.; Fyfe, M. C. T. Lysine-specific demethylase 1 inhibitors and their use. 2011.

139. Maes, T.; Carceller, E.; Salas, J.; Ortega, A.; Buesa, C., Advances in the development of histone lysine demethylase inhibitors. *Curr Opin Pharmacol* **2015,** *23*, 52-60.

140. Huang, Y.; Greene, E.; Stewart, T. M.; Goodwin, A. C.; Baylin, S. B.; Woster, P. M.; Casero, R. A., Inhibition of lysine-specific demethylase 1 by polyamine analogues results in reexpression of aberrantly silenced genes. *Proc. Nat'l. Acad. Sci. U.S.A.* **2007,** *104*, 8023-8028.

141. Sharma, S.; Wu, Y.; Steinbergs, N.; Crowley, M.; Hanson, A.; Casero, R. A. J.; Woster, P., (Bis)urea and (bis)thiourea inhibitors of lysine-specific demethylase 1 as epigenetic modulators. *J. Med. Chem.* **2010,** *53* (14), 5197–5212.

142. Sharma, S. K.; Hazeldine, S.; Crowley, M. L.; Hanson, A.; Beattie, R.; Varghese, S.; Sennanayake, T. M. D.; Hirata, A.; Hirata, F.; Huang, Y.; Wu, Y.; Steinbergs, N.; Murray-Stewart, T.; Bytheway, I.; Casero, J., R.A.; Woster, P. M., Polyamine-based small molecule epigenetic modulators. *MedChemComm* **2012,** *3*, 14-21.

143. Kutz, C. J.; Holshouser, S. L.; Marrow, E. A.; Woster, P. M., 3,5-Diamino-1,2,4-triazoles as a novel scaffold for potent, reversible LSD1 (KDM1A) inhibitors. *MedChemComm* **2014,** *5* (12), 1863-1870.

144. Zheng, Y. C.; Duan, Y. C.; Ma, J. L.; Xu, R. M.; Zi, X.; Lv, W. L.; Wang, M. M.; Ye, X. W.; Zhu, S.; Mobley, D.; Zhu, Y. Y.; Wang, J. W.; Li, J. F.; Wang, Z. R.; Zhao, W.; Liu, H. M., Triazole-Dithiocarbamate Based Selective Lysine Specific Demethylase 1 (LSD1) Inactivators Inhibit Gastric Cancer Cell Growth, Invasion, and Migration. *J. Med. Chem.* **2013,** *56*, 8543-8560.

145. Gottesfeld, J. M.; Pandolfo, M., Development of histone deacetylase inhibitors as therapeutics for neurological disease. *Future Neurol* **2009,** *4* (6), 775-784.

146. Lakowski, B.; Roelens, I.; Jacob, S., CoREST-like complexes regulate chromatin modification and neuronal gene expression. *J Mol Neurosci* **2006,** *29* (3), 227-39.

147. Ginder, G. D., Epigenetic regulation of fetal globin gene expression in adult erythroid cells. *Translational Res.* **2015,** *165*, 115-125.

148. Shi, L.; Cui, S.; Engel, J. D.; Tanabe, O., Lysine-specific demethylase 1 is a therapeutic target for fetal hemoglobin induction. *Nature medicine* **2013,** *19* (3), 291-4.

149. Liang, Y.; Quenelle, D.; Vogel, J. L.; Mascaro, C.; Ortega, A.; Kristie, T. M., A novel selective LSD1/KDM1A inhibitor epigenetically blocks herpes simplex virus lytic replication and reactivation from latency. *mBio* **2013,** *4* (1), e00558-12.

150. Mishra, M.; Zhong, Q.; Kowluru, R. A., Epigenetic modifications of Nrf2-mediated glutamate-cysteine ligase: implications for the development of diabetic retinopathy and the metabolic memory phenomenon associated with its continued progression. *Free Radic Biol Med* **2014,** *75*, 129-139.

151. Pan, D.; Mao, C.; Wang, Y. X., Suppression of gluconeogenic gene expression by LSD1-mediated histone demethylation. *PLoS ONE* **2013,** *8* (6), e66294.

152. Yang, I. V.; Schwartz, D. A., Epigenetics of idiopathic pulmonary fibrosis. *Translational Res.* **2014,** *165*, 48-60.

153. Wang, J.; Saijo, K.; Skola, D.; Jin, C.; Ma, Q.; Merkurjev, D.; Glass, C. K.; Rosenfeld, M. G., Histone demethylase LSD1 regulates hematopoietic stem cells homeostasis and protects from death by endotoxic shock. *Proceedings of the National Academy of Sciences* **2018,** *115* (2), E244-E252.

154. Haines, R. R.; Barwick, B. G.; Scharer, C. D.; Majumder, P.; Randall, T. D.; Boss, J. M., The Histone Demethylase LSD1 Regulates B Cell Proliferation and Plasmablast Differentiation. *The Journal of Immunology* **2018,** *201* (9), 2799-2811.

155. Labbé, R. M.; Holowatyj, A.; Yang, Z. Q., Histone lysine demethylase (KDM) subfamily 4: structures, functions and therapeutic potential. *American Journal of Translational Research* **2014,** *6* (1), 1-15.

156. Su, Z.; Wang, F.; Lee, J. H.; Stephens, K. E.; Papazyan, R.; Voronina, E.; Krautkramer, K. A.; Raman, A.; Thorpe, J. J.; Boersma, M. D.; Kuznetsov, V. I.; Miller, M. D.; Taverna, S. D.; Phillips, G. N., Jr.; Denu, J. M., Reader domain specificity and lysine demethylase-4 family function. *Nat Commun* **2016,** *7*, 13387.

157. Kim, T. W.; Lee, S. J.; Oh, B. M.; Lee, H.; Uhm, T. G.; Min, J. K.; Park, Y. J.; Yoon, S. R.; Kim, B. Y.; Kim, J. W.; Choe, Y. K.; Lee, H. G., Epigenetic modification of TLR4 promotes activation of NF-κB by regulating methyl-CpG-binding domain protein 2 and Sp1 in gastric cancer. *Oncotarget* **2016,** *7* (4), 4195-209.

158. Gazzar, M. E.; Yoza, B. K.; Chen, X.; Hu, J.; Hawkins, G. A.; McCall, C. E., G9a and HP1 Couple Histone and DNA Methylation to TNFα Transcription Silencing during Endotoxin Tolerance. *Journal of Biological Chemistry* **2008,** *283* (47), 32198-32208.

159. Li, M. F.; Zhang, R.; Li, T. T.; Chen, M. Y.; Li, L. X.; Lu, J. X.; Jia, W. P., High Glucose Increases the Expression of Inflammatory Cytokine Genes in Macrophages Through H3K9 Methyltransferase Mechanism. *J Interferon Cytokine Res* **2016,** *36* (1), 48-61.

160. Fu, X.; Wang, X.; Duan, Z.; Zhang, C.; Fu, X.; Yang, J.; Liu, X.; He, J., Histone H3k9 and H3k27 Acetylation Regulates IL-4/STAT6-Mediated Igepsilon Transcription in B Lymphocytes. *Anatomical record (Hoboken, N.J. : 2007)* **2015,** *298* (8), 1431-9.

161. Hachiya, R.; Shiihashi, T.; Shirakawa, I.; Iwasaki, Y.; Matsumura, Y.; Oishi, Y.; Nakayama, Y.; Miyamoto, Y.; Manabe, I.; Ochi, K.; Tanaka, M.; Goda, N.; Sakai, J.; Suganami, T.; Ogawa, Y., The H3K9 methyltransferase Setdb1 regulates TLR4-mediated inflammatory responses in macrophages. *Sci Rep* **2016,** *6*.

162. Das, N. D.; Choi, M. R.; Jung, K. H.; Park, J. H.; Lee, H. T.; Das, A.; Kim, S. H.; Chai, Y. G., Functional Analysis of Histone Demethylase Jmjd2b on Lipopolysaccharide-Treated Murine Neural Stem Cells (NSCs). *Neurotoxicity Research* **2013,** *23* (2), 154-165.

163. Calapkorur, M. U.; Alkan, B. A.; Tasdemir, Z.; Akcali, Y.; Saatci, E., Association of peripheral arterial disease with periodontal disease: Analysis of inflammatory cytokines and an acute phase protein in gingival crevicular fluid and serum. *Journal of Periodontal Research* **2016**.

164. Ye, L.; Fan, Z.; Yu, B.; Chang, J.; Al Hezaimi, K.; Zhou, X.; Park, N. H.; Wang, C. Y., Histone demethylases KDM4B and KDM6B promotes osteogenic differentiation of human MSCs. *Cell stem cell* **2012,** *11* (1), 50-61.

165. Han, F.; Ren, J.; Zhang, J.; Sun, Y.; Ma, F.; Liu, Z.; Yu, H.; Jia, J.; Li, W., JMJD2B is required for Helicobacter pylori-induced gastric carcinogenesis via regulating COX-2 expression. *Oncotarget* **2016,** *7* (25), 38626-37.

166. Busslinger, M.; Tarakhovsky, A., Epigenetic Control of Immunity. *Cold Spring Harbor Perspectives in Biology* **2014,** *6* (6).

167. Xu, G.; Liu, G.; Xiong, S.; Liu, H.; Chen, X.; Zheng, B., The histone methyltransferase Smyd2 is a negative regulator of macrophage activation by suppressing interleukin 6 (IL-6) and tumor necrosis factor α (TNF-α) production. *The Journal of biological chemistry* **2015,** *290* (9), 5414-23.

168. Fu, L.; Chen, L.; Yang, J.; Ye, T.; Chen, Y.; Fang, J., HIF-1α-induced histone demethylase JMJD2B contributes to the malignant phenotype of colorectal cancer cells via an epigenetic mechanism. *Carcinogenesis* **2012,** *33* (9), 1664-1673.

169. Liu, L.; Lu, Y.; Martinez, J.; Bi, Y.; Lian, G.; Wang, T.; Milasta, S.; Wang, J.; Yang, M.; Liu, G.; Green, D. R.; Wang, R., Proinflammatory signal suppresses proliferation and shifts macrophage metabolism from Myc-dependent to HIF1α-dependent. *Proceedings of the National Academy of Sciences* **2016,** *113* (6), 1564-1569.

170. O'Neill, Luke A. J., A Broken Krebs Cycle in Macrophages. *Immunity* **2015,** *42* (3), 393-394.

171. Wu, N.; Yang, M.; Gaur, U.; Xu, H.; Yao, Y.; Li, D., Alpha-Ketoglutarate: Physiological Functions and Applications. *Biomolecules & Therapeutics* **2016,** *24* (1), 1-8.

172. Rose, N. R.; Ng, S. S.; Mecinovic, J.; Lienard, B. M.; Bello, S. H.; Sun, Z.; McDonough, M. A.; Oppermann, U.; Schofield, C. J., Inhibitor scaffolds for 2-oxoglutarate-dependent histone lysine demethylases. *J Med Chem* **2008,** *51* (22), 7053-6.

173. Wang, L.; Chang, J.; Varghese, D.; Dellinger, M.; Kumar, S.; Best, A. M.; Ruiz, J.; Bruick, R.; Pena-Llopis, S.; Xu, J.; Babinski, D. J.; Frantz, D. E.; Brekken, R. A.; Quinn, A. M.; Simeonov, A.; Easmon, J.; Martinez, E. D., A small molecule modulates Jumonji histone demethylase activity and selectively inhibits cancer growth. *Nat Commun* **2013,** *4*, 2035.

174. King, O. N.; Li, X. S.; Sakurai, M.; Kawamura, A.; Rose, N. R.; Ng, S. S.; Quinn, A. M.; Rai, G.; Mott, B. T.; Beswick, P.; Klose, R. J.; Oppermann, U.; Jadhav, A.;

Heightman, T. D.; Maloney, D. J.; Schofield, C. J.; Simeonov, A., Quantitative high-throughput screening identifies 8-hydroxyquinolines as cell-active histone demethylase inhibitors. *PLoS ONE* **2010,** *5* (11), e15535.

175. Schiller, R.; Scozzafava, G.; Tumber, A.; Wickens, J. R.; Bush, J. T.; Rai, G.; Lejeune, C.; Choi, H.; Yeh, T. L.; Chan, M. C.; Mott, B. T.; McCullagh, J. S.; Maloney, D. J.; Schofield, C. J.; Kawamura, A., A cell-permeable ester derivative of the JmjC histone demethylase inhibitor IOX1. *ChemMedChem* **2014,** *9* (3), 566-71.

176. Rai, G.; Kawamura, A.; Tumber, A.; Liang, Y.; Vogel, J. L.; Arbuckle, J. H.; Rose, N. R.; Dexheimer, T. S.; Foley, T. L.; King, O. N.; Quinn, A.; Mott, B. T.; Schofield, C. J.; Oppermann, U.; Jadhav, A.; Simeonov, A.; Kristie, T. M.; Maloney, D. J., Discovery of ML324, a JMJD2 demethylase inhibitor with demonstrated antiviral activity. In *Probe Reports from the NIH Molecular Libraries Program*, National Center for Biotechnology Information (US): Bethesda (MD), 2010.

177. Duan, L.; Rai, G.; Roggero, C.; Zhang, Q. J.; Wei, Q.; Ma, S. H.; Zhou, Y.; Santoyo, J.; Martinez, E. D.; Xiao, G.; Raj, G. V.; Jadhav, A.; Simeonov, A.; Maloney, D. J.; Rizo, J.; Hsieh, J. T.; Liu, Z. P., KDM4/JMJD2 Histone Demethylase Inhibitors Block Prostate Tumor Growth by Suppressing the Expression of AR and BMYB-Regulated Genes. *Chemistry & biology* **2015,** *22* (9), 1185-96.

178. Chu, C. H.; Wang, L. Y.; Hsu, K. C.; Chen, C. C.; Cheng, H. H.; Wang, S. M.; Wu, C. M.; Chen, T. J.; Li, L. T.; Liu, R.; Hung, C. L.; Yang, J. M.; Kung, H. J.; Wang, W. C., KDM4B as a target for prostate cancer: structural analysis and selective inhibition by a novel inhibitor. *J Med Chem* **2014,** *57* (14), 5975-85.

179. Kim, T. D.; Fuchs, J. R.; Schwartz, E.; Abdelhamid, D.; Etter, J.; Berry, W. L.; Li, C.; Ihnat, M. A.; Li, P. K.; Janknecht, R., Pro-growth role of the JMJD2C histone

demethylase in HCT-116 colon cancer cells and identification of curcuminoids as JMJD2 inhibitors. *American Journal of Translational Research* **2014,** *6* (3), 236-47.

180. Bavetsias, V.; Lanigan, R. M.; Ruda, G. F.; Atrash, B.; McLaughlin, M. G.; Tumber, A.; Mok, N. Y.; Le Bihan, Y. V.; Dempster, S.; Boxall, K. J.; Jeganathan, F.; Hatch, S. B.; Savitsky, P.; Velupillai, S.; Krojer, T.; England, K. S.; Sejberg, J.; Thai, C.; Donovan, A.; Pal, A.; Scozzafava, G.; Bennett, J. M.; Kawamura, A.; Johansson, C.; Szykowska, A.; Gileadi, C.; Burgess-Brown, N. A.; von Delft, F.; Oppermann, U.; Walters, Z.; Shipley, J.; Raynaud, F. I.; Westaway, S. M.; Prinjha, R. K.; Fedorov, O.; Burke, R.; Schofield, C. J.; Westwood, I. M.; Bountra, C.; Müller, S.; van Montfort, R. L.; Brennan, P. E.; Blagg, J., 8-Substituted Pyrido[3,4-d]pyrimidin-4(3H)-one Derivatives As Potent, Cell Permeable, KDM4 (JMJD2) and KDM5 (JARID1) Histone Lysine Demethylase Inhibitors. *J Med Chem* **2016,** *59* (4), 1388-409.

181. Yang, J.; Jubb, A. M.; Pike, L.; Buffa, F. M.; Turley, H.; Baban, D.; Leek, R.; Gatter, K. C.; Ragoussis, J.; Harris, A. L., The histone demethylase JMJD2B is regulated by estrogen receptor alpha and hypoxia, and is a key mediator of estrogen induced growth. *Cancer research* **2010,** *70* (16), 6456-66.

182. Coffey, K.; Rogerson, L.; Ryan-Munden, C.; Alkharaif, D.; Stockley, J.; Heer, R.; Sahadevan, K.; O'Neill, D.; Jones, D.; Darby, S.; Staller, P.; Mantilla, A.; Gaughan, L.; Robson, C. N., The lysine demethylase, KDM4B, is a key molecule in androgen receptor signalling and turnover. *Nucleic Acids Res* **2013,** *41* (8), 4433-46.

183. Janzer, A.; Lim, S.; Fronhoffs, F.; Niazy, N.; Buettner, R.; Kirfel, J., Lysine-specific demethylase 1 (LSD1) and histone deacetylase 1 (HDAC1) synergistically repress proinflammatory cytokines and classical complement pathway components. *Biochemical and Biophysical Research Communications* **2012,** *421* (4), 665-670.

184. Shi, L.; Sun, L.; Li, Q.; Liang, J.; Yu, W.; Yi, X.; Yang, X.; Li, Y.; Han, X.; Zhang, Y.; Xuan, C.; Yao, Z.; Shang, Y., Histone demethylase JMJD2B coordinates H3K4/H3K9 methylation and promotes hormonally responsive breast carcinogenesis. *Proceedings of the National Academy of Sciences of the United States of America* **2011,** *108* (18), 7541-7546.

185. Ghare, S. S.; Joshi-Barve, S.; Moghe, A.; Patil, M.; Barker, D. F.; Gobejishvili, L.; Brock, G. N.; Cave, M.; McClain, C. J.; Barve, S. S., Coordinated histone H3 methylation and acetylation regulate physiologic and pathologic fas ligand gene expression in human CD4+ T cells. *Journal of immunology (Baltimore, Md. : 1950)* **2014,** *193* (1), 412-21.

186. Eke, P. I.; Dye, B. A.; Wei, L.; Slade, G. D.; Thornton-Evans, G. O.; Borgnakke, W. S.; Taylor, G. W.; Page, R. C.; Beck, J. D.; Genco, R. J., Update on Prevalence of Periodontitis in Adults in the United States: NHANES 2009 to 2012. *J Periodontol* **2015,** *86* (5), 611-22.

187. Klein, S. L.; Flanagan, K. L., Sex differences in immune responses. *Nature Reviews Immunology* **2016,** *16*, 626.

188. Coffey, K.; Rogerson, L.; Ryan-Munden, C.; Alkharaif, D.; Stockley, J.; Heer, R.; Sahadevan, K.; O'Neill, D.; Jones, D.; Darby, S.; Staller, P.; Mantilla, A.; Gaughan, L.; Robson, C. N., The lysine demethylase, KDM4B, is a key molecule in androgen receptor signalling and turnover. *Nucleic Acids Research* **2013,** *41* (8), 4433-4446.

189. Pollock, J. A.; Larrea, M. D.; Jasper, J. S.; McDonnell, D. P.; McCafferty, D. G., Lysine-specific histone demethylase 1 inhibitors control breast cancer proliferation in ERalpha-dependent and -independent manners. *ACS chemical biology* **2012,** *7* (7), 1221-31.

190. Gaughan, L.; Stockley, J.; Coffey, K.; O'Neill, D.; Jones, D. L.; Wade, M.; Wright, J.; Moore, M.; Tse, S.; Rogerson, L.; Robson, C. N., KDM4B is a Master Regulator of the Estrogen Receptor Signalling Cascade. *Nucleic Acids Research* **2013,** *41* (14), 6892-6904.

191. Kawazu, M.; Saso, K.; Tong, K. I.; McQuire, T.; Goto, K.; Son, D.-O.; Wakeham, A.; Miyagishi, M.; Mak, T. W.; Okada, H.; Shioda, T., Histone Demethylase JMJD2B Functions as a Co-Factor of Estrogen Receptor in Breast Cancer Proliferation and Mammary Gland Development. *PLoS ONE* **2011,** *6* (3), e17830.

192. Choi, J. Y.; Yoon, S. S.; Kim, S. E.; Ahn Jo, S., KDM4B histone demethylase and G9a regulate expression of vascular adhesion proteins in cerebral microvessels. *Sci Rep* **2017,** *7*.

193. Dandona, P.; Aljada, A.; Bandyopadhyay, A., Inflammation: the link between insulin resistance, obesity and diabetes. *Trends in immunology* **2004,** *25* (1), 4-7.

194. Salvi, G. E.; Yalda, B.; Collins, J. G.; Jones, B. H.; Smith, F. W.; Arnold, R. R.; Offenbacher, S., Inflammatory mediator response as a potential risk marker for periodontal diseases in insulin-dependent diabetes mellitus patients. *J Periodontol* **1997,** *68* (2), 127-35.

195. Salvi, G. E.; Collins, J. G.; Yalda, B.; Arnold, R. R.; Lang, N. P.; Offenbacher, S., Monocytic TNF alpha secretion patterns in IDDM patients with periodontal diseases. *Journal of clinical periodontology* **1997,** *24* (1), 8-16.

196. Stewart, M. D.; Li, J.; Wong, J., Relationship between Histone H3 Lysine 9 Methylation, Transcription Repression, and Heterochromatin Protein 1 Recruitment. *Molecular and Cellular Biology* **2005,** *25* (7), 2525-38.

197. Chatterjee, B.; Wolff, D. W.; Jothi, M.; Mal, M.; Mal, A. K., p38α MAPK disables KMT1A-mediated repression of myogenic differentiation program. *Skeletal muscle* **2016,** *6*.

198. Filgueiras, L. R.; Brandt, S. L.; Ramalho, T. R. d. O.; Jancar, S.; Serezani, C. H., Imbalance between HDAC and HAT activities drives aberrant STAT1/MyD88 expression in macrophages from type 1 diabetic mice. *Journal of Diabetes and its Complications*.

199. Brasacchio, D.; Okabe, J.; Tikellis, C.; Balcerczyk, A.; George, P.; Baker, E. K.; Calkin, A. C.; Brownlee, M.; Cooper, M. E.; El-Osta, A., Hyperglycemia induces a dynamic cooperativity of histone methylase and demethylase enzymes associated with gene-activating epigenetic marks that coexist on the lysine tail. *Diabetes* **2009,** *58* (5), 1229-36.

200. Suvan, J. E.; Finer, N.; D'Aiuto, F., Periodontal complications with obesity. *Periodontol 2000* **2018,** *78* (1), 98-128.

201. Martinez-Herrera, M.; Lopez-Domenech, S.; Silvestre, F. J.; Silvestre-Rangil, J.; Banuls, C.; Hernandez-Mijares, A.; Rocha, M., Dietary therapy and non-surgical periodontal treatment in obese patients with chronic periodontitis. *Journal of clinical periodontology* **2018,** *45* (12), 1448-1457.

202. Kato, T.; Yamazaki, K.; Nakajima, M.; Date, Y.; Kikuchi, J.; Hase, K.; Ohno, H.; Yamazaki, K., Oral Administration of Porphyromonas gingivalis Alters the Gut Microbiome and Serum Metabolome. *mSphere* **2018,** *3* (5).

203. Wu, Y.; Chi, X.; Zhang, Q.; Chen, F.; Deng, X., Characterization of the salivary microbiome in people with obesity. *PeerJ* **2018,** *6*, e4458.

204. Damanaki, A.; Memmert, S.; Nokhbehsaim, M.; Sanyal, A.; Gnad, T.; Pfeifer, A.; Deschner, J., Impact of obesity and aging on crestal alveolar bone height in mice.

Annals of anatomy = Anatomischer Anzeiger : official organ of the Anatomische Gesellschaft **2018,** *218*, 227-235.

205. Lizcano, F.; Romero, C.; Vargas, D., Regulation of adipogenesis by nuclear receptor PPARγ is modulated by the histone demethylase JMJD2C. *Genetics and Molecular Biology* **2011,** *34* (1), 19-24.

206. Tateishi, K.; Okada, Y.; Kallin, E. M.; Zhang, Y., Role of Jhdm2a in regulating metabolic gene expression and obesity resistance. *Nature* **2009,** *458* (7239), 757-761.

207. Inagaki, T.; Tachibana, M.; Magoori, K.; Kudo, H.; Tanaka, T.; Okamura, M.; Naito, M.; Kodama, T.; Shinkai, Y.; Sakai, J., Obesity and metabolic syndrome in histone demethylase JHDM2a-deficient mice. *Genes to cells : devoted to molecular & cellular mechanisms* **2009,** *14* (8), 991-1001.

208. Kang, C.; Saso, K.; Ota, K.; Kawazu, M.; Ueda, T.; Okada, H., JMJD2B/KDM4B inactivation in adipose tissues accelerates obesity and systemic metabolic abnormalities. *Genes to cells : devoted to molecular & cellular mechanisms* **2018,** *23* (9), 767-777.

209. Cheng, Y.; Yuan, Q.; Vergnes, L.; Rong, X.; Youn, J. Y.; Li, J.; Yu, Y.; Liu, W.; Cai, H.; Lin, J. D.; Tontonoz, P.; Hong, C.; Reue, K.; Wang, C. Y., KDM4B protects against obesity and metabolic dysfunction. *Proc Natl Acad Sci U S A* **2018,** *115* (24), E5566-e5575.

210. Nagpal, R.; Yamashiro, Y.; Izumi, Y., The Two-Way Association of Periodontal Infection with Systemic Disorders: An Overview. *Mediators of Inflammation* **2015,** *2015*.

211. Wang, W.-C., Chu, C.-H., Chen, C.-C., 4LXL Crystal structure of JMJD2B complexed with pyridine-2,4-dicarboxylic acid and H3K9me3 In *Classification: OXIDOREDUCTASE / PEPTIDE*, Deposited: 2013-07-30 Released: 2014-07-30.

212. Rai G, K. A., Tumber A, et al. *Discovery of ML324, a JMJD2 demethylase inhibitor with demonstrated antiviral activity.*; Bethesda (MD): National Center for Biotechnology Information (US): 2012 Dec 17 [Updated 2013 Sep 16].

213. Zhang, X.; Goncalves, R.; Mosser, D. M., The Isolation and Characterization of Murine Macrophages. *Current protocols in immunology / edited by John E. Coligan ... [et al.]* **2008,** *Chapter*, Unit-14.1.

214. Weischenfeldt, J.; Porse, B., Bone Marrow-Derived Macrophages (BMM): Isolation and Applications. *Cold Spring Harbor Protocols* **2008,** *2008* (12), pdb.prot5080.

215. Valerio, M. S.; Herbert, B. A.; Basilakos, D. S.; Browne, C.; Yu, H.; Kirkwood, K. L., Critical Role of MKP-1 in Lipopolysaccharide-Induced Osteoclast Formation through CXCL1 and CXCL2. *Cytokine* **2015,** *71* (1), 71-80.

216. Loe, H., The Gingival Index, the Plaque Index and the Retention Index Systems. *J Periodontol* **1967,** *38* (6), Suppl:610-6.

217. Herbert, B. A.; Steinkamp, H. M.; Gaestel, M.; Kirkwood, K. L., Mitogen-Activated Protein Kinase 2 Signaling Shapes Macrophage Plasticity in Aggregatibacter actinomycetemcomitans-Induced Bone Loss. *Infection and immunity* **2017,** *85* (1).

218. Pettersen, E. F.; Goddard, T. D.; Huang, C. C.; Couch, G. S.; Greenblatt, D. M.; Meng, E. C.; Ferrin, T. E., UCSF Chimera--a visualization system for exploratory research and analysis. *Journal of computational chemistry* **2004,** *25* (13), 1605-12.

219. Irwin, J. J.; Sterling, T.; Mysinger, M. M.; Bolstad, E. S.; Coleman, R. G., ZINC: A Free Tool to Discover Chemistry for Biology. *Journal of Chemical Information and Modeling* **2012,** *52* (7), 1757-1768.

220. Backman, T. W.; Cao, Y.; Girke, T., ChemMine tools: an online service for analyzing and clustering small molecules. *Nucleic Acids Res* **2011,** *39* (Web Server issue), W486-91.

221. Labute, P., Binary QSAR: a new method for the determination of quantitative structure activity relationships. *Pacific Symposium on Biocomputing. Pacific Symposium on Biocomputing* **1999**, 444-55.

222. Ijjaali, I.; Petitet, F.; Dubus, E.; Barberan, O.; Michel, A., Assessing potency of c-Jun N-terminal kinase 3 (JNK3) inhibitors using 2D molecular descriptors and binary QSAR methodology. *Bioorganic & Medicinal Chemistry* **2007,** *15* (12), 4256-4264.

223. Hinsberger, S.; Hüsecken, K.; Groh, M.; Negri, M.; Haupenthal, J.; Hartmann, R. W., Discovery of Novel Bacterial RNA Polymerase Inhibitors: Pharmacophore-Based Virtual Screening and Hit Optimization. *Journal of Medicinal Chemistry* **2013,** *56* (21), 8332-8338.

224. Chen, Z.-W.; Zhu, Y.-Z.; Ou, J.-W.; Wang, Y.-P.; Zheng, J.-Y., Metal-Free Iodine(III)-Promoted Synthesis of Isoquinolones. *The Journal of Organic Chemistry* **2014,** *79* (22), 10988-10998.

225. Park, S. R.; Kim, D. J.; Han, S. H.; Kang, M. J.; Lee, J. Y.; Jeong, Y. J.; Lee, S. J.; Kim, T. H.; Ahn, S. G.; Yoon, J. H.; Park, J. H., Diverse Toll-Like Receptors Mediate Cytokine Production by Fusobacterium nucleatum and Aggregatibacter actinomycetemcomitans in Macrophages. *Infection and Immunity* **2014,** *82* (5), 1914-20.

226. Binda, O.; LeRoy, G.; Bua, D. J.; Garcia, B. A.; Gozani, O.; Richard, S., Trimethylation of histone H3 lysine 4 impairs methylation of histone H3 lysine 9: Regulation of lysine methyltransferases by physical interaction with their substrates. *Epigenetics* **2010,** *5* (8), 767-75.

227. Berghaus, L. J.; Moore, J. N.; Hurley, D. J.; Vandenplas, M. L.; Fortes, B. P.; Wolfert, M. A.; Boons, G. J., Innate immune responses of primary murine macrophage-lineage cells and RAW 264.7 cells to ligands of Toll-like receptors 2, 3, and 4. *Comp Immunol Microbiol Infect Dis* **2010,** *33* (5), 443-54.

228. Satoh, T.; Takeuchi, O.; Vandenbon, A.; Yasuda, K.; Tanaka, Y.; Kumagai, Y.; Miyake, T.; Matsushita, K.; Okazaki, T.; Saitoh, T.; Honma, K.; Matsuyama, T.; Yui, K.; Tsujimura, T.; Standley, D. M.; Nakanishi, K.; Nakai, K.; Akira, S., The Jmjd3-Irf4 axis regulates M2 macrophage polarization and host responses against helminth infection. *Nat Immunol* **2010,** *11* (10), 936-44.

229. Wang, X.; Wang, S.; Yao, G.; Yu, D.; Chen, K.; Tong, Q.; Ye, L.; Wu, C.; Sun, Y.; Li, H.; Hermann, D. M.; Doeppner, T. R.; Jin, F.; Dai, Y.; Wu, J., Identification of the histone lysine demethylase KDM4A/JMJD2A as a novel epigenetic target in M1 macrophage polarization induced by oxidized LDL. *Oncotarget* **2017,** *8* (70), 114442-114456.

230. Van den Bossche, J.; Baardman, J.; de Winther, M. P., Metabolic Characterization of Polarized M1 and M2 Bone Marrow-derived Macrophages Using Real-time Extracellular Flux Analysis. *Journal of visualized experiments : JoVE* **2015,** (105).

231. Heinrich, F.; Lehmbecker, A.; Raddatz, B. B.; Kegler, K.; Tipold, A.; Stein, V. M.; Kalkuhl, A.; Deschl, U.; Baumgärtner, W.; Ulrich, R.; Spitzbarth, I., Morphologic, phenotypic, and transcriptomic characterization of classically and alternatively activated canine blood-derived macrophages in vitro. *PLoS ONE* **2017,** *12* (8), e0183572.

232. Kirkpatrick, J. E.; Kirkwood, K. L.; Woster, P. M., Inhibition of the Histone Demethylase KDM4B Leads to Activation of KDM1A, Attenuates Bacterial-Induced Pro-Inflammatory Cytokine Release, and Reduces Osteoclastogenesis. *Epigenetics* **2018**.

233. Mombelli, A., Microbial colonization of the periodontal pocket and its significance for periodontal therapy. *Periodontol 2000* **2018,** *76* (1), 85-96.

234. Zhuang, Z.; Yoshizawa-Smith, S.; Glowacki, A.; Maltos, K.; Pacheco, C.; Shehabeldin, M.; Mulkeen, M.; Myers, N.; Chong, R.; Verdelis, K.; Garlet, G. P.; Little, S.; Sfeir, C., Induction of M2 Macrophages Prevents Bone Loss in Murine Periodontitis Models. *J Dent Res* **2018**, 22034518805984.

235. Redlich, K.; Smolen, J. S., Inflammatory bone loss: pathogenesis and therapeutic intervention. *Nat Rev Drug Discov* **2012,** *11* (3), 234-250.

236. Saurav Pathak, S.; Maitra, S.; Chakravarty, S.; Kumar, A., *Histone Lysine Demethylases of JMJD2 or KDM4 Family are Important Epigenetic Regulators in Reward Circuitry in the Etiopathology of Depression*. 2016; Vol. 42.

237. Sterling, T.; Irwin, J. J., ZINC 15 – Ligand Discovery for Everyone. *Journal of Chemical Information and Modeling* **2015,** *55* (11), 2324-2337.

238. Aldrich, C.; Bertozzi, C.; Georg, G. I.; Kiessling, L.; Lindsley, C.; Liotta, D.; Merz, K. M.; Schepartz, A.; Wang, S., The Ecstasy and Agony of Assay Interference Compounds. *Journal of Medicinal Chemistry* **2017,** *60* (6), 2165-2168.

239. Lipinski, C. A., Lead- and drug-like compounds: the rule-of-five revolution. *Drug Discovery Today: Technologies* **2004,** *1* (4), 337-341.

240. Charifson, P. S.; Corkery, J. J.; Murcko, M. A.; Walters, W. P., Consensus Scoring: A Method for Obtaining Improved Hit Rates from Docking Databases of Three-

Dimensional Structures into Proteins. *Journal of Medicinal Chemistry* **1999,** *42* (25), 5100-5109.

241. Backman, T. W. H.; Cao, Y.; Girke, T., ChemMine tools: an online service for analyzing and clustering small molecules. *Nucleic Acids Research* **2011,** *39* (suppl_2), W486-W491.

242. Wang, L.; Chang, J.; Varghese, D.; Dellinger, M.; Kumar, S.; Best, A. M.; Ruiz, J.; Bruick, R.; Peña-Llopis, S.; Xu, J.; Babinski, D. J.; Frantz, D. E.; Brekken, R. A.; Quinn, A. M.; Simeonov, A.; Easmon, J.; Martinez, E. D., A small molecule modulates Jumonji histone demethylase activity and selectively inhibits cancer growth. *Nature communications* **2013,** *4*, 2035-2035.

243. Chu, C.-H.; Wang, L.-Y.; Hsu, K.-C.; Chen, C.-C.; Cheng, H.-H.; Wang, S.-M.; Wu, C.-M.; Chen, T.-J.; Li, L.-T.; Liu, R.; Hung, C.-L.; Yang, J.-M.; Kung, H.-J.; Wang, W.-C., KDM4B as a Target for Prostate Cancer: Structural Analysis and Selective Inhibition by a Novel Inhibitor. *Journal of Medicinal Chemistry* **2014,** *57* (14), 5975-5985.

244. Meng, S.; Zhang, L.; Tang, Y.; Tu, Q.; Zheng, L.; Yu, L.; Murray, D.; Cheng, J.; Kim, S.; Zhou, X.; Chen, J., BET Inhibitor JQ1 Blocks Inflammation and Bone Destruction. *Journal of Dental Research* **2014,** *93* (7), 657-62.

245. Herbert, B. A.; Steinkamp, H. M.; Gaestel, M.; Kirkwood, K. L., MK2 Signaling Shapes Macrophage Plasticity in Aggregatibacter actinomycetemcomitans-induced Bone Loss. *Infection and Immunity* **2016**.

246. Yates, A.; Akanni, W.; Amode, M. R.; Barrell, D.; Billis, K.; Carvalho-Silva, D.; Cummins, C.; Clapham, P.; Fitzgerald, S.; Gil, L.; Girón, C. G.; Gordon, L.; Hourlier, T.; Hunt, S. E.; Janacek, S. H.; Johnson, N.; Juettemann, T.; Keenan, S.; Lavidas, I.; Martin, F. J.; Maurel, T.; McLaren, W.; Murphy, D. N.; Nag, R.; Nuhn, M.; Parker, A.; Patricio,

M.; Pignatelli, M.; Rahtz, M.; Riat, H. S.; Sheppard, D.; Taylor, K.; Thormann, A.; Vullo, A.; Wilder, S. P.; Zadissa, A.; Birney, E.; Harrow, J.; Muffato, M.; Perry, E.; Ruffier, M.; Spudich, G.; Trevanion, S. J.; Cunningham, F.; Aken, B. L.; Zerbino, D. R.; Flicek, P., Ensembl 2016. *Nucleic Acids Research* **2016,** *44* (D1), D710-D716.

247. The KDM4B inhibition assay procedure was run by BPS Biosciences (San Diego, CA) using AlphaScreen® technology.

248. Papadopoulos, G.; Weinberg, E. O.; Massari, P.; Gibson, F. C.; Wetzler, L. M.; Morgan, E. F.; Genco, C. A., Macrophage-Specific TLR2 Signaling Mediates Pathogen-Induced TNF-Dependent Inflammatory Oral Bone Loss. *The Journal of Immunology* **2013,** *190* (3), 1148-1157.

249. Dunmyer, J.; Herbert, B.; Li, Q.; Zinna, R.; Martin, K.; Yu, H.; Kirkwood, K. L., Sustained mitogen-activated protein kinase activation with Aggregatibacter actinomycetemcomitans causes inflammatory bone loss. *Molecular oral microbiology* **2012,** *27* (5), 397-407.

250. Zhang, X.; Hyer, J. M.; Yu, H.; D'Silva, N. J.; Kirkwood, K. L., DUSP1 Phosphatase Regulates the Proinflammatory Milieu in Head and Neck Squamous Cell Carcinoma. *Cancer research* **2014,** *74* (24), 7191-7197.

251. Herbert, B. A.; Novince, C. M.; Kirkwood, K. L., Aggregatibacter actinomycetemcomitans, a potent immunoregulator of the periodontal host defense system and alveolar bone homeostasis. *Molecular oral microbiology* **2016,** *31* (3), 207-227.

252. Madeira, M. F. M.; Queiroz-Junior, C. M.; Costa, G. M.; Santos, P. C.; Silveira, E. M.; Garlet, G. P.; Cisalpino, P. S.; Teixeira, M. M.; Silva, T. A.; Souza, D. d. G., MIF

induces osteoclast differentiation and contributes to progression of periodontal disease in mice. *Microbes and Infection* **2012,** *14* (2), 198-206.

253. Ye, L.; Fan, Z.; Yu, B.; Chang, J.; Hezaimi, K. A.; Zhou, X.; Park, N. H.; Wang, C. Y., Histone Demethylases KDM4B and KDM6B Promotes Osteogenic Differentiation Of Human MSCs. *Cell stem cell* **2012,** *11* (1), 50-61.

254. Valerio, M. S.; Basilakos, D. S.; Kirkpatrick, J. E.; Chavez, M.; Hathaway-Schrader, J.; Herbert, B. A.; Kirkwood, K. L., Sex-based differential regulation of bacterial-induced bone resorption. *J Periodontal Res* **2017,** *52* (3), 377-387.

255. Whetstine, J. R.; Nottke, A.; Lan, F.; Huarte, M.; Smolikov, S.; Chen, Z.; Spooner, E.; Li, E.; Zhang, G.; Colaiacovo, M.; Shi, Y., Reversal of Histone Lysine Trimethylation by the JMJD2 Family of Histone Demethylases. *Cell* **2006,** *125* (3), 467-481.

256. Ponnaluri, V. K. C.; Vavilala, D. T.; Putty, S.; Gutheil, W. G.; Mukherji, M., Identification of non-histone substrates for JMJD2A–C histone demethylases. *Biochemical and biophysical research communications* **2009,** *390* (2), 280-284.

257. Vazquez, D., Inhibitors of protein synthesis. *FEBS Letters* **1974,** *40*, S48-S62.

258. Berry, W. L.; Janknecht, R., KDM4/JMJD2 Histone Demethylases: Epigenetic Regulators in Cancer Cells. *Cancer research* **2013,** *73* (10), 2936-42.

259. Schukin, S. I.; Zinkovsky, V. G.; Zhuk, O. V., Elimination kinetics of the novel prodrug cinazepam possessing psychotropic activity in mice. *Pharmacological Reports* **2011,** *63* (5), 1093-1100.

260. Peloquin, C. A.; James, G. T.; Craig, L. D.; Kim, M.; McCarthy, E. A.; Ikle, D.; Iseman, M. D., Pharmacokinetic evaluation of aconiazide, a potentially less toxic isoniazid prodrug. *Pharmacotherapy* **1994,** *14* (4), 415-23.

261. Miller, W. D.; Fray, A. H.; Quatroche, J. T.; Sturgill, C. D., Suppression of a Palladium-Mediated Homocoupling in a Suzuki Cross-Coupling Reaction. Development of an Impurity Control Strategy Supporting Synthesis of LY451395. *Organic Process Research & Development* **2007,** *11* (3), 359-364.